Single Molecule Studies of hGSTA1-1: Binding Kinetics and Active Site Dynamics

By

John R. Pettersson

A dissertation submitted in partial fulfillment of the requirements for the degree of

Doctor of Philosophy in Biological Sciences

Carnegie Mellon University

4400 Fifth Avenue

Pittsburgh, PA 15213

November 13th 2015

Thesis Advisors: Dr Frederick Lanni & Dr. Gordon Rule

Thesis Committee: Dr. Marcel Bruchez, Dr. David Hackney, Dr. Linda Peteanu

Table of Content

Abstract

The human detoxification enzyme glutathione s-transferase alpha 1 (GSTA1-1) is known for its ability to conjugate a variety of different hydrophobic xenobiotics to the tripeptide glutathione. The conjugation can be catalyzed through either a substitution or an addition reaction. Which reaction mechanism is being used affects the cooperativity of the enzyme. GST is also capable of catalyzing isomerization reactions of particular substrates without conjugation to GSH which further extends its repertoire. The C-terminal of the enzyme transitions from a random loop to an α-helix that localizes over the active site as a ligand binds. The α-helix is also involved in product release. We hypothesize that the broad substrate specificity and the catalytic flexibility of GST is a result of a heterogeneous protein population where multiple conformers with different properties coexist. To identify different conformers in a population a single molecule approach is needed. Fluorescently tagged substrates and products of GSTA1-1 have been imaged as they bind immobilized GSTA1-1 using TIRF microscopy. Single molecule binding events can be analyzed to characterize different binding states of the enzyme. The observation of at least two average occupancy times suggests that there are multiple binding states and conformations of the enzyme. One of these binding states is dominating the population and a large number of binding events has to be sampled to pick up the more rare states.

To further characterize the behavior of GSTA1-1 FRET and DEER have been used to study the active site dynamics during binding of a ligand. Unlike X-ray crystallography, DEER and FRET provide a distribution in a distance between groups, and not just an average. Our data suggest that binding of S-hexylglutathione does not localize the C-terminal helix which is contrary to what can be observed in the X-ray crystal structure. Glutathione alone is sufficient to localize the helix. This highlights the importance of using proteins in solution to study their conformation.

Acknowledgements

Advisors:
Dr. Frederick Lanni
Dr. Gordon Rule

Committee:
Dr. Marcel Bruchez
Dr. David Hackney
Dr. Linda Peteanu

Lab members:
Dr. Jigar V. Desai
Sahil Sangani
Dr. Kaustubh Sinha
Dr. Andrew Kehr
Paul Barton
Ian Fucci

Biological Sciences:
Minden Lab: Dr. Phu Van, Brendan Redler
Bruchez Lab: Dr. Dmytro Yushchenko**,** Lydia Perkins
Administration: Ena Miceli, Shoba Subramanian, Nate Frezzell, Emily Stark, Matthew Salyers

MBIC:
Dr. Marcel Bruchez
Dr. Alan Waggoner
Dr. Lauren Ernst
Dr. Brigitte Schmidt
Dr. Haibing Teng
Mike Patrick
Sue Andreko

Chemistry:
Sourav Dey
Dr. Matteus Tanha
Hadi Abroshan
Dr. Samya Sourav
Dr. James Woods
[10]

2010 Students:
Gino, Han, Jigar, Karen, Liz, Madhu, Olivia, Sahil, Salini, Shanna, Ting, Yi, Zhongling

Saxena Lab:
Dr. Sunil Saxena
Matthew Lawless

Family and Friends:
Stephanie Makin
Dr. Anton Fagerström
Annika & Lennart Pettersson
Friends

Figure List

Chapter 1:

Chapter 2:

Chapter 3:

List of Abbreviations

Ar	Argon gas
BME	β-mercaptoethanol
CDNB	1-chloro-2,4-dinitrobenzene
CW	Continuous Wave
DEER	Double Electron-Electron Resonance
DHAR	Dehydroascorbate reductases
EA	Ethacrynic Acid
EPR	Electron Paramagnetic Resonance
FRET	Förster Resonance Energy Transfer
FCS	Fluorescence Correlation Spectroscopy
f.l.	Focal Lenght
fps	Frames Per Second
GOC	Glucose Oxidase and Catalase deoxygenation system
GS-DNB	S-dinitrobenzyl glutathione
GSH	Glutathione
GS-hex	S-hexyl glutathione
GST	Glutathione S-transferase
HPLC	High Performance Liquid Chromatography
ips	Images Per Second
ITC	Isothermal Titration Calorimetry
MAPEG	Membrane Associated Proteins in Eicosanoid and Glutathione Metabolism
MS	Mass Spectrometry
NMR	Nuclear Magnetic Resonance
P2	Extended linker including 2 polyethylene glycol residues
PDA/PCD	Protocatechuic Acid/Protocatechuate 3,4-dioxygenase deoxygenation system
PIFE	Protein Induced Fluorescence Enhancement
PTM	Post Translational Modification
SDSL	Site Directed Spin Labeling
S_NAr	Nucleophilic aromatic substitution
SM	Single Molecule
TIRF	Total Internal Reflection Fluorescence
UV	Ultraviolet

Chapter 1 – General Background

1.1 - Introduction

The human body is constantly exposed to harmful substances and has developed a sophisticated detoxification system to help prevent cellular damage. Our liver is crucial to this detoxification process and contains enzymes that can neutralize and enable excretion of unwanted molecules. Detoxification can be divided into two phases, phase I where a variety of enzymes introduce reactive groups into the unwanted substance, and phase II where enzymes conjugate the metabolite into charged species. Phase II detoxification generates a more polar product which is unable to pass across the cell membrane and has to be actively transported out of the cell, whereupon it cannot easily re-enter due to its polarity.[1]

Glutathione S-transferase (GST) is one of the most abundant phase II detoxification enzymes and conjugates a variety of different electrophilic xenobiotics to the tripeptide glutathione (GSH).[2] GSTs comprise as much as 4% of the soluble protein in the liver so mammals seem to be primed to deal with a variety and fairly large quantity of unwanted reactive species, some of which are endogenous oxidation products.[3] A few other examples of natural GST substrates are isothiocyanates[4] and peroxides[5].

Decades of extensive research on GST has shown a complex and broad functionality. GST is not only a detoxification enzyme but participates in a variety of different cellular processes like cell signaling[6] and propagation of cancer[7]. The fact that GST has multiple functions may explain the high abundance in some tissues. Both the broad substrate specificity and functional flexibility of GST has been established, but there are still many unanswered questions regarding the biochemical significance of its dimeric structure, and the molecular

features giving rise to its functional plasticity. I have in my work focused on one of the best characterized GSTs, the human alpha class 1 (GSTA1-1), a cytosolic enzyme that has the capability to catalyze detoxification reactions of reactive species that differ greatly in both size and structure.

1.2 - Glutathione S-Transferases

The broad substrate specificity of GSTA1-1 must be the result of unusual structural features of the enzyme. The active site is able to accommodate and conjugate a plethora of different molecules and further characterization of the enzymes structure is needed to better understand the reason for the substrate plasticity.

GST has the enzyme classification number 2.5.1.18 describing that it is a transferase (2), transferring alkyl or aryl groups, other than methyl groups (2.5), transferring alkyl or aryl groups, other than methyl groups (2.5.1), called glutathione S-transferase (2.5.1.18).

There are both cytosolic and non-cytosolic GSTs. Since the cytosolic classes are much more abundant they have historically been more frequently studied and are therefore more well characterized than the other more rare classes of the enzyme.[8,9,10]

All cytosolic GSTs are dimers and each monomer has a GSH binding site (G-site) and a hydrophobic binding site (H-site) located at the dimer interface (**Figure 1.1**). There are no solvent channels running through the interface between the monomers, but there is a V-shaped cleft about 40Å long with one active site at each side separated by 14Å.[11]

Cytosolic GST is found in all aerobic organisms with 15-20 genes identified in mammals, 10-15 in bacteria and over 10 in insects. The cytosolic GSTs have been divided into seven classes

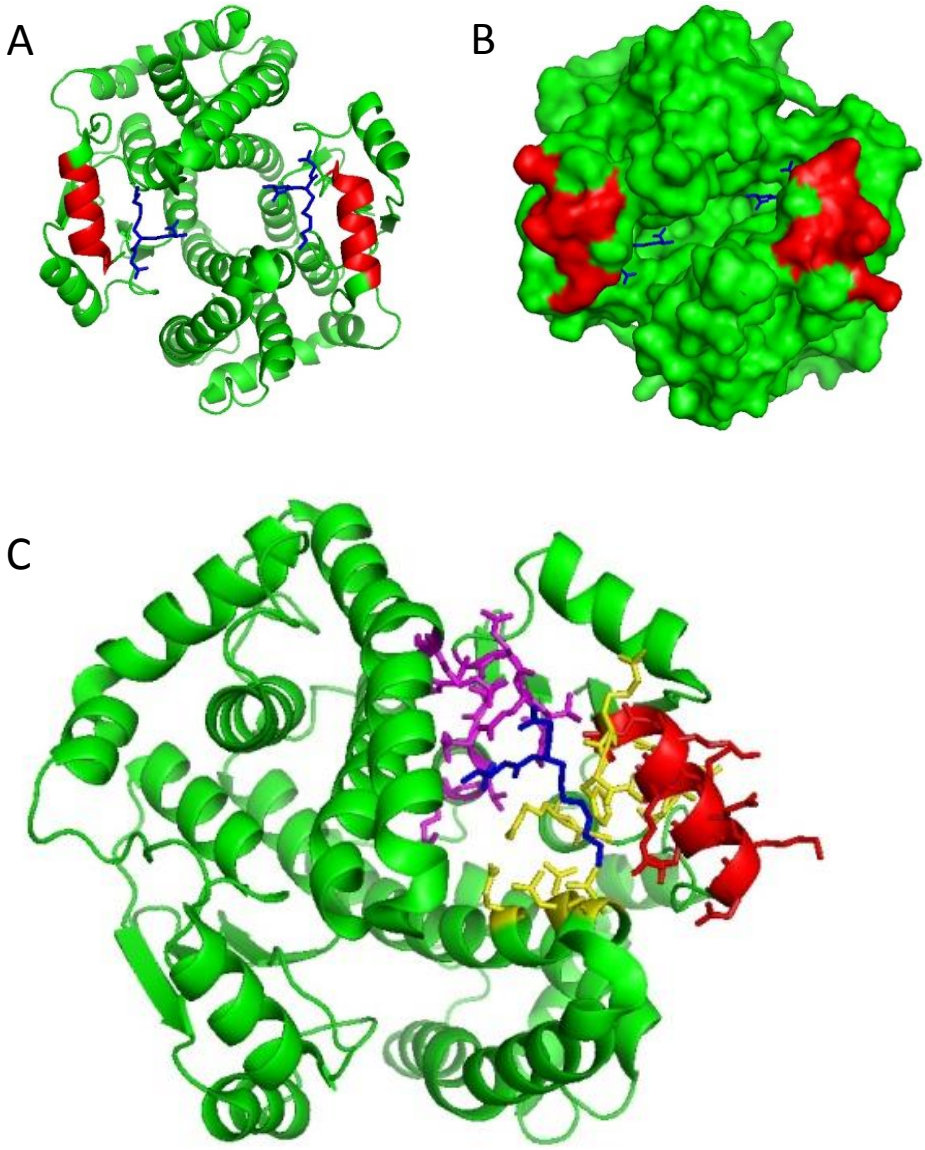

Figure 1.1: Structure of GSTA1-1 (PDB- entry IK3L) with the ligand S-hexyl glutathione colored blue and the C-terminal helix α9 colored red. **A**: Secondary structure of GSTA1-1. **B**: Space filled model of A. **C**: A rotation of A with residues in the G-site colored magenta, and residues in the H-site colored yellow. As can be seen α9 is localized on top of the H-site with ligand bound. Only one active site has been colored in C to avoid confusion.

in mammals based on sequence identity, gene structure, and immunoreactivity properties; Alpha, Mu, Pi, Sigma, Theta, Zeta and Omega. There are six cytosolic classes in plants; Lambda, Phi, Tau, DHAR (dehydroascorbate reductases), Theta and Zeta. Insects have five cytosolic classes; Delta, Sigma, Theta, Zeta and Omega. The number of classes in bacteria is less characterized but a specific Beta class and enzymes related to the Theta class have been identified. Dimerization is restricted to monomers of the same class and even if each subunit is catalytically independent all active cytosolic GSTs found in nature are dimers.[12,10,13]

There are two classes of non-cytosolic GSTs that are quite different from the cytosolic classes. The dimeric mammalian Kappa class has both GSH and peroxidase activity. It has a wide tissue expression profile but has been detected in mitochondria and peroxisomes and not in the cytosol. The Kappa class has been suggested to be involved in β-oxidation of fatty acids and in detoxification of lipid peroxides.[13,14]

In addition to the Kappa class there are also the trimeric membrane associated proteins in eicosanoid and glutathione metabolism (MAPEGs) that are smaller and have a different fold compared to cytosolic GSTs. MAPEGs are present in a variety of organisms but are much less abundant and less characterized than cytosolic GSTs. MAPEGs are involved in synthesis of eicosanoids, leukotrienes and prostaglandins, but many of them have glutathione transferase and peroxidase activity as well.[13,15]

All types of GSTs have detoxification activity and the enzyme family possesses an incredible width of activities and substrate specificity. This in itself would be sufficient to motivate further characterization of the enzyme. However, GST is also involved in drug

metabolism and cancer progression which makes it even more important to understand and modulate its activity.

1.3 - GST Activity

To better understand the functional flexibility of GST both the catalytic mechanism and the conformation of the active site has to be studied. Since GST can use a variety of different substrates there must me some flexibility in the active site of the enzyme (**Figure 1.1**).

GSTs catalyze the nucleophilic attack of the sulfur atom of the tripeptide GSH (γ-Glu-Cys-Gly) on the electrophilic group of xenobiotics, carcinogens and endogenous hydrophobic compounds.[16,17] The conjugation plays an important role in detoxification by inactivating hydrophobic compounds that contain reactive centers. A single GST isoform is capable of conjugating GSH to many different hydrophobic substrates (**Figure 1.2**).[18,19,20]

GSH plays a vital role in maintaining proper redox status within the cell and eliminating toxic compounds like alkylating compounds, peroxides and disulfides. GSH will react spontaneously with some substrates, but these reactions are also catalyzed by GSTs.[21] GSTs also have ligandin activity, the ability to bind different hydrophobic substrates without catalytic turnover, which is important for sequestration and transportation of hydrophobic compounds.[22]

A fundamental mechanism of GST is the deprotonation of GSH to form the GS^- thiolate anion since only deprotonated GSH is reactive. By binding GSH, GSTs decrease the thiol pKa which promotes deprotonation and increases the effective concentration of the active thiolate.[12,16,21,23,24,25] Nucleophilic GS^- reacts with an electrophilic substrate through a

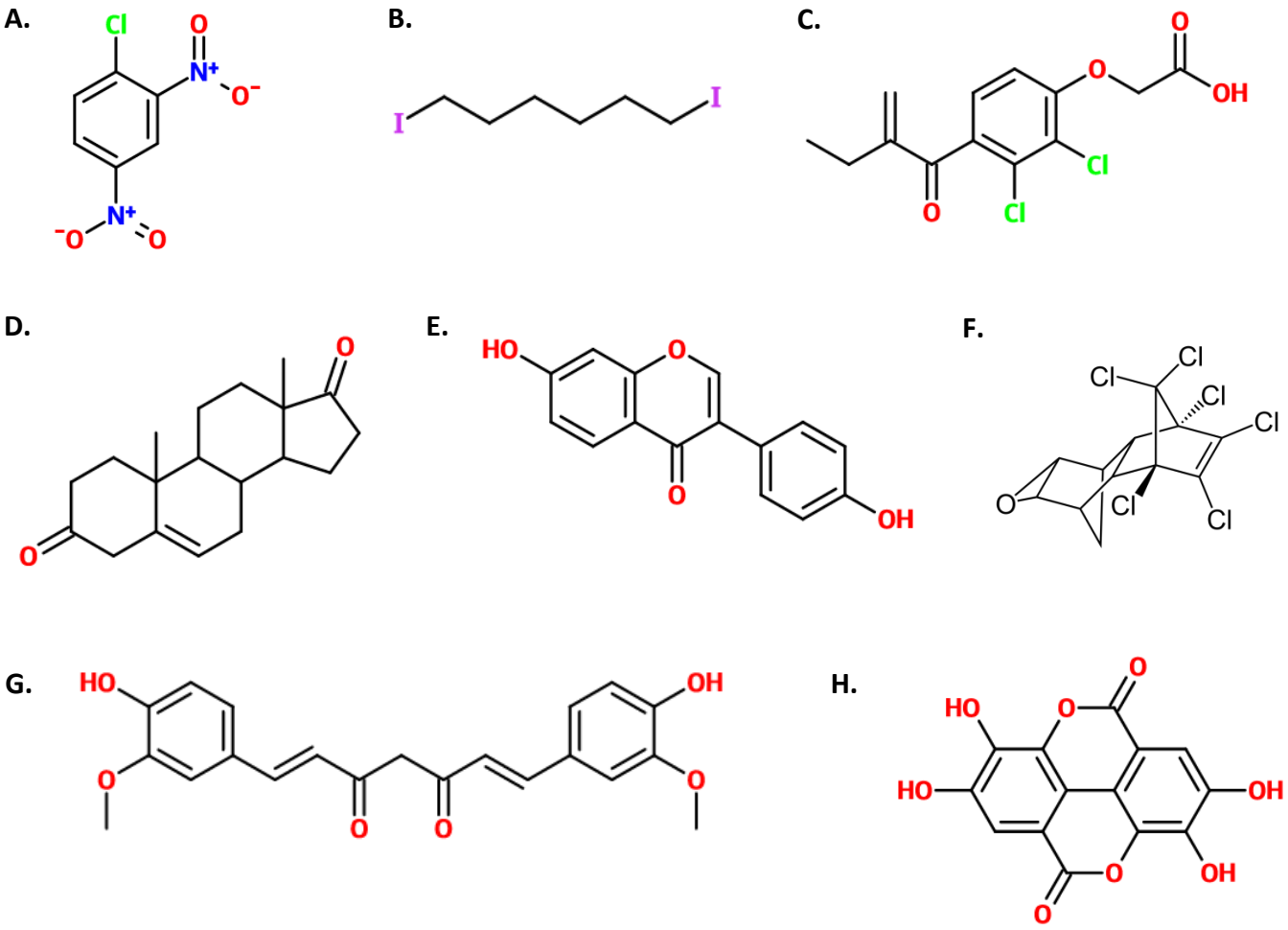

Figure 1.2: The structural diversity of GSTA1-1 substrates and inhibitors. **A:** 1-chloro-2,4-dinitrobenzene[85] (substrate) **B:** Diiodohexane[86] (substrate) **C:** Ethacrynic Acid[87] (substrate) **D:** Δ5 -Androstene- 3,17-dione[40] (substrate) **E:** Daidzein[88] (inhibitor) **F:** Dieldrin[89] (inhibitor) **G:** Curcumin[88] (inhibitor) **H:** Ellagic Acid[88] (inhibitor).

substitution reaction via a high-energy anionic transition state, or with an aromatic electrophilic substrate in a S_NAr via the Meisenheimer complex. [12,16,21,23,24] GST can also conjugate GSH to substrate through addition reactions.[26]

1.4 - GST Structure

The relationship between GSTA1-1s structure and function has to be further studied to understand the activities of the enzyme. The homodimeric GSTA1-1 monomer consists of 222 residues separated into two domains. Domain 1 adopts a thioredoxin-like fold (βαβαββα) consisting of the N-terminal β1α1β2 and the C-terminal β3β4α3 linked by a loop containing helix α2. A beta-sheet is formed by the parallel β1, β2, β4 and the antiparallel β3 with α2 on one side and α1 and α3 on the other side. Domain 2 is positioned downstream of domain1 and contains 5 α-helices. The C-terminal part of GSTA1-1 contains another α-helix, α9.[12,13]

The two active sites are located at the interface of the dimer. The G-site is formed by the N-terminal thioredoxin domain and is highly conserved among soluble GSTs. The high level of conservation is ensuring high specificity towards GSH. The H-site is very variable between different classes and determines the substrate specificity. The H-site can fit substrates of different sizes but large molecules would protrude into the crevice between the monomers and potentially affect the domain interface and the stability of the dimer.[17,27] Tyr9 is the catalytic residue of GSTA1-1 and is located in the H-site. It acts as a hydrogen bond donor stabilizing the deprotonated form of GSH but also controls the arrangement of the substrate and therefore binding and dissociation rates.[28]

The rate limiting step for alpha class GSTs is the release of product, and the conformation of α9 is important for substrate binding, catalysis and product release.[11,29] GSH binding is sufficient to stabilize the C-terminal helix.[12] The carboxylate of glycine in GSH interacts with Arg45 which influences the ionic interaction between Arg221 and Asp42 which in turn triggers the fixation of the C-terminal lid over the binding site. The interaction of the GSH glycine with the binding site is also believed to influence the binding of the second substrate.[30] Mobility examination of GSTA1-1 crystal structures revealed that the ends of α4 and α5 also show high mobility, that the structure of the loop between α6 and α7 can sometimes not be determined, and that there is break in α5 as it kinks.[11] These regions might also be involved in the dynamics determining the substrate specificity of the enzyme.

1.5 - The C-terminal Region of GST

The conformation of the C-terminal region of GSTA1-1 is determined by the presence of ligand. The region adopts an α-helix that localizes over the active site as ligand binds, while the conformation of the region is non-structured and delocalized without ligand present. The helix is believed to undergo transitions between different conformations in the unligated enzyme but is closing in over the active site upon binding of GSH or electrophilic substrate. GSH binding alone is sufficient to stabilize the C-terminal helix. Without the presence of a ligand the C-terminal region cannot be detected in crystal structures. [12,27,31] The C-terminal region consists of residues 208-222, where residues 210-220 form α9 (**Figure 1.1**).[27]

X-ray crystallography has shown that the two residues Arg221 and Phe222 are not part of the helix, but Arg221 seems to be involved in anchoring the helix against the protein by an

ionic interaction with Asp42.[11] Tyr9, Phe10, Phe220, and Phe222 are part of the H-site hydrophobic cavity and form an aromatic cluster which helps to position the β-carbon of the cysteinyl sidechain of glutathione.[11] The catalytic residue Tyr9 controls the positioning of the ligand as well as the binding and dissociation rates.[32] Phe10 is mobile and can change conformation upon ligand binding. Phe10 and Phe220 compete for the same position in the active site and cannot be present simultaneously. Ligand binding displaces Phe10 generating space for Phe220 and thereby help to localize the helix. Phe220 can interact with both GSH and the substrate which supports the observation that either ligand can trigger localization of the helix. Mutation of Phe220 decreases the catalytic activity, and mutation of Phe222 further decreases activity of the enzyme. Interaction of Tyr9 and Phe220 locks the α9-helix in place over the active site.[11] Increasing the viscosity by addition of sucrose or glycerol further decreases the activity by lowering both k_{cat} and k_{cat}/k_m suggesting that mobility is important for activity and that product release is the rate limiting step for a substrate saturated enzyme.[31,12,27] Thermodynamic studies suggest that open and closed conformations of the GSTA1-1 C-terminal coexist in a protein population.[28,32] Ile219 is involved in the stability of the region through tertiary interactions. Mutating Ile219 to alanine reduced the stability of the C-terminal region in human GSTA1-1 resulting in reduced acticity.[12,27]

Isothermal Titration Calorimetry (ITC) and stopped-flow experiments have previously been used to study the thermodynamics of ligand binding to GSTA1-1.[28,27] The experiments show that GSTA1-1 is following a two-step binding mechanism for the conjugate of ethacrynate and glutathione (GS-EA) where binding is followed by isomerization and ordering of the C-terminal helix. Before the ligand can bind the active site has to be desolvated. This step is

entropically driven. After the ligand has bound an ordering of the enzyme occurs by localizing the C-terminal helix. This step is enthalpically driven. The C-terminal is crucial for efficient desolvation of the active site which is necessary for ligand binding. A GSTA1-1 mutant lacking the C-terminal is more than 100-fold less active than wild-type enzyme due to its inability to efficiently desolvate the active site.[28]

In addition to the C-terminal's role in binding of a ligand it is also believed to be involved in the release of product. The free energy of GS-EA binding to GSTA1-1 is lower than that of the two substrates and the enzyme has to cross a thermodynamic barrier to be able to release product. Disordering of the C-terminal helps provide positive entropy which is needed for product release and recycling of the enzyme.[27]

1.6 – GST Activity Assay

The standard way of determining GST activity is with the 1-chloro-2,4-dinitrobenzene (CDNB) assay. The dinitrobenzyl thioether (GS-DNB) product formed by GST after GSH conjugation to CDNB absorbs light at 340nm which enables detection of the catalytic progress in a spectrophotometer (**Figure 1.3**).[23,33] In order to investigate the binding of other substrates, products, or inhibitors these molecules can be added in the assay, and the decrease in activity can be monitored.

GST follows a sequential binding scheme with the S-conjugation reaction occurring in a ternary complex of enzyme, activated glutathione and hydrophobic electrophile. By keeping GSH concentration high and varying the substrate concentration the enzyme act as a single substrate enzyme and can be analyzed using Michaelis-Menten kinetics.[29,34,35,36,37] No sigmoidal

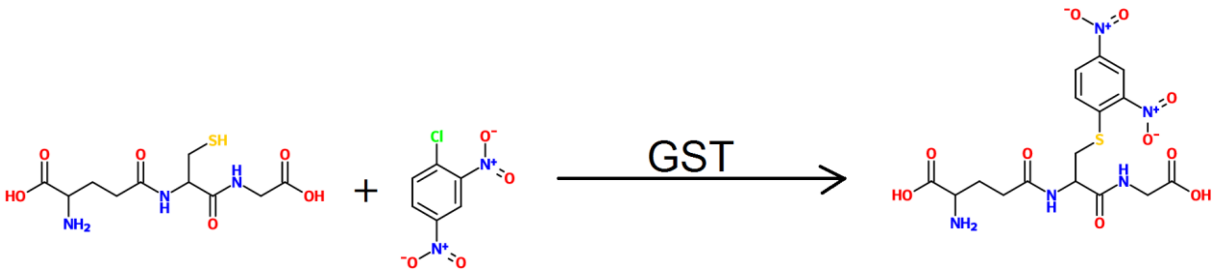

Figure 1.3: The GSTA1-1 catalyzed CDNB reaction. The standard assay to determine GST activity. GST is catalyzing the conjugation of GSH to CDNB through a substitution reaction forming a thioether. The reaction can be monitored colorimetrically as an increase in absorbance at 340nm. Visually, the reaction causes the solution to turn deeper yellow.

rate curves have been observed using CDNB as a substrate indicating that GSTA1-1 is not cooperative in S_NAr, acting non-cooperativiely following Michaelis-Menten kinetics. In the case of addition reactions, where GSH is added to the substrate, negative cooperativity can be observed with non-hyperbolic rate curves, not following Michaelis-Menten kinetics.[34,38,39] There is likely some kind of allosteric regulation and communication between the binding sites since negative cooperativity is obtained for addition reactions.[26]

1.7 - GST Promiscuity

GSTA1-1 has both broad substrate specificity and the capability of using different reaction mechanisms to conjugate GSH and substrate and thereby express what is called enzyme promiscuity. Enzyme promiscuity refers to having more than one function and can be divided in to three types of behavior; substrate promiscuity, catalytic promiscuity and product promiscuity. Substrate promiscuity describes the ability of an enzyme to utilize different substrates and catalytic promiscuity is when one active site of an enzyme can catalyze different reactions. Product promiscuity is when an enzyme can use one substrate to produce different products. GSTA1-1 expresses both substrate and catalytic promiscuity.

GSTA1-1 can for example conjugate hexyl iodide to GSH through a substitution reaction while ethacrynate (EA) is conjugated to GSH through an addition reaction. The enzyme can also isomerize the steroid hormone Δ^5-androstene-3,17-dione to Δ^4-androstene-3,17-dione.[40] GST was previously known as Ligandin due to its ability to bind and transport hydrophobic molecules.[22] This multifunctionality, especially the capability of GSTA1-1 to bind so many different molecules, makes characterization a challenge. The experimental conditions used

during an experiment will have a big effect on the activity of GST, and some of the enzyme's properties might have been mischaracterized due to experiments carried out in a non-optimal environment.[41] Every chemical in a sample has to be tested to make sure it is not interfering with any of the enzyme's functions. The activity towards a substrate molecule, the reaction mechanism used, and the cooperativity of the enzyme are all intertwined, and certain properties might be enhanced in certain conditions.

Promiscuity is a common feature of detoxification enzymes where conjugation of a variety of different compounds is an evolutionary advantage. Another example of a promiscuous enzyme is the detoxification enzyme Cytochrome P450 that actually expresses all three types of promiscuity.[42]

To enable functional flexibility in a single catalytic site the enzyme must express some structural flexibility. If an enzyme has multiple functions it should also have multiple conformations. A promiscuous enzyme must therefore be able to interconvert between different conformers and a chemically identical population of enzymes might make up a conformationally heterogeneous population.

1.8 - Protein Heterogeneity

The term protein heterogeneity refers to conformational transitions occurring over time that are slow compared to the dynamics associated with the catalytic cycle of the enzyme. A protein might at one time be in one conformation with characteristic dynamics and rate constants, while at a different time be in another state with different dynamics and rate

constants. It is possible that protein heterogeneity, substrate-dependent dynamics, and reaction mechanism are not mutually exclusive.

Static and dynamic heterogeneity may both contribute to the heterogeneity found among ensembles of molecules. Static heterogeneity refers to properties of a molecule which don't change on the timescale of the experiment while the fluctuations that occur in a property over the timescale of the experiment constitute dynamic heterogeneity.[43]

Enzymes are dynamic in their structure even without conformational changes occurring due to interaction with or binding to another molecule. It is believed that these dynamics are unsynchronized, and that proteins go through conformational selection. If there is a subpopulation of one conformation binding a molecule the equilibrium will shift in favor of that population.[44]

Post translational modifications (PTMs) can also contribute to protein heterogeneity. The major reasons for this kind of heterogeneity are proteolytic cleavage, glycosylation, additions of lipids, modifications of single amino acids, and other secondary modifications. PTMs are important for stability, folding, binding, and function of proteins.[45]

The only post-translational modifications detected with electro-spray ionization-MS for GSTA1-1 is acetylation of N-terminal residues.[46] This acetylation might not be present in a recombinant protein. Even if hGSTA1-1 expressed in *E.coli* is acetylated on the N-terminal it is not expected to have any effect on the dynamics of the active site and the C-terminal since these regions are spatially separated.

An interesting observation is that many acetylated proteins, including GST, seem to be involved in tumorigenesis, cancer cell proliferation, and immune functions. Lysines are targets

for both acetylation and ubiquitylation. Acetylation can thereby block ubiquitylation and bypass proteasomal degradation.[47]

1.9 - Single Molecule Experiments

Single Molecule (SM) detection of biomolecules has created a field of study at the interface of biology, chemistry, and physics, enabling characterization of both binding kinetics and dynamics. Although x-ray crystallography has been a powerful tool for obtaining the structure of a protein it tells us very little about the dynamics of an enzyme. NMR can be used to study dynamics in a small protein but the experiments are expensive, elaborate, and labor intensive to perform. NMR would just provide data related to the ensemble average, and not individual molecules. An alternative is SM-imaging which enables us to follow the dynamics of biomolecules in real time.

The traditional enzyme assays only report the average properties of the enzyme during optimal conditions for maximum activity. The activity of the enzyme will depend on the environment it is in and the activity obtained in vitro under assay conditions says very little about how an enzyme works in its natural environment, with less substrate available, at non-optimal temperature, pH etc. Single molecule enzymology would enable characterization of the range of activity and not just the average activity in an enzyme population.[48] It could also reveal how changing the environment changes the properties of individual enzymes.

To understand asynchronous biological processes real time studies at the single molecule level are required. Even though two biomolecules are chemically identical they may display different physiological properties at different times.[44] NMR experiments suggest that

structural dynamics are limiting for substrate binding rates.[49] Protein dynamics play an essential role in enzyme catalysis, but the relationship between dynamics and catalytic function is poorly understood. Allosteric transitions and conformational selection occur at the slower end of the spectrum, on millisecond to second timescales.[50,51,52,53] However, even the second timescale is fast compared to many rate assays.

Although a single enzyme displays an average catalytic rate over time, the catalytic efficiency can vary considerable from time to time. Conformational changes of an enzyme are often triggered by substrate binding and catalytic turnover, and are essential for the activity of the enzyme. Interconverting conformers can thereby have differences in enzymatic activity depending on what conformation they are in at a particular period of time.[54] If single enzymes show differences in binding rates they might have adapted different conformations. Novel experimental approaches where spectroscopic techniques are used to measure time-resolved protein motions are needed to further characterize the dynamics of enzymes.

The previously discussed two states of GSTA1-1, without and with bound ligand should be able to be observed in a single-molecule binding kinetics experiment. One could imagine that two different dissociation rates could be observed for the different states; one for ligand binding and dissociation with disordered helix, and one for ligand binding and dissociation with ordering of the helix.

1.10 - Total Internal Reflection Fluorescence Microscopy

One of the most important factors for single molecule detection is to reduce the excitation volume such that the signal from a single molecule can be observed. Total Internal

Reflection Fluorescence (TIRF) microscopy is a powerful method to visualize events in a thin region of fluorescence excitation without interference from other regions in the sample.[55] The result is an image with very low background fluorescence.

In TIRF microscopy an evanescent field is produced when an excitation beam in a refractive solid hits a lower refractive index material with a high angle of incidence. The angle has to be above the critical angle (θ_c) so that the light is totally internally reflected. This generates a thin electromagnetic field at the surface interface with the same frequency as the excitation light which can be used to excite fluorophores. The evanescent filed is produced in the low-index material. The critical angle (θ_c) can be obtained from the refractive indices on either side of the interface, the low-index material (n_1) and the substratum (n_2).

$$\theta_c = \sin^{-1}\left(\frac{n_1}{n_2}\right) \qquad \text{(Eq. 1.1)}$$

The intensity (I) of the evanescent field decreases exponentially into the specimen with the distance from the surface (z).

$$I(z) = I(\theta)e^{-z/d} \qquad \text{(Eq. 1.2)}$$

The attenuation length, or depth, (d) of the evanescent field can be determined from the wavelength (λ), incidence angle (θ_i) and the refractive indices (n).

$$d = \frac{\lambda_0}{4\pi n_2\left(\sin^2\theta_i - \frac{n_1^2}{n_2^2}\right)^{1/2}} \qquad \text{(Eq. 1.3)}$$

In TIRF a prism or a high numeric aperture (NA) objective is used to send the light into the sample with a high angle (θ_m), determined by the NA of the objective and the refractive index of the immersion fluid (usually oil for high-NA objectives).

$$\mathrm{NA} = n_{oil} \sin\theta_m \qquad \text{(Eq. 1.4)}$$

There are two commonly used optical TIRF setups, one using a high NA objective and one using a prism. In objective type TIRF, excitation light is sent though the side of a high NA objective generating an incident angle high enough for total reflection. In a prism type system the excitation light is refracted in the prism so that it hits the interface of a fused silica slide and sample buffer above the critical angle and is totally reflected (**Figure 1.4**).

Both setups have their advantages and shortcomings. In an objective type system samples can be placed right on top of the objective which allows for easier sample manipulation, but both excitation light and emitted light have the same light path which tends to generate a higher background, sometimes due to low levels of non-evanescent light that excites fluorophores that are detected by the CCD-camera. In the prism based system the sample is in between the prism and the objective which restricts sample manipulation and that is why some sort of flow cell is commonly used. Since excitation light and emission light are separated, prism

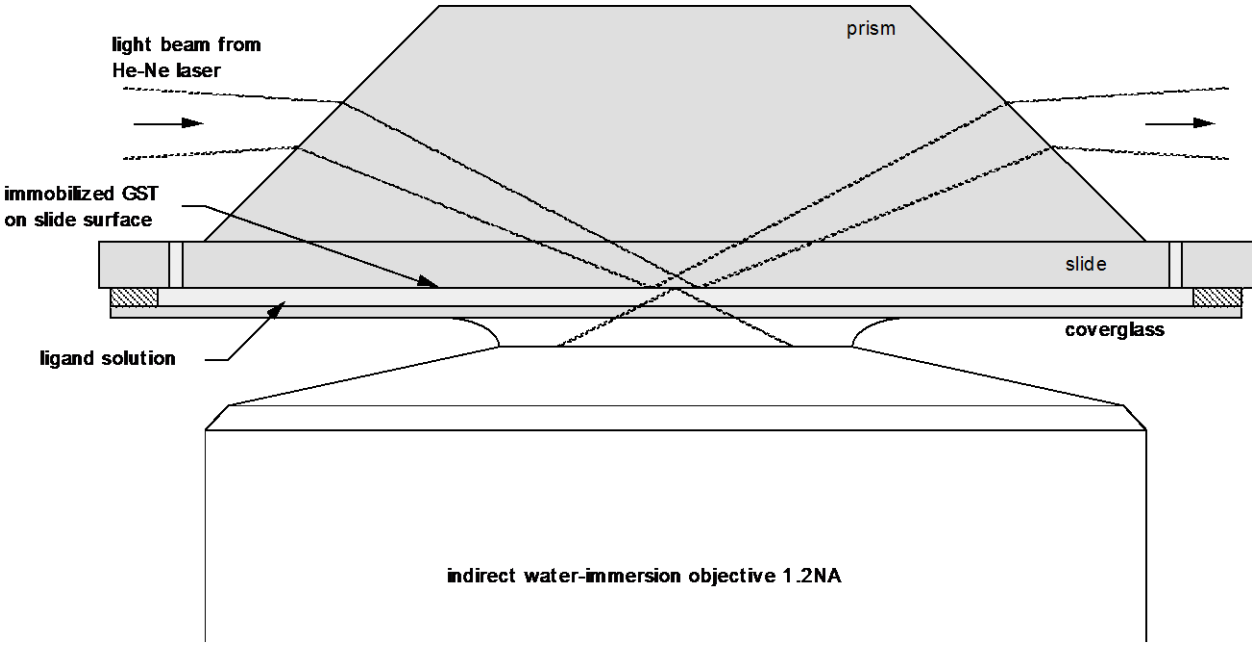

Figure 1.4: The prism TIRF setup used in our single-molecule kinetics experiments. A 633nm He-Ne laser is used to excite fluorescent ligands as they are binding immobilized GST in the evanescent field at the interface of the fused silica slide and the ligand solution.

based systems tend to generate a cleaner fluorescence signal with lower fluorescent background.

The polarization of the evanescent wave depends on the polarization of incident light. If s-polarized light is used, perpendicular to the plane of incidence, the electric field vector remains perpendicular to the plane of incidence. If p-polarized light is used, polarized in the plane of incidence, the evanescent field contains components that are normal to the substratum surface, and parallel to the surface.[56,57]

1.11 - Förster Resonance Energy Transfer

In addition to the two workhorses of structural biology, X-ray crystallography and NMR, there are optical methods that can be used for structural studies of biomolecules. One of these methods is called Förster Resonance Energy Transfer (FRET). FRET is used to study intramolecular distances and changes in these distances, and can be used to determine the dynamics of particular regions of a molecule.

An excited donor fluorophore can non-radiatively transfer energy and excite an acceptor fluorophore which then can emit a photon that can be detected. The rate of energy transfer depends on the distance between the fluorophores where faster transfer occurs at shorter distances. FRET also requires overlap of the emission spectra of the donor with the absorption spectra of the acceptor. FRET can be observed as acceptor sensitization or donor quenching.

FRET is commonly used to study dynamics and molecular motions of biomolecules. By labeling dynamic regions different levels of energy transfer, acceptor emission, will be obtained as the molecule moves and the distance between the fluorophores is changing. R_0 is the Förster

radius, the distance between the donor and acceptor generating 50% energy transfer. The FRET efficiency (E_T) at a known distance can be used to calculate acceptor-donor distance R_{DA}.

$$E_T = \frac{1}{1+\left(\frac{R_{DA}}{R_0}\right)^6} \quad \text{(Eq. 1.5)}$$

Where the FRET efficiency (E_T) depends on the rate of energy transfer (k_{ET}), the rate of non-radiative decay (k_{NR}) and the rate of fluorescence (k_F).

$$E_T = \frac{k_{ET}}{k_{NR}+k_F+k_{ET}} \quad \text{(Eq. 1.6)}$$

SM-FRET is therefore a suitable method to identify sample heterogeneity and can be used to find rare events that are hidden in the averages of ensemble measurements. This can be used to characterize kinetics and structural changes in non-synchronized systems such as motions associated with the activity of a biomolecule.[58,59]

Some features of a good fluorescent dye are brightness, photostability, conjugatability, size, low intensity fluctuation, and to be excitable and emitting photons of a visible wavelength. Cy3 and Cy5 is one of the most common FRET pairs with an R_0 of 60Å making it suitable for enzyme dynamics.[59,60]

1.12 - Protein Induced Fluorescence Enhancement

The quantum yield of a fluorophore is the number of emitted photons per number of absorbed photons. Since a fluorescent dye has an optimal conformation for maximum fluorescence, the conformation where the quantum yield is the highest, the quantum yield can sometimes be altered by changing the environment of the dye.

The quantum yield of some fluorescent dyes, like Cy3 and Cy5, are known to increase in close proximity to the surface of a protein generating a brighter fluorescent signal. Although this phenomena has been long known it has recently started to become referred to as Protein Induced Fluorescence Enhancement (PIFE).[61] The proposed mechanism for the increase in brightness is a stabilization of the fluorescent conformation of the dye in proximity to a protein surface. The method is sensitive enough to study binding kinetics. PIFE can be applied in the 0-40Å range and is therefore useful to study short distances not accessible with FRET.[61]

Heavy water (D_2O) is also known to increase the quantum yield of fluorescent dyes by decreasing the quenching due to vibrational coupling between dye and solvent. D_2O is heavier than water and has lower vibrational frequencies which result in the decrease in quenching.[62] The PIFE signal can therefore be enhanced by replacing water with D_2O.

1.13 - Fluorescence Correlation Spectroscopy

Both translational and rotational diffusion depend on the radius of the molecule. As a consequence the diffusion constant of a small molecule will decrease as it is binding to large molecule. This can be used in Fluorescence Correlation Spectroscopy (FCS) to learn about the binding kinetics of a molecule.[63]

FCS is not a single molecule technique as normally observed but still a powerful tool to study interactions of biomolecules. The average concentration of fluorescent molecules in a small observation volume of a sample is constant over time, but there will be small fluctuations in the number due to Brownian motion of the molecules in and out of the volume. Molecules will constantly diffuse in and out of the volume generating fluctuations in the detected fluorescence. It can be shown that for a Poisson variable, the mean square fluctuation is equal to the mean, therefore measuring fluorescence fluctuations can give an estimate of the average number of molecules being observed (N).

An autocorrelation function, *G(τ)*, can be used to analyze fluorescent fluctuations and extract information about molecular dynamic processes using detected fluorescence intensity *I(t)*, and fluctuations $\delta I(t)$ around the mean intensity *<I>*.[64,65]

$$G(\tau) = \frac{\langle I(t)I(t+\tau)\rangle}{\langle I\rangle^2} = \frac{\langle[\langle I\rangle+\delta I(t)][\langle I\rangle+\delta I(t+\tau)]\rangle}{\langle I\rangle^2} = 1 + \frac{\langle \delta I(t)\delta I(t+\tau)\rangle}{\langle I\rangle^2} \qquad \text{(Eq. 1.7)}$$

The decay of *G(τ)* is related to the diffusion coefficient of the molecule and the correlation when τ is zero*, G(0),* is related to the average numbers of fluorescent particles, *<N>,* in the excitation volume.

$$G(0) = 1 + \frac{1}{\langle N\rangle} \qquad \text{(Eq. 1.8)}$$

FCS can be used to excite fluorescent particles in solution (3D diffusion) or in a cell membrane (2D diffusion). Ideally, the laser beam has a 3D profile given by the Gaussian beam

equations derived by Kogelnik and Li.[66] Since the beam profile is non-uniform within the observation volume, the resulting weighting of the fluorescence affects the mathematical form of the autocorrelation.

$$G(\tau) = 1 + \frac{1}{\langle N \rangle}\left(1 + \frac{4D\tau}{w_0^2}\right)^{-1}\left(1 + \frac{4D\tau}{z_0^2}\right)^{-1/2} \quad \text{(Eq. 1.9)}$$

Where w_0 is the Gaussian beam radius at the focus and z_0 is the Gaussian beam depth-of-field. In the case of 2D diffusion, (where $z_0 \rightarrow \infty$), the equation can be simplified.

$$G(\tau) = 1 + \frac{1}{\langle N \rangle}\left(1 + \frac{4D\tau}{w_0^2}\right)^{-1} \quad \text{(Eq. 1.10)}$$

In both cases *G(0)* is decaying down to unity. By fitting *G(τ)* to the above relation, the diffusion coefficient (*D*) of the Brownian particles can be found.

$$D = \frac{w_0^2}{4\tau_D} \quad \text{(Eq. 1.11)}$$

The diffusion coefficient can together with Boltzmann's constant, k_B, the viscosity, η, and the temperature, *T*, be used to obtain the radius, *R*, of the fluorescent molecule.

$$D = \frac{k_b T}{8\pi\eta R^3} \quad \text{(Eq. 1.12)}$$

1.14 - Fluorescence Polarization

Fluorescence polarization can be used as an alternative way to obtain the binding constant of a ligand. A small molecule has a faster rotational diffusion coefficient than a large molecule. If a small fluorescent molecule binds to a larger molecule the depolarization of light due to rotational diffusion between excitation and emission will decrease. The difference in intensity between light parallel to the plane of incidence (I_{VV}) and light perpendicular to the plane of incidence (I_{VH}) can be used to calculate the fluorescence anisotropy (A). The fluorescence anisotropy at different concentrations of ligand can be used to construct a binding curve and extract a binding constant.

$$A = \frac{I_{VV} - I_{VH}}{I_{VV} + 2I_{VH}} \qquad \text{(Eq. 1.13)}$$

An example of a biding curve generated from the fluorescence anisotropy of a fluorescent ligand (Cy5-GS-hex) as it is binding GSTA1-1 can be seen in **Figure 1.5**.

1.15 - Photostability

Fluorescent molecules can undergo a number of processes that can transiently or permanently turn them non-fluorescent. Photobleaching is a photochemical alteration of a fluorophore that permanently renders it non-fluorescent. Singlet oxygen produced by photo-excitation of the fluorophore is the primary species reacting with the fluorophore and removing oxygen with an oxygen scavenger system can eliminate this particular reaction pathway.[59]

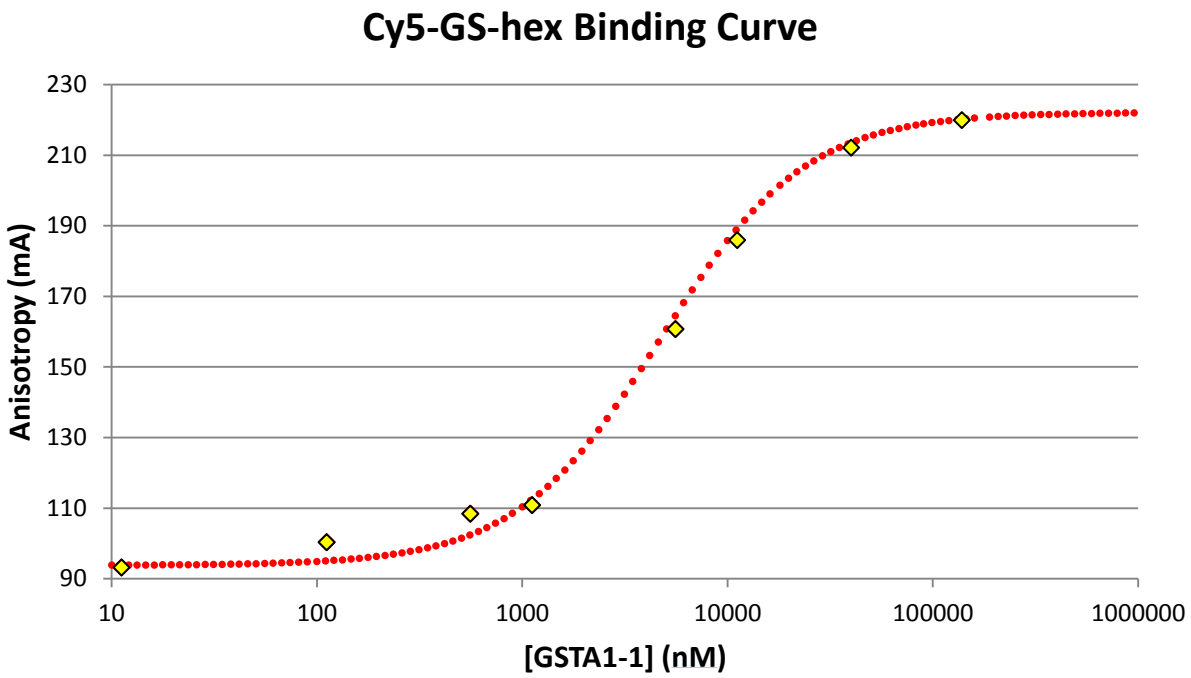

Figure 1.5: An example of a fluorescence polarization experiment where the fluorescent anisotropy increases as a fluorescent ligand (Cy5-GS-hex) bind GSTA1-1. The ligand concentration is fixed at 500nM while the concentration of enzyme is increased.

Glucose oxidase, Catalase and glucose (GOC) is one of the most common systems for deoxygenation (**Figure 1.6**) but protocatechuic acid and protocatechuate 3,4-dioxygenase (PDA/PCD) is another system that has gained more popularity lately.[67] Antioxidants like Trolox and Ascorbate are commonly added to prevent oxygen species reacting with the fluorescent dye. The antioxidants can also reduce a photo-oxidized dye and bring it back to a fluorescent state.[68,69]

There is a risk of using a highly efficient deoxygenation system. Dioxygen (O_2) in its ground state is a triplet that is an efficient triplet state quencher and removing oxygen can reduce the fluorescent signal by an accumulation of the triplet state of the dye. In addition to formation of a dark triplet state some antioxidants can at low oxygen concentrations reduce the fluorophore into the colorless and non-fluorescent leuco form of the dye. This is accomplished by reducing a double bond and breaking the conjugated system of the dye. The GOC deoxygenation system and the concentration of antioxidants have to be carefully tuned to maximize the fluorescent signal from the dye.

In addition to photobleaching many dyes can go into metastable states, which may be conformational isomers, or covalent adducts. These metastable states may be non-fluorescent or may have altered emission properties. There is an equilibrium between Cy5 isomers where approximately 50% of the Cy5 molecules can be expected to be in a weak fluorescent state. This has to be considered when setting up single molecule experiments.[64]

Cyanine dyes have strong absorbance, good quantum yields, good photostability, low pH sensitivity, and have been widely used in biological imaging since their spectral bands can be

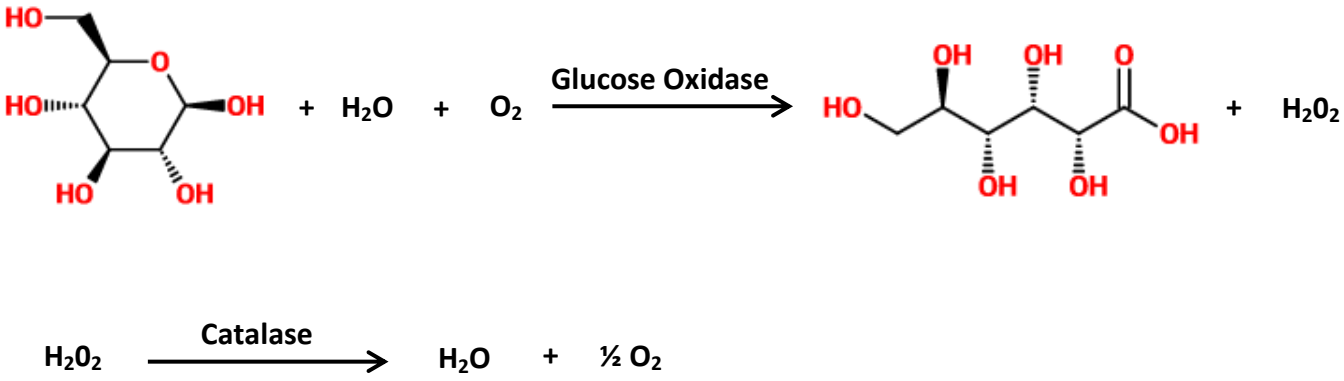

Figure 1.6: The Glucose Oxidase Catalase reaction showing the process of deoxygenation. In my experiments 7µg/ml Glucose Oxidase and 1.5µg/ml Catalase was added to the sample buffer together with 0.8% glucose.

tuned across the visible spectra by varying the polymethinic chain connecting the end groups. The polarity of the solvent has a low effect on cyanine dye isomerization while high viscosity slows down the isomerization rate. Adding substituents to the dyes will increase the fluid resistance and thereby decrease the isomerization rate.[64,70]

1.16 – Double Electron-Electron Resonance

A non-optical ensemble method that can be used to study intramolecular distances, and thereby used to obtain information about the structure of a biological molecule, is Electric Paramagnetic Resonance (EPR). EPR is spectroscopic method similar to NMR but electron spins are excited instead of the spins of the atomic nuclei.

One type of EPR called the Double Electron-Electron Resonance (DEER) is particularly useful to study distance distributions in protein structures.[71,72] Similarly to FRET a protein can be labeled with two probes to determine the distance between the labeling sites. In a DEER experiment two unpaired electrons are introduced through site directed spin labeling (SDSL). DEER is a pulsed experiment where a microwave pulse is used to align the magnetization vector. Fourier transformation of the emitted microwave signal is used to obtain the EPR spectra. The change in peak intensities as a ligand is introduced in to the system can be measured.[73] Just like FRET DEER provides the distance distribution and not only an average distance.

1.17 - Significance

There is no general theory for the stability and specificity of binding sites in proteins, and this is an area of much current research.[74,75,76] The broad substrate specificity and functional flexibility of GSTA1-1 makes it an excellent candidate to study protein heterogeneity. The main reason why we are studying GST is the collective evidence suggesting the possibility of multiple conformations existing simultaneously within a population of enzymes, as multiple conformers, and potentially undergoing interconversions. From the specific activity of GSTA1-1 with CDNB the average time for a catalytic conversion can be calculated to approximately 50ms, and we would expect that the binding and dissociation of a ligand would occur on the same time scale.

GST is a very abundant protein with many different biological functions. Further characterization of GST will not only increase our knowledge in protein heterogeneity and enzymatic detoxification, but also has many potential applications in biotechnology and medicine. For example, there are agricultural applications for GST such as drug resistant plants that would enable selection for specific crops. Another potential application is constructing bio-sensors where GST could be used to detect toxic compounds.[77] It has been speculated that bacteria can be genetically designed to degrade toxic and carcinogenic compounds.[13]

GST levels are elevated in many types of cancers and in liver and kidney disease and can be used as a marker for diagnostics of disease.[78] Development of sensitive detection systems for these enzyme markers would be useful for the diagnosis of early stages of disease.[79]

GSH is the major endogenous antioxidant of the cell decreasing the levels of reactive oxygen species (ROS) and protecting the cell from damage. Unfortunately a high GSH

concentration is an advantage for a cancerous cell since it lowers the level of ROS that would normally kill rapidly dividing cells.[80] Manipulating GSH activity, which is obviously related to GST activity, specifically in a particular cell type could restore ROS levels. In a similar manner tuning GST activity could prevent detoxification of chemotherapeutics or used to activate a prodrug.

GST is involved in detoxification of carcinogenic metabolites and chemotherapeutic agents like Thiotepa and Busulfan.[81] The GST dependent decrease in concentration and lifetime of the administrated drug makes dosing difficult. This property can however be circumvented and used as an advantage. GST can be utilized as a pro-drug activator in treatment of cancer. One example is the GST catalyzed conversion of Azathioprine to 6-mercaptopurine (6MP) and a glutathione-imidazole conjugate. The purine analogue 6MP is active against tumors by inhibiting purine utilization. Since 6MP also suppresses the immune system Azathioprine has been most widely used to prevent rejection during transplantations.[82]

1.18 - Summary of Thesis Research

Recent work studying the dynamics of GSTA1-1[11,27,] and the promiscuity of the enzyme suggests the existence of more than one conformational population.[83,84] The traditional methods of structural biology are limited in their ability to study protein heterogeneity and novel approaches are necessary to deepen our understanding in this area. GSTA1-1 has to our knowledge never before been characterized using single molecule imaging techniques. We have employed a wide repertoire of single molecule imaging and optical techniques for thorough biophysical characterization of the enzymes properties.

This thesis shows that GSTA1-1 ligands can be fluorescently tagged and still maintain high affinity for the enzyme (Chapter 2). These fluorescently tagged ligands express binding statistics corresponding to more than one binding state suggesting the existence of multiple conformers (Chapter 3). We have also used a new method to confirm that the C-terminal is adopting a different conformation as a ligand occupies the active site (Chapter 4).

Chapter 2 – Synthesis of Fluorescent hGSTA1-1 Ligands

2.1 – Introduction

There are several possible approaches to observe the state of individual GST molecules: fluorescent ligands, fluorescent substrates, fluorescent tags on the enzyme, or a combination of these different approaches. I have in my thesis research tested and evaluated all of these methods. Whether to fluorescently label a GST ligand or GST itself depends on what question we are trying to answer and what experiment is being conducted. One of the main objectives in my work is to study GST in action, as it is conjugating GSH to a hydrophobic substrate.

In an attempt to identify and characterize different conformational sub-populations of GSTA1-1 a suite of fluorescent ligands has been constructed. These fluorescent ligands can be used in single-molecule imaging experiments to measure the occupancy time of a single ligand to a single dimer. If there are different groups of occupancy times identified these are likely to correspond to different conformational populations.

2.2 - GST Ligands

One approach to observe binding-site occupancy statistics is to use a fluorescent ligand. With GSTA1-1's broad substrate specificity there are a variety of ligands that can be used and modified for single molecule imaging.

In some initial trials the binding and conjugation of the fluorogenic GSTA1-1 substrates bromobimane and 4-chloro-7-nitrobenzofurazan (NBD-chloride) were studied.[19,90] The bimane adduct was excited by a 405nm near-UV laser, but unfortunately the background fluorescence from the glass slide was high at this wavelength and the experiment had to be abandoned. NBD

was studied using a fused silica slide, which slightly reduced the fluorescent background, but the NBD-chloride GSH conjugate (GS-NBD) was quenched upon binding to GST and was not suitable to study binding. The fluorescence of 50µM GS-NBD decreases when GST is added (**Figure 2.1**). The quenching can be disrupted by adding the competing ligand S-hexyl glutathione (GS-hex) which displaces GS-NBD and restores the fluorescence intensity to some extent (**Figure 2.2**). GS-hex has high affinity for GSTA1-1[25] (70nM) and the fact that 100µM GS-hex cannot restore the fluorescence of GS-NBD completely suggest that GS-NBD has very high affinity for the enzyme as well. A ligand that loses fluorescence intensity upon binding to GST was considered unsuitable for single-molecule experiments and an alternative ligand had to be found.

Since no high affinity fluorogenic substrates were identified an alternative approach had to be used where a well characterized high affinity ligand is fluorescently tagged. Adding a fluorescent tag will most likely decrease the ligand's affinity somewhat, but we predict it should still be high enough for our applications. In support of this approach we know that GST is commonly used as a fusion protein to facilitate protein purification. In the S-hexylglutathione agarose resin (Sigma) S-hexylglutathione (GS-hex), a high affinity GST ligand, is linked to agarose beads through an alkane linker. The linker is attached to the N-terminal of GS-hex. Since this resin has very high affinity for GST a high affinity GSH-conjugate with a fluorescent dye linked to the N-terminal should behave similarly.

There are a variety of GSTA1-1 ligands that could be fluorescently tagged and used to study binding to the enzyme. To be able to study the rate at which GSTA1-1 conjugates GSH to an electrophilic substrate, GSH would have to be fluorescently labeled. Many GSH conjugates

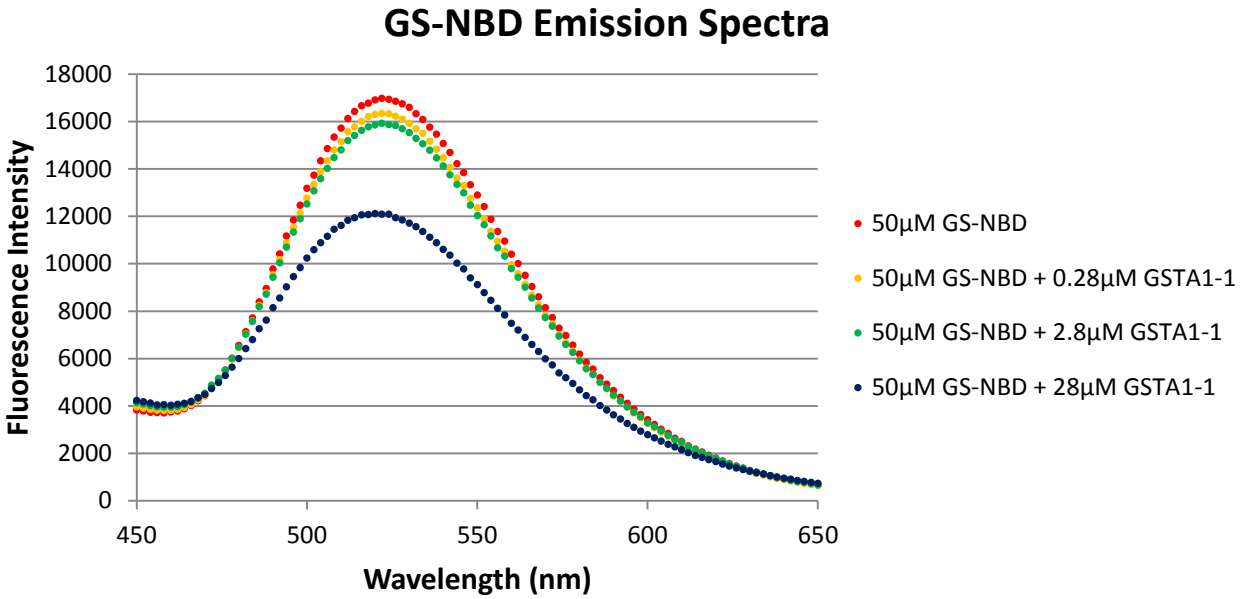

Figure 2.1: The quenching effect of GS-NBD binding to GSTA1-1. The fluorescence intensity decreases with higher concentrations of GST since a larger fraction of the ligand is bound to the enzyme. This ligand is not well suited for single-molecule experiments since a ligand has to maintain its fluorescence when it binds to the enzyme.

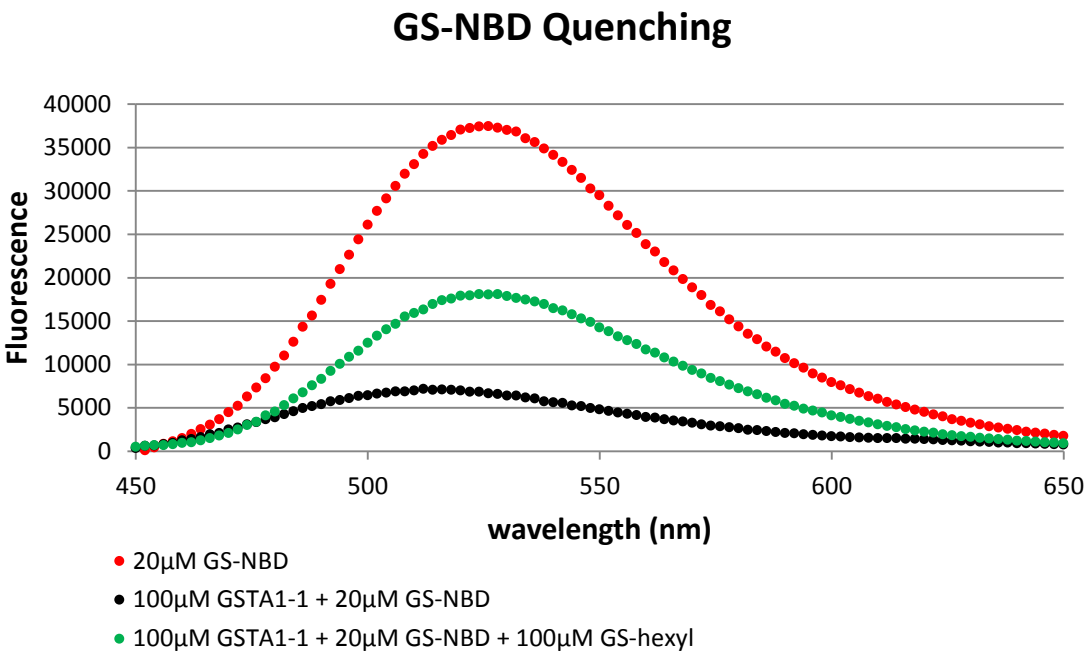

Figure 2.2: The quenching of GS-NBD by GST can be disrupted by addition of GS-hex. GS-hex has high affinity for GSTA1-1 and the fact that 100µM GS-hex cannot restore the fluorescence completely suggest that GS-NBD must have high affinity for the enzyme as well.

are known to have a higher affinity to GST than GSH alone. With this in mind GS-hex and S-dinitrobenzyl glutathione (GS-DNB) were also fluorescently tagged. GS-hex and GS-DNB are both the result of a substitution reaction but the GSTA1-1 is capable of using other reaction mechanisms as well. GSTA1-1 conjugates ethacrynic acid to GSH through an addition reaction and studying the GS-EA might reveal reaction dependent binding properties. There is a stereocenter in the GS-EA conjugate and GSTA1-1 produces different quantities of the stereoisomers.[91] GSTP1-1 only produces isomer A and can be used to enzymatically produce one enantiomer.[91]

2.3 - Types of ligands

I have used the cyanine dyes Cy3 and Cy5 as tags for my fluorescent ligands due to their high molar extinction coefficient and quantum yield. The disulfonated dyes were used since they are more water soluble and less prone to dye-stacking interactions, and therefore better suited for biological applications. To enable conjugation to the N-terminal amine of GSH the active N-hydroxy-succinimidyl-ester (NHS-ester) of the dye was used. The commercially available dyes generally have a hexyl linker between the head group of the dye and the reactive NHS-ester which generates a fluorescent tag that is at least somewhat spatially separated from the ligand. The molar extinction coefficient for sulfo-Cy3-NHS is $162000M^{-1}cm^{-1}$ and $271000M^{-1}cm^{-1}$ for sulfo-Cy5-NHS (Lumiprobe Corporation).

Despite the close proximity of the active sites in GSTA1-1 the Cy5-ligands are not quenched upon binding to GSTA1-1 (**Figure 2.3**). This result suggests that Cy5-labeling of high

affinity GST ligands is superior to the conjugates of a fluorogenic substrate and GSH previously tested.

The cyanine dyes are large compared to GSH and will most likely to some extent interfere with binding and decrease the affinity to GST. The increased size of a labeled ligand will extend the number of non-favorable interactions that can occur between the ligand and the enzyme and work against tight binding. Using PyMOL to inspect the active site of GSTA1-1 (PDB entry 1K3L) revealed that there is not a lot of space in the active site to accommodate a cyanine dye. Due to the proximity of the two active sites of the enzyme dimer the dyes of two bound ligands would have to compete for the same limited space in the crevice in between the active sites (**Figure 2.3**). Further separating the dyes from the ligand, and thereby from the enzyme, with a longer linker might prevent this from happening. The standard hexyl linker is also quite hydrophobic and might not be optimal in the environment of the active site. To rest whether the linker itself interferes with binding a tetra-oxyethylene (P4) was conjugated to the N-terminal of GS-hex (**Figure 2.4**). Due to the difficulty of quantifying the colorless P4-GS-hex at low concentrations the ligand was never fully characterized. However, P4-GS-hex does inhibit the CDNB assay which validates that a ligand with an N-terminal substitution can bind the active site.

With the observed results of the P4-GS-hex linker in mind, an amine reactive Cy5 with an extended and more polar linker was synthesized by Dr. Brigitte Schmidt at Molecular Biosensor and Imaging Center, Carnegie Mellon University. In the extended linker, called P2, the hexamethylene chain has been extended with two PEG residues followed by an amide and the reactive NHS ester (**Figure 2.4**).

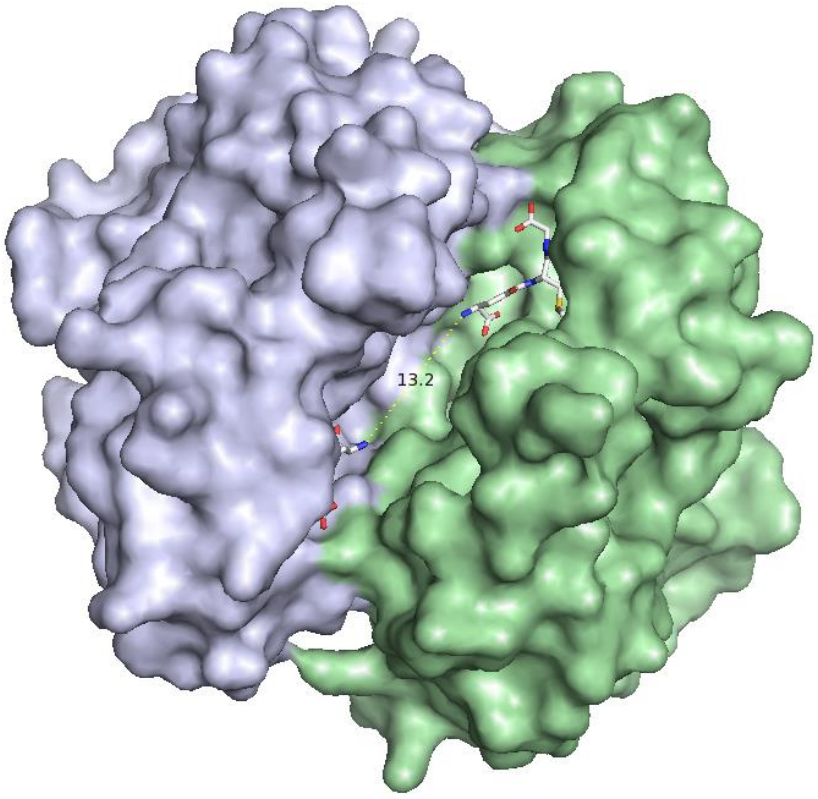

Figure 2.3: Space filled model of GSTA1-1 with two GS-hex bound (PDB entry 1K3L). The distance between the N-terminal amines of GS-hex to which the Cy-dyes have been conjugated is 13.2Å. The narrow crevice between the active sites that has to accommodate the fluorescent dye can also be seen in the structure. The narrow opening of the crevice suggests that a dye can only fit sideways, which might restrict intramolecular rotation and isomerization of the dye thereby increasing the quantum yield of the dye.

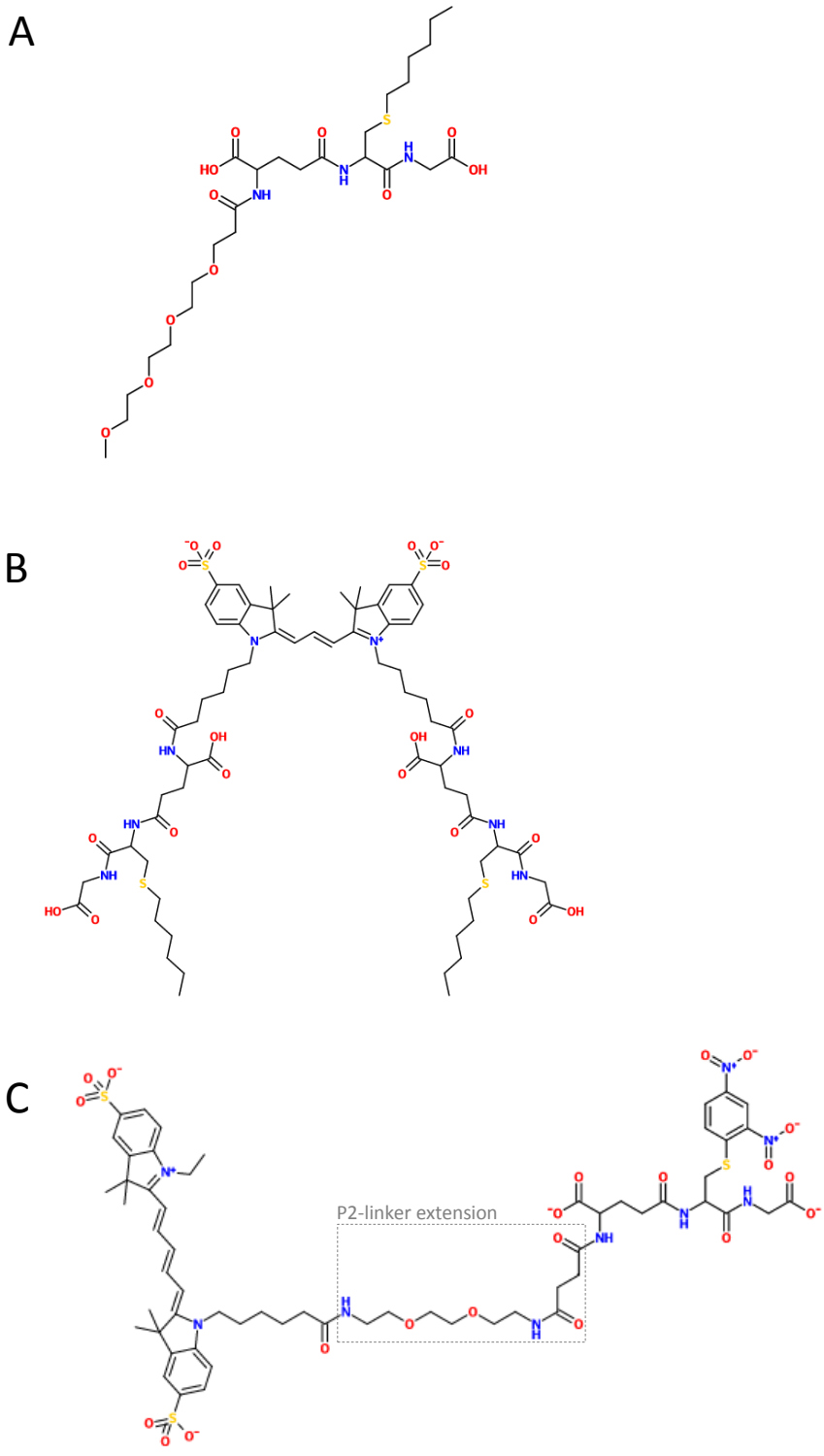

Figure 2.4: The chemical structure of P4-GS-hex (**A**), the bis-ligand Cy3-(GS-hex)$_2$ (**B**) and the longer linker ligand Cy5-P2-GS-DNB (**C**). The P2 extension of the normal hexyl linker is marked with a box.

The GSTA1-1 dimer has two active sites which can be occupied by ligands simultaneously.[11] The close proximity of the active sites can be taken advantage of by constructing a bifunctional ligand where two product inhibitors are linked by a fluorescent dye (**Figure 2.4**). Linking two ligands could increase the affinity of the conjugate by reducing the number of fluorescent tags to one, thus minimizing competition for the space between the active sites which should promote binding. Linking two ligands would also increase the local concentration of ligand as one side of the bifunctional ligand binds which will promote binding of the second ligand. Since both ligands must dissociate simultaneously for the bifunctional ligand to dissociate completely from the enzyme a greater binding affinity is expected.[18]

2.4 - Ligand labeling and purification

All the GST ligands were labeled using Cy3-succinimidyl ester or Cy5-succinimidyl ester in dimethyl sulfoxide (DMSO) with 1% N,N-diisopropylethylamine (DIPEA) as a H^+ acceptor at room temperature overnight. The reaction mixture is loaded on to a Sep-Pak® C18 desalting column (Waters Corporation) which retains the dye conjugate but not DMSO. The dye conjugate is eluted from the column in 50% acetonitrile (ACN) (**Figure 2.5**).

The labeled ligands were then purified with RP-HPLC using Waters Prep LC 4000 system with a Waters 2487 Dual λ Absorbance Detector and a µBondapak™ C18 10µm 125Å 19x300mm Prep Column. The purified ligand was verified and analyzed for purity with mass spectrometry using a Thermo-Fisher LCQ ESI/APCI Ion Trap in negative mode (**Figure 2.6**).

Cy5 labeling of GSH resulted in a mix of thiol and amine labeled product. Both products bind GSTA1-1 but since the thioester of glutathione and Cy5 no longer contains a thiol group it

cannot be used to study catalysis. Oxidized GSH (GSSG) was instead labeled to ensure 100% labeling of the amine. The doubly labeled GSSG was then reduced with dithiothreitol before HPLC purification.

Approximately half of the reactive NHS dye is hydrolyzed and not conjugated in a ligand labeling reaction and is eluted as a separate peak in the HPLC. Some dye is hydrolyzed in the reaction mixture before reacting with the amine of GSH, but the dye also hydrolyzes over time and some dye was likely hydrolyzed before the reaction was started. The eluted hydrolyzed dye can be collected and reactivated using *N*,*N*,*N*′,*N*′′-Tetramethyl-*O*-(*N*-succinimidyl)uronium tetrafluoroborate (TSTU). The reactivation is carried out in dry dimethylformamide (DMF) with 1% DIPEA. Reactivated dye is extracted in diethyl ether and dried. Mass spectrometry show that almost all dye has been reactivated. There might be some TSTU remaining in the dried reactivated dye but this should be eliminated after desalting and HPLC purification of labeled ligand.

Three different types of fluorescent GST ligands have been constructed and characterized: products, substrates, and bis-ligands. Labeled GS-hex and GS-DNB are product ligands since they are the result of a conjugation of GSH and a hydrophobic substrate. GSH has been labeled on the N-terminal and retains reactivity through its thiol. Labeled GSH is therefore classified as a substrate ligand. The bis-ligands are made using a bis-reactive Cy3 or Cy5 to link two product inhibitors. The bis-reactive dyes have been used to link two GS-hex or two GS-DNB. Amine reactive Cy5-NHS is available with and without the longer P2-linker and both forms of the dye have been used to label product and substrate ligands. Cy5-P2-NHS is monoreactive and cannot be used to construct a bis-ligand. The bis-ligands therefore all have the shorter

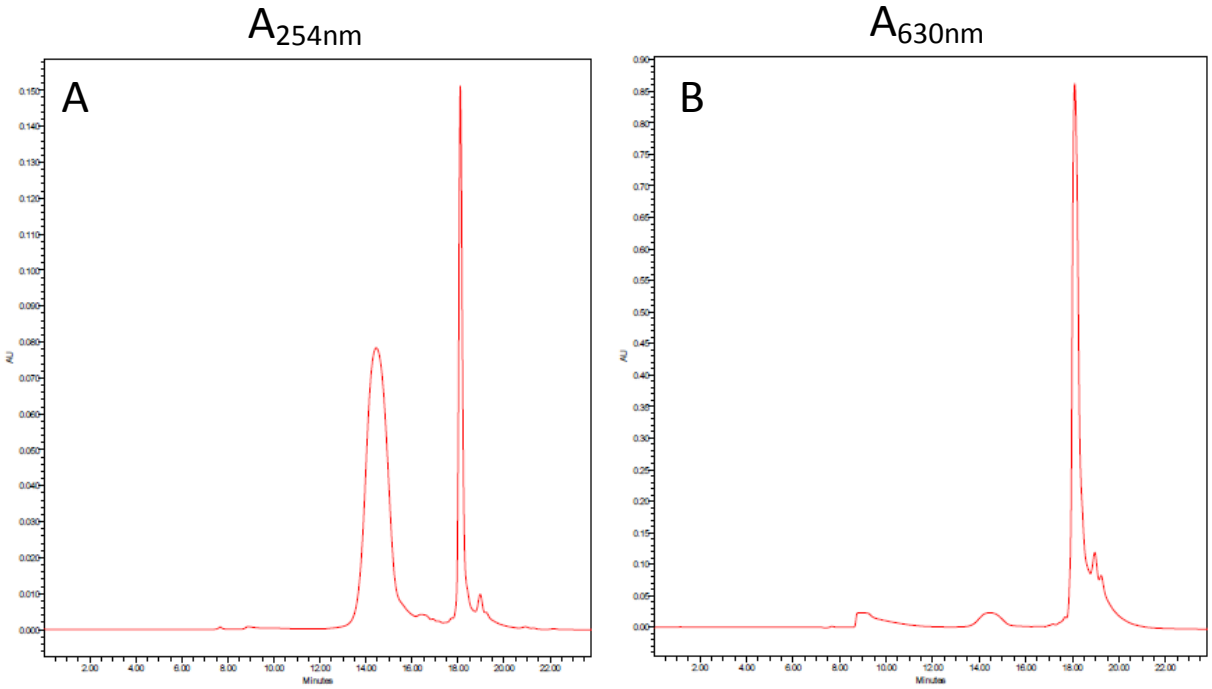

Figure 2.5: Chromatogram from HPLC purification of Cy5-GS-DNB with 254nm absorption (**A**) and 630nm absorption (**B**). The peak at 14min is representing GS-DNB, the peak at 18min is from Cy5-GS-DNB, and the peak at 19min representing hydrolyzed dye. The small shoulder of hydrolyzed dye peak might represent non-reactive dye isoform. The low fraction of hydrolyzed dye and the high peak from GS-DNB suggest that Cy5-NHS was not used in excess for this particular reaction.

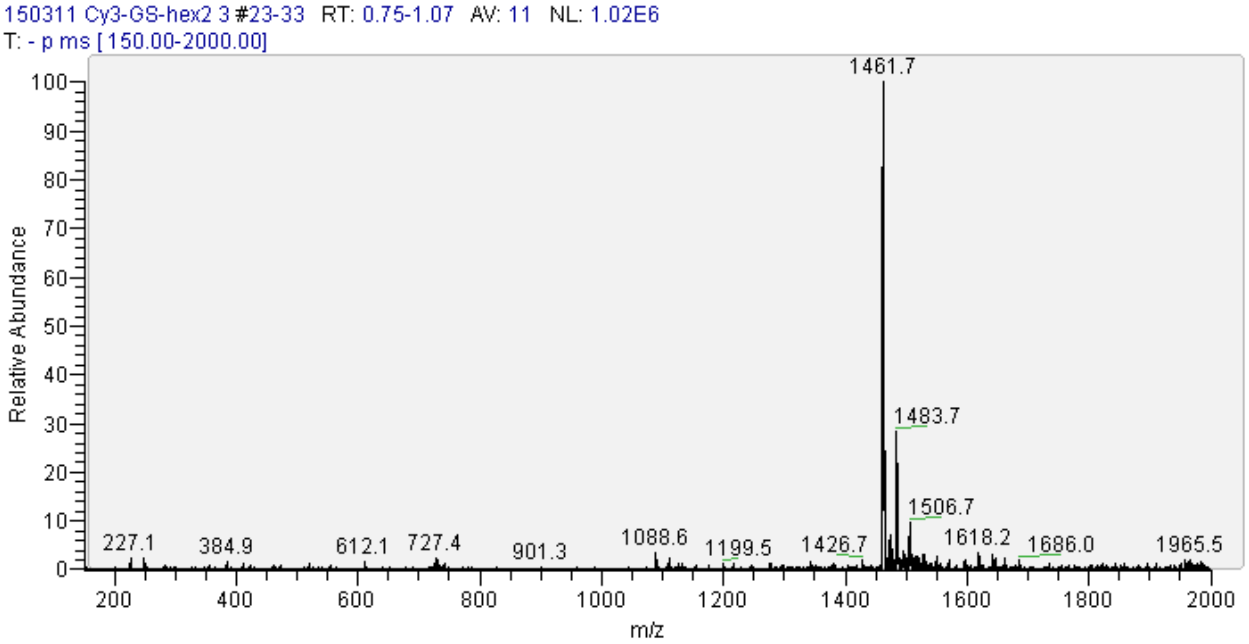

Figure 2.6: Mass spectra of Cy5-(GS-hex)$_2$ in negative mode. The major peak at 1461.7m/z represent the -1 ion of Cy5-(GS-hex)$_2$. A small peak for the -2 ion can be observed at approximately 730m/z. The sodium salt ions (+22m/z) of the conjugate can be observed as well.

linker. Cy3 is only available with the shorter linker so no Cy3-P2-conjugates have been constructed.

The following labeled ligands have been made and characterized: Cy5-GSH, Cy5-P2-GSH, Cy5-GS-hex, Cy5-P2-GS-hex, Cy5-$(GS\text{-}hex)_2$, Cy5-GS-DNB, Cy5-P2-GS-DNB, Cy5-$(GS\text{-}DNB)_2$, Cy3-GS-hex, Cy3-$(GS\text{-}hex)_2$. The general chemical structure of the ligands can be seen in **Figure 2.4 and 2.7**.

2.5 - Expression of Biotinylated GSTA1-1

To ensure that the different ligands bind to GST the enzyme has to be expressed and the ligand binding properties evaluated. To enable immobilization of the enzyme without interfering with the active sites it was engineered to carry a N-terminal biotin.

Biotinylated GSTA1-1 was expressed in *E. coli* C2992 (New England Biolabs) by heat shock co-transformation of a PKK-D plasmid containing the GSTA1-1 gene (*gsta1*) and a RSFDuet-1 plasmid containing the *E.coli* biotin ligase gene (*birA*). Both vectors are under the regulatory control of a *Lac* promoter and can be IPTG induced. The birA plasmid carries kanamycin resistance and the gsta1 plasmid ampicillin resistance enabling selection for co-transformed cells. The gsta1 encodes an N-terminal Avitag that BirA will biotinylate.[92,93] The protein was purified using a GS-hex agarose affinity column (Sigma-Aldrich) with gravity flow. To ensure that the co-expression of GSTA1-1 and birA had worked properly and that the purified GSTA1-1 was biotinylated the HABA assay[94] and a gel shift assay[95] with NeutrAvidin (Thermo) was used. Both assays confirmed GSTA1-1 had been successfully biotinylated.

A

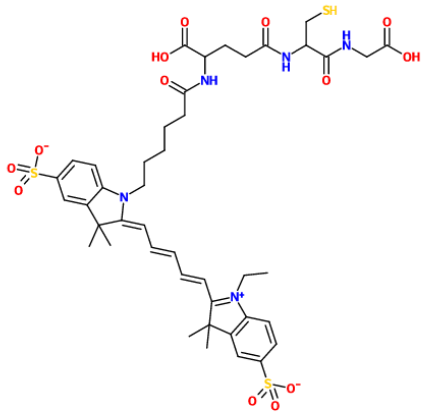

B

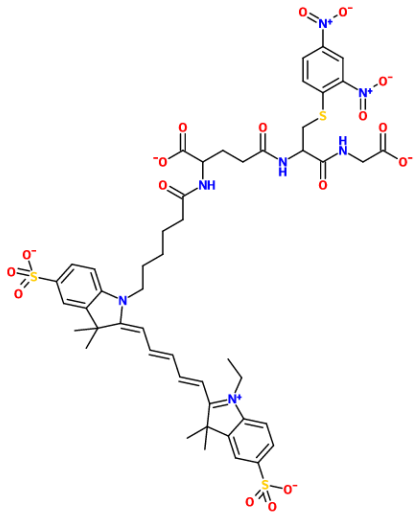

C

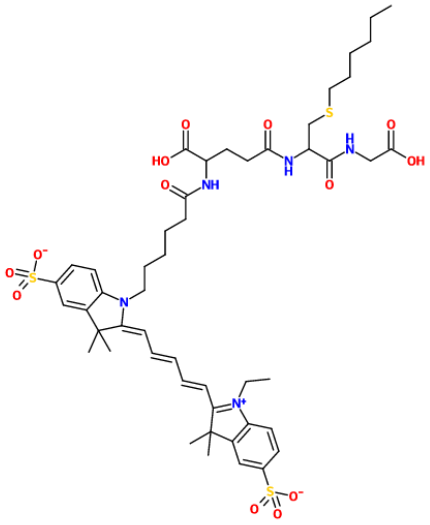

Figure 2.7: Chemical structure of Cy5-GSH (**A**), Cy5-GS-hex (**B**), and Cy5-GS-DNB (**C**). The relative size of the ligand and the dye can be seen in the structure.

Throughout this thesis GSTA1-1 refers to wild type GSTA1-1 where cysteine 112 has been replaced with a serine. The cysteine is surface exposed and can over time conjugate to electrophiles. Even if such conjugation has no effect on enzyme activity the possibility of having a chemically heterogeneous population of enzyme has to be eliminated.[27]

2.6 - Conjugation of labeled GSH

I am studying GSTA1-1 in an attempt to identify and characterize conformational subpopulations of the enzyme. If there are multiple conformations of the enzyme they are likely to have different activities towards a particular substrate. One important experiment to do is to image GST during conjugation of GSH to a hydrophobic substrate. This would reveal the kinetic properties of single enzymes as they catalyze a reaction. Since the GSH conjugates of the fluorogenic substrates are quenched upon binding this would require a fluorescently tagged GSH or hydrophobic substrate. GSH can be easily labeled on the N-terminal with an amine reactive dye. Labeling GSH would also be more efficient than labeling all of the different substrates that could potentially be conjugated with GSH. Another benefit of labeling GSH with a fluorescent dye instead of using a fluorogenic substrate is that a brighter fluorophore can be used which is beneficial in single molecule experiments. Extending GSH with a large fluorescent dye like Cy5 will most likely affect the catalytic rate of the enzyme, but my experiments show that GST is still capable of conjugating both Cy5-GSH and Cy5-P2-GSH to CDNB (**Figure 2.8**).

Conjugation of labeled GSH reveals some information about the structure of the active site during catalysis. The rate of conjugating Cy5-P2-GSH to CDNB is faster than that of Cy5-GSH suggesting that by separating Cy5 from the active site by using a linker restriction of catalysis is

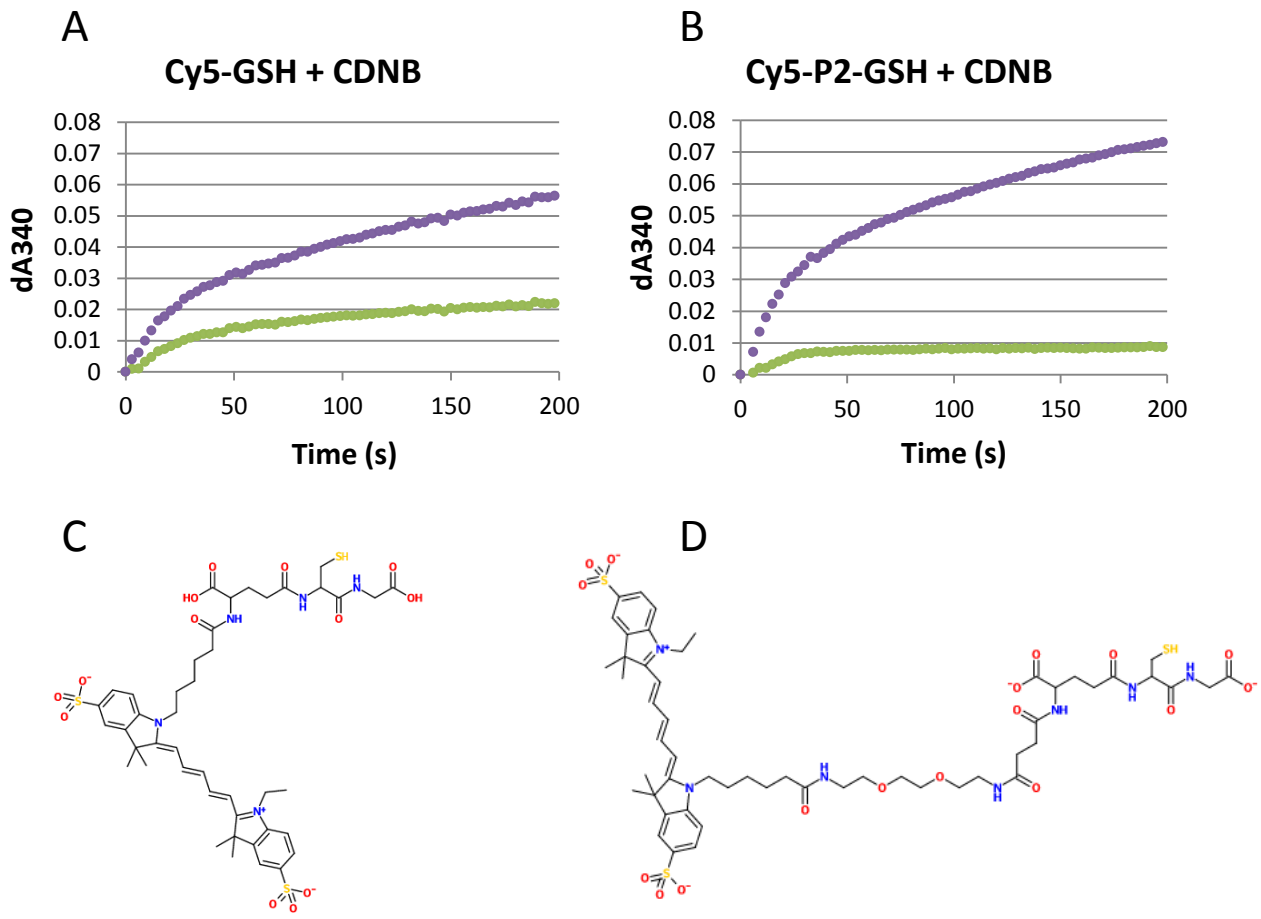

Figure 2.8: Non-catalyzed (green curve) and GSTA1-1 catalyzed (purple curve) conjugation of Cy5-GSH and CDNB (**A**), non-catalyzed and GSTA1-1 catalyzed conjugation of Cy5-P2-GSH and CDNB (**B**), chemical structure of Cy5-GSH (**C**), chemical structure of Cy5-P2-GSH (**D**).

somewhat prevented. The enzymatic rate with labeled GSH, however, is still much slower than that of non-labeled GSH implying that Cy5-labeling is restricting the access to the active site (**Figure 2.9**). Despite this, GST is capable of conjugating a labeled GSH to CDNB which should enable single molecule analysis of such an event.

2.7 - Ligand Binding to GST

A number of experiments were performed to investigate how a labeled ligand is affected by binding to GST, more specifically to ensure the ligand stays fluorescent and is not quenched like the fluorogenic substrates and their GSH-conjugates.

Unlike the previously tested substrates the fluorescence of Cy5-GS-hex was not quenched when binding GST, instead a slight increase in fluorescence can be seen. When adding GST to a fixed concentration of ligand there will be three different states of the enzyme: free enzyme, singly occupied enzyme, and doubly occupied enzyme. An approximate K_d of 500nM was used to calculate the fraction of enzyme in each state as the concentration of enzyme was increased (**Equation 2.1-2.4**). The total concentration of inhibitor in complex is described by *C*.

$$[I] + [sites] \leftrightarrow [C] \qquad \text{(Eq. 2.1)}$$

$$[C] = \frac{[I]_0+[sites]+K_d}{2} * \left(1 - \sqrt{1 - \frac{4[I]_0[sites]}{[I]_0+[sites]+K_d}}\right) \qquad \text{(Eq. 2.2)}$$

$$[EI] = 2[E]_0 * \frac{[C]}{[sites]} * \left(1 - \frac{[C]}{[sites]}\right) \quad \text{(Eq. 2.3)}$$

$$[EI_2] = [E]_0 * \left(\frac{[C]}{[sites]}\right)^2 \quad \text{(Eq. 2.4)}$$

As the concentration of enzyme in proportion to the concentration of ligand was increased a small increase in fluorescence could be seen, even at the concentration at which most enzymes would be doubly occupied and most likely to quench the fluorescence of the ligand. At the higher enzyme concentrations almost all of the ligand should be bound to GST, and the increase in fluorescence became smaller (**Figure 2.10**). In conclusion Cy5-GS-hex is not quenched when binding to GST, and if anything the fluorescence was increased.

In a bulk experiment the enzyme and ligand concentration can be tuned to get a large fraction of doubly occupied enzyme. A possible explanation to why no quenching is observed in such an experiment, at a GST concentration where a large fraction of enzyme should be occupied by two ligands, could be that only one ligand is bound. Double occupancy of a fluorescently labeled ligand could be sterically hindered resulting in strong negative cooperativity where two ligands will never bind.

Another interesting observation is a red-shift in the absorbance of Cy5-GS-hex as it binds GST (**Figure 2.11**). This further supports previous results where the physical properties of the dye change as a result of the environment. The increase in emission intensity observed upon binding to GST could be a result of less dye isomerization as it is confined to the limited space around the active site. This would, however, not explain the absorbance red shift

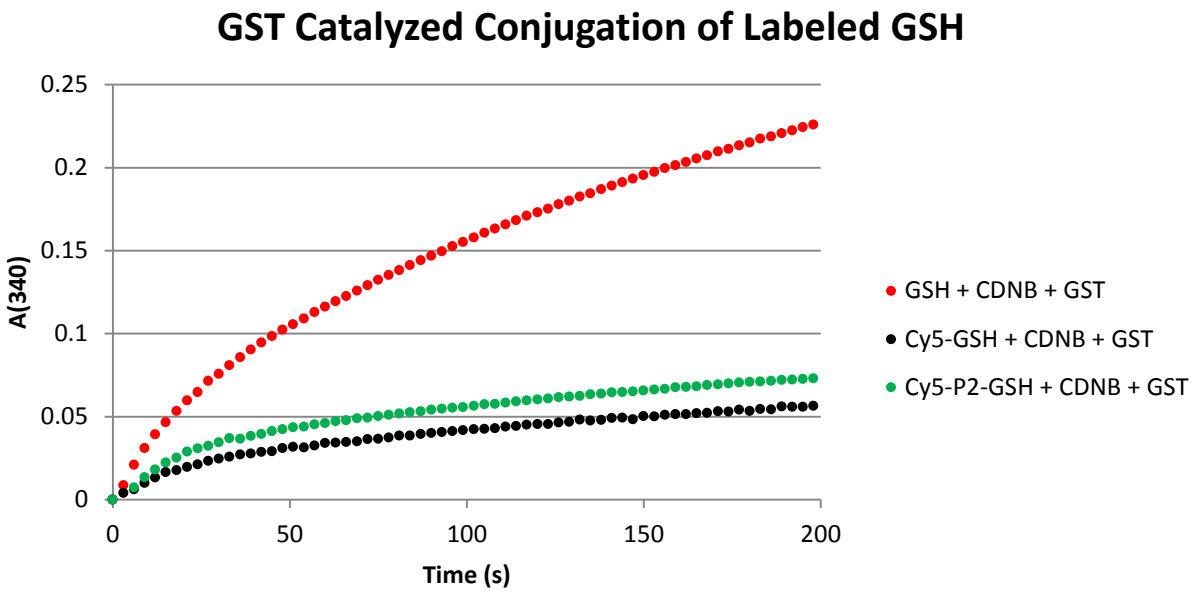

Figure 2.9: Rate of GST catalyzed conjugation of GSH, Cy5-GSH and Cy5-P2-GSH to CDNB. GST can conjugate Cy5-P2-GSH to CDNB faster than Cy5-GSH due to the longer linker separating the dye from the active site. The conjugation of Cy5-P2-GSH is still much slower than the conjugation to non-labeled GSH.

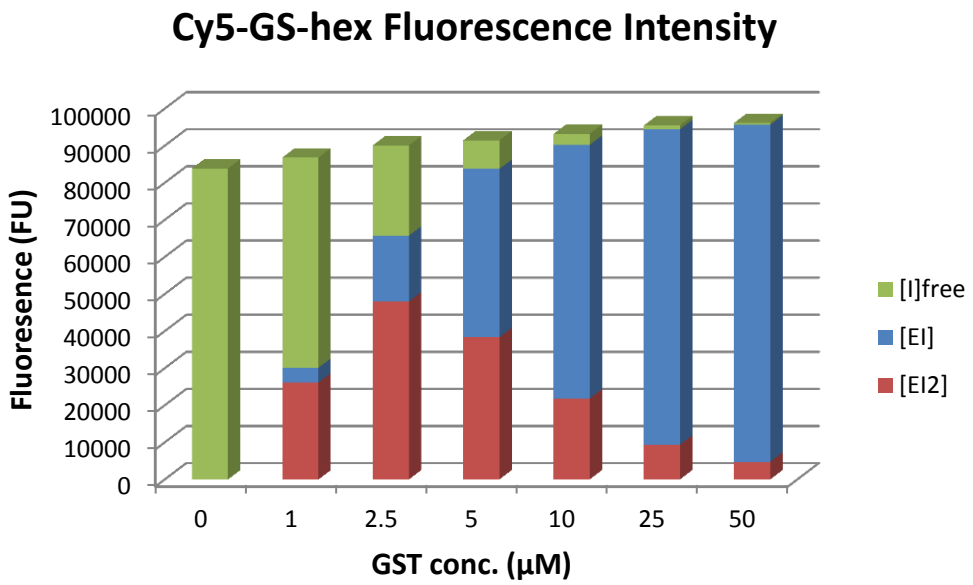

Figure 2.10: Fluorescence intensity and the calculated state of the ligand using 5µM Cy5-GS-hex assuming a K_d of 500nM. In the experiment 650nm excitation was used to measure the emission at 670nm. The fluorescence intensity increases when GST is added suggesting stabilization of a more fluorescent state of the dye which increases the quantum yield. No decrease in fluorescence due to quenching can be seen at any GST concentration, not even at the concentration generating the larges fraction of doubly occupied GST where two dyes are the closest to each other and should most likely to be quenched.

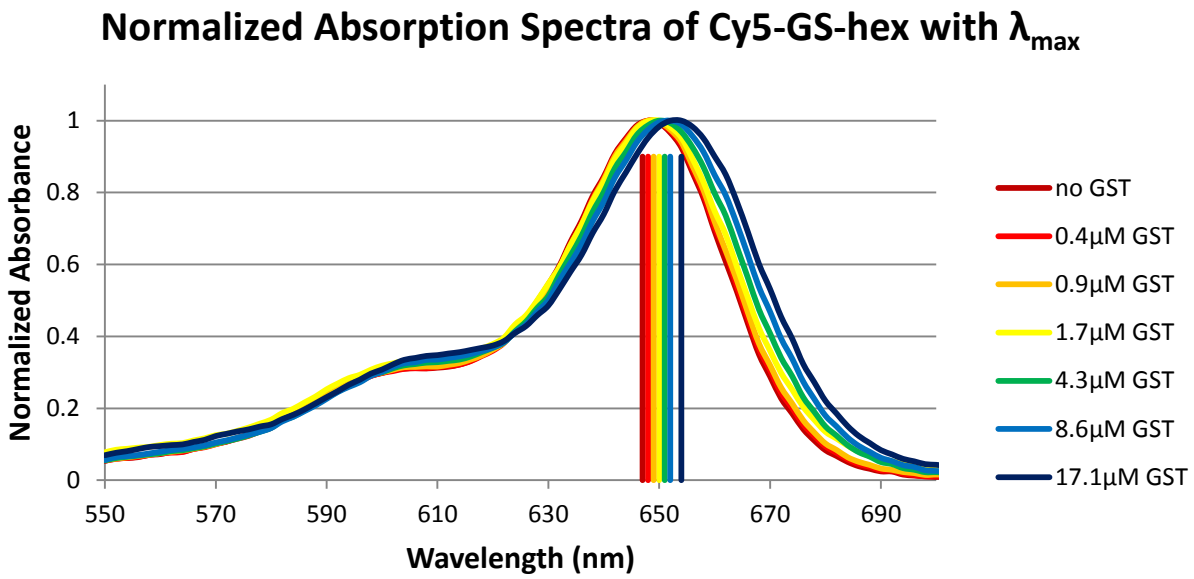

Figure 2.11: Shift in peak absorbance of Cy5-GS-hex (1.75uM) as it binds GST. The shift in peak absorbance increases with the fraction of ligand bound (higher GST concentration). The shift is likely a result of the change in environment the dye experiences as it binds the active site of the enzyme.

observed. The shift in peak absorbance is likely due to the change in environment. A combination of steric hindrance and a PIFE-like effect due to the charged or hydrophobic environment close to the active site is possible. It is possible that in a well calibrated system the degree of red shift or increase in fluorescence intensity can be used as a direct way to study binding.

2.8 - Characterization of Ligand Binding Through Inhibition of CDNB Assay

To further characterize the ligands their affinity towards GST was determined. A high affinity ligand is desired in single molecule experiments since a lower concentration can be used in order to reduce the fluorescent background in the sample.

The IC_{50} is the inhibitor concentration at which 50% of the non-inhibited reaction rate is obtained. The IC_{50} can be used to calculate the inhibition constant (K_I) of the inhibitor, which is the same as the binding constant (K_d) of the inhibitor. The observed IC_{50} depends on the concentration and binding constants of the substrates, which in this activity assay are GSH and CDNB. When inhibiting the CDNB assay the concentration and K_d of both CDNB and GSH have to be used to calculate K_I. The CDNB assay has traditionally been done at saturating substrate levels with 1mM GSH and CDNB. These concentrations are too high to obtain a large decrease in the catalytic rate upon addition of inhibitor. If the substrate concentration is decreased there will be a lower fraction of occupied binding sites, and the inhibitor is more likely to bind and block some percentage of those otherwise available sites. I have therefore used 100µM GSH and 100µM CDNB together with 45nM GSTA1-1 (**Figure 2.12**). The lower substrate concentrations increased the inhibitory effect of the inhibitor.

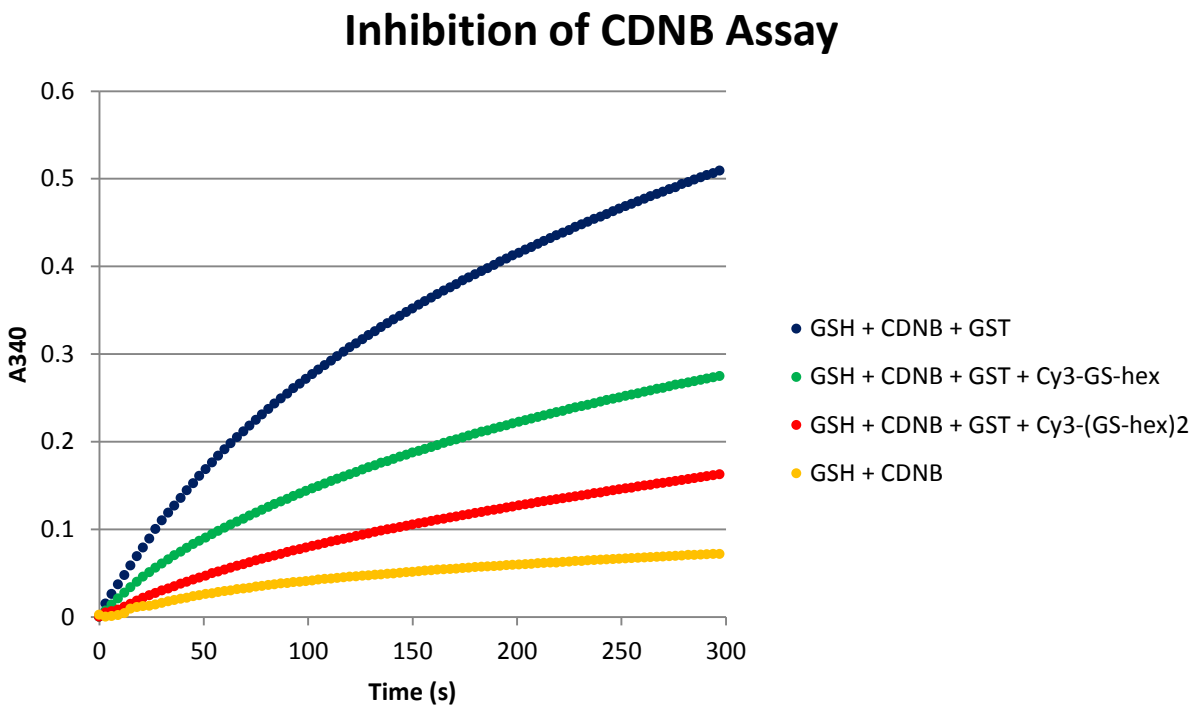

Figure 2.12: Example of GST ligands inhibiting the CDNB assay. Both Cy3-GS-hex and Cy3-$(GS\text{-}hex)_2$ have a strong inhibitory effect on the enzyme. The concentration of Cy3-GS-hex is 2.02µM and the concentration of Cy3-$(GS\text{-}hex)_2$ is 1.59µM. The non-catalyzed conjugation of CDNB and GSH is also displayed. The concentrations of GSH and CDNB are 100µM.

The equation for conversion of IC_{50} to K_I for a multisubstrate enzyme under steady state conditions is well-known.[96] The definition of the equilibrium constants (K_n) can be found in Appendix 1.

$$IC_{50} = K_I \left(1 + \frac{[A]}{K_1} + \frac{[B]}{K_3} + \frac{[A][B]}{K_3 K_4}\right) \quad \text{(Eq. 2.5)}$$

By rearranging the equation for fractional rate found in Appendix 1 the IC_{50} at any rate can be calculated from the non-inhibited rate (R_0), the inhibited rate (R), and the inhibitor concentration ([I]).

$$IC_{50} = \frac{[I]}{\frac{R_0}{R} - 1} \quad \text{(Eq. 2.6)}$$

The K_d of GSH can be found in literature[19] but only the K_M of CDNB has been reported[33]. K_M can still be used in the conversion of inhibitors IC_{50} to K_I. Since the K_M term contains the product dissociation rate (k_2) and the sum of the substrate on-rate (k_1) and off-rate (k_{-1}) it can be used as an upper limit for the calculated K_d. Especially since product release has been determined to be the rate limiting step in catalysis[11,29], and that term should be significant.

$$K_d = \frac{k_{-1}}{k_1} \quad \text{(Eq. 2.7)}$$

$$K_M = \frac{k_{-1} + k_2}{k_1} \quad \text{(Eq. 2.8)}$$

To ensure that Cy5 has no, or very low, absorbance at 340nm, which might influence the readout of inhibition assay, the absorption spectra of the assay components was obtained (**Figure 2.13**). Cy5 and Cy5-GS-hex shows very low absorbance at 340nm.

The K_I obtained from the inhibition of the CDNB assay is 67.8nM for Cy5-GS-hex, 40.7nM for Cy5-P2-GS-hex, 8.2nM for Cy5-$(GS\text{-}hex)_2$, 37.6nM for Cy5-GS-DNB, 12.7nM for Cy5-P2-GS-DNB, 15.9nM Cy5-$(GS\text{-}DNB)_2$, 65.1nM for Cy3-GS-hex, 4.2nM for Cy3-$(GS\text{-}hex)_2$ (**Table 2.1**).

The low inhibition constants obtained indicate very tight binding of the inhibitors. The bis-inhibitors express particularly high affinity for the enzyme. The type of dye used to label the ligand, Cy3 or Cy5, seems to have no effect on the affinity towards the enzyme since Cy3-GS-hex and Cy5-GS-hex have very similar affinity. It was speculated whether the slightly smaller size of Cy3 would interfere less with binding to GST, generating a higher affinity, but this does not seem to be the case. For the bis-inhibitor the type of dye used seems to have an effect on affinity. The dye has to bridge the two active sites and the length of the dye will determine if the two ends of the bis-ligand can simultaneously access the enzyme.

To ensure that Cy5 in itself is not affecting the activity of the GST hydrolyzed Cy5-NHS was added to the CDNB assay. The hydrolyzed Cy5-NHS has no inhibitory effect on the CDNB assay ensuring that the observed inhibition of a labeled ligand is caused by the ligand and not the dye (**Figure 2.14**).

When using the CDNB assay to determine the activity of GST a decrease in the catalytic rate can be observed over time as a result of product inhibition (**Figure 2.12**). It is therefore crucial to only use the initial rate, the rate before product inhibition becomes detectable, when determining the activity and the binding constant.

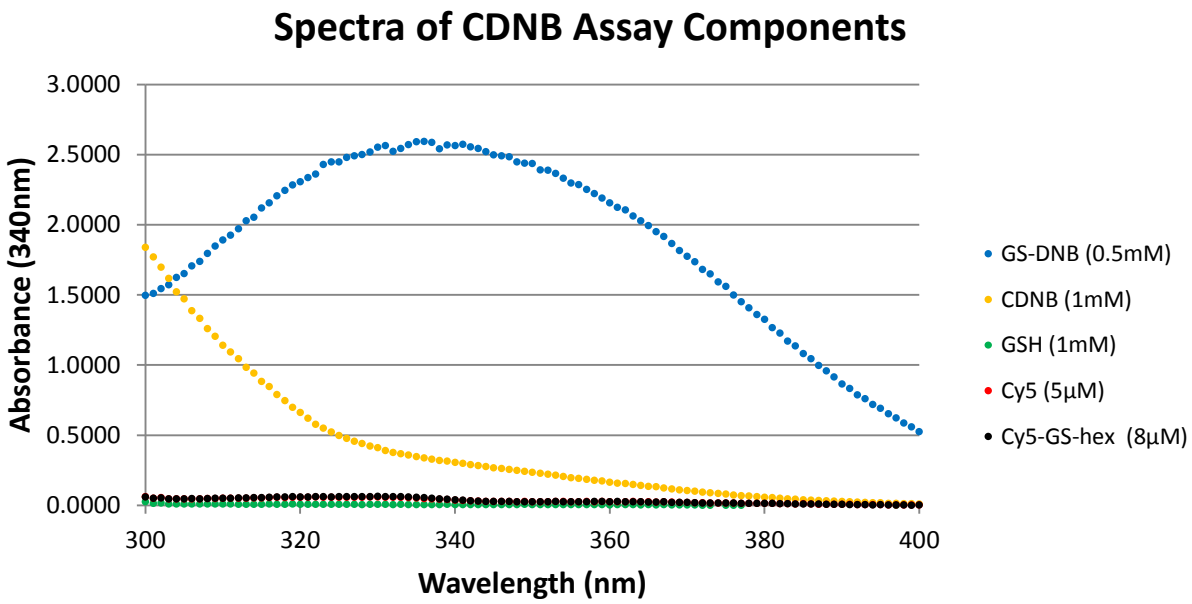

Figure 2.13: Absorption spectra of CDNB inhibition assay components to ensure that Cy5 has no significant absorption at 340nm. Only GS-DNB and CDNB have any significant absorbance at 340nm. The CDNB concentration is kept high and its contribution to the overall absorbance will not change when a fraction of it is converted to GS-DNB.

Table 2.1: IC_{50} and K_I of labeled GSTA1-1 ligands calculated from the inhibited rate of the CDNB assay. K_I was calculated using equation 2.4. The labeled ligands all show high affinity towards the enzyme. Ligands with the P2 linker have a slightly lower K_I than the same ligands with the shorter linker. The ligands expressing the absolute highest affinity are the bis-ligands.

Ligand	**IC_{50} (μM)**	**K_I (μM)**
Cy3-GS-hex	4.5	0.065
Cy5-GS-hex	4.7	0.068
Cy5-GS-DNB	2.6	0.038
Cy5-P2-GS-hex	2.8	0.041
Cy5-P2-GS-DNB	0.88	0.013
Cy3-$(GS\text{-}hex)_2$	0.29	0.0042
Cy5-$(GS\text{-}hex)_2$	0.57	0.0082
Cy5-$(GS\text{-}DNB)_2$	1.1	0.016

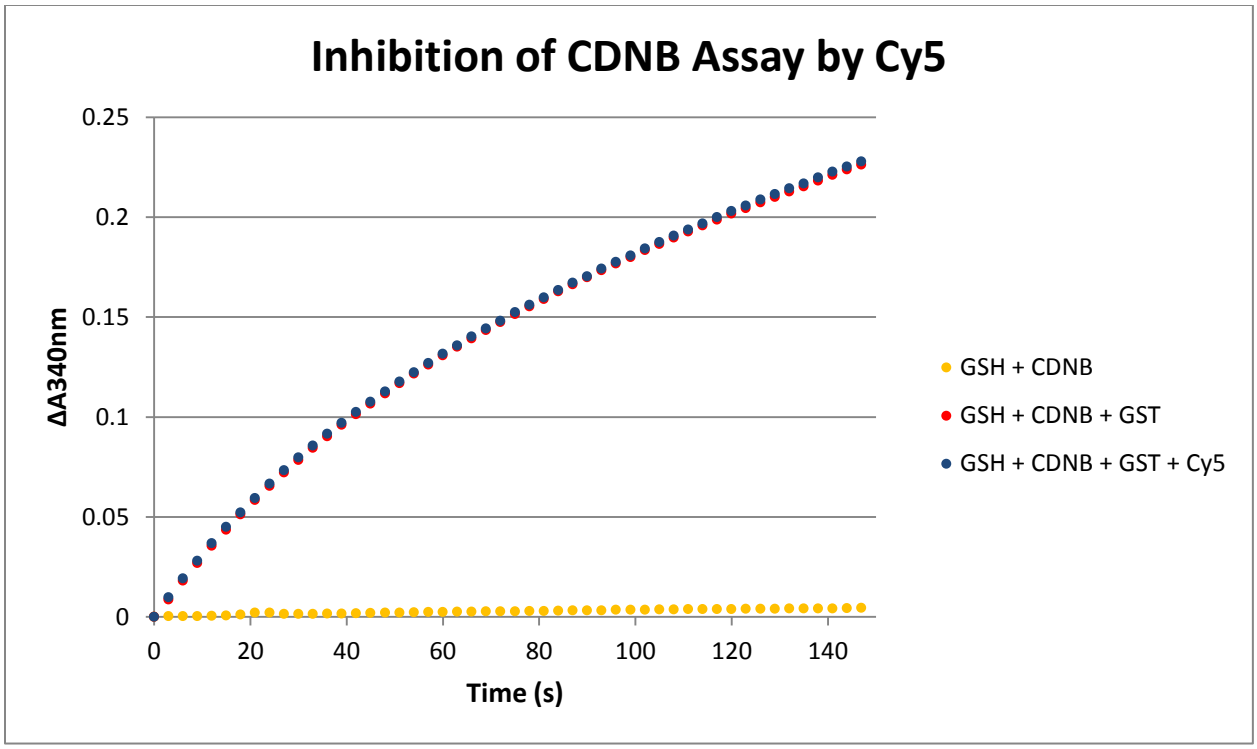

Figure 2.14: The inhibitory effect of 24.39µM hydrolyzed Cy5-NHS. The CDNB and GSH concentration in this particular experiment is 10µM instead of 100µM resulting in the lower non-catalyzed rate.

It is important to ensure that the fluorescently tagged ligands bind to the active site of GST and decrease the activity by preventing the substrates from accessing the active site, and not through allosteric effects. I will in the next chapter show that the binding of a fluorescently tagged ligand is competitive as its binding to GST can be restricted by the addition of a non-labeled ligand. This shows that the labeled and non-labeled ligand compete for the same binding site.

With the ligands exceptionally low inhibition constants it is possible that our conversion from IC_{50} to K_I is overcompensating for the substrate concentration results in a lower K_I. The conversion is based on independent binding of the two substrates. If this is not the case it might affect the calculated K_I.

2.9 - Characterization of Ligand Binding by Fluorescence Polarization

Fluorescence polarization was used as an additional way to confirm that a particular ligand was binding GSTA1-1. The polarization was used to calculate the fluorescence anisotropy at different ligand concentrations which were used to construct a binding curve from which a binding constant was extracted. The obtained K_d does not always match the K_d obtained from the inhibition assay. One reason could be an over-compensation in adjusting IC_{50} to K_d. The fluorescence polarization method has been useful to study the properties of labeled GSH. Since GSH is the substrate of GST, and not a product inhibitor which is occupying both the G-site and the H-site preventing catalysis, the CDNB inhibition assay cannot be used to obtain or compare observed binding constants.

In the general experiment a 200um flat capillary (Vitrotubes^{TM}) was filled with approximately 10µl sample, sealed with VALAP, and imaged using a Zeiss Axiovert 200 microscope with a 20x 0.75NA plan apochromat objective. Polarized light from a Sutter xenon illuminator was used together with a Cy5 filterset (Chroma HQ620/60x, Q660LP, HQ700/75m) and a rotatable analyzer (**Figure 2.15**). The polarized excitation defined the "V" axis, and the analyzer was therefore rotated 90° to obtain the "VV" or "VH" measurements. The intrinsic polarization selectivity of the microscope was obtained by measurement of the VH to VV ratio for free dye, for which the anisotropy should be low. After an image was recorded the analyzer was rotated and another image recorded so that the anisotropy of the sample could be calculated. The anisotropy was calculated for samples with constant ligand concentration and increasing protein concentration. The Cy5-ligands are expensive to make and have therefore only been made in small quantities. GST on the other hand is easy and cheap to express. This is the reason the enzyme concentration is varied and not the ligand concentration.

A binding curve was fitted to the data points using Equation 2.9 where *r* is the anisotropy and *n* is the Hill coefficient.

$$r = \frac{max \cdot [GST]^n}{K_d^n + [GST]^n} \qquad \text{(Eq. 2.9)}$$

The K_d obtained from the fluorescence polarization measurements, with non-cooperative binding, is 4.7µM for Cy5-GS-hex (**Figure 2.16**), 19.1µM for Cy5-P2-GSH, and 52µM for Cy5-GSH (**Table 2.2**). As a control the K_d of Cy5 was determined to be 125µM (**Figure 2.17**). Cy5 in itself might have low affinity towards GST, but this could in theory also be a result of a non-specific

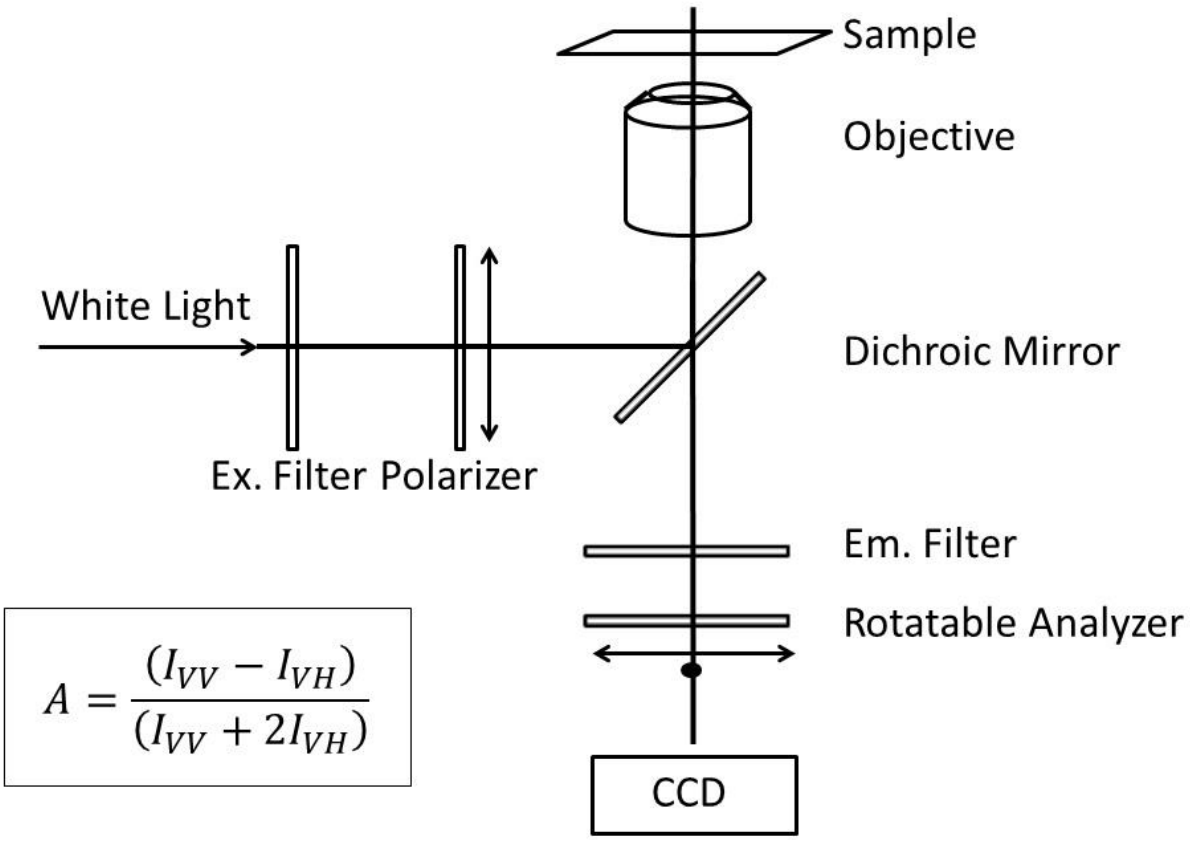

Figure 2.15: The fluorescence polarization setup used to obtain the fluorescence anisotropy. White light is passed through a Cy5 excitation filter, a polarizer, and reflected in a dichroic before reaching the sample. Emitted fluorescence passes through the same dichroic, a Cy5 emission filter, and a rotatable analyzer before reaching the CCD chip on the camera. The anisotropy (*A*) can be calculated from the intensity of emitted light parallel to excitation polarization (I_{VV}) and the intensity of emitted light perpendicular to the incident polarization (I_{VH}).

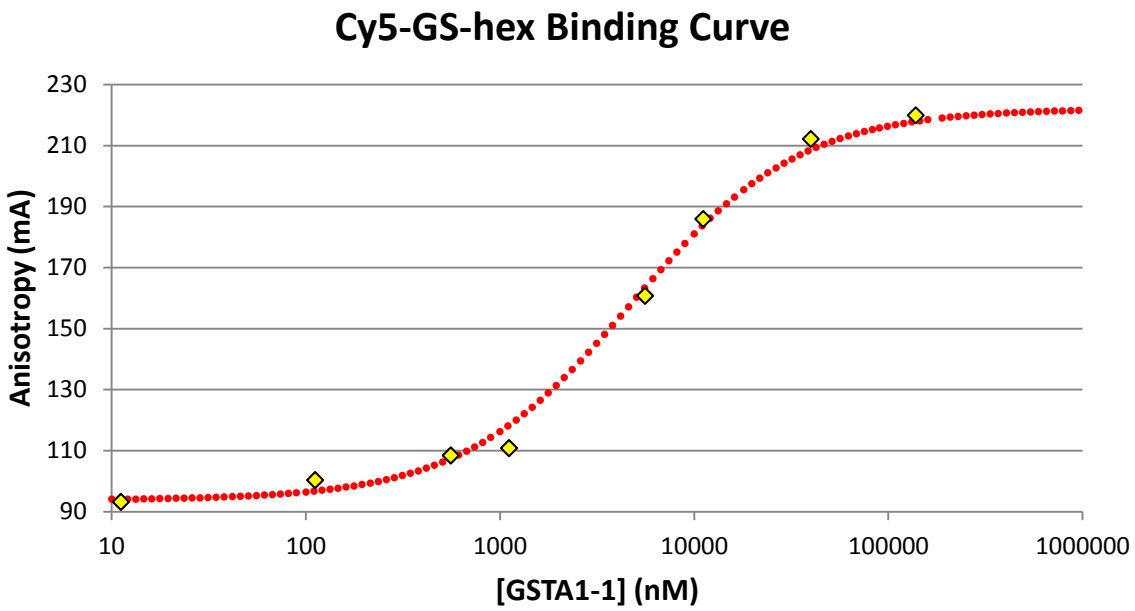

Figure 2.16: Fluorescence anisotropy binding curve of Cy5-GS-hex to GSTA1-1. The extracted K_d is 4.7µM for non-cooperative binding (n=1).

Tabel 2.2: The k_ds obtained from the fluorescence polarization experiments.

Ligand	k_d **(µM)**
Cy5-GS-hex	4.7
Cy5-GSH	52
Cy5-GSH + CDNB	42
Cy5-GSH + CDNB 20h	20
Cy5-P2-GSH	19.1
Cy5	152

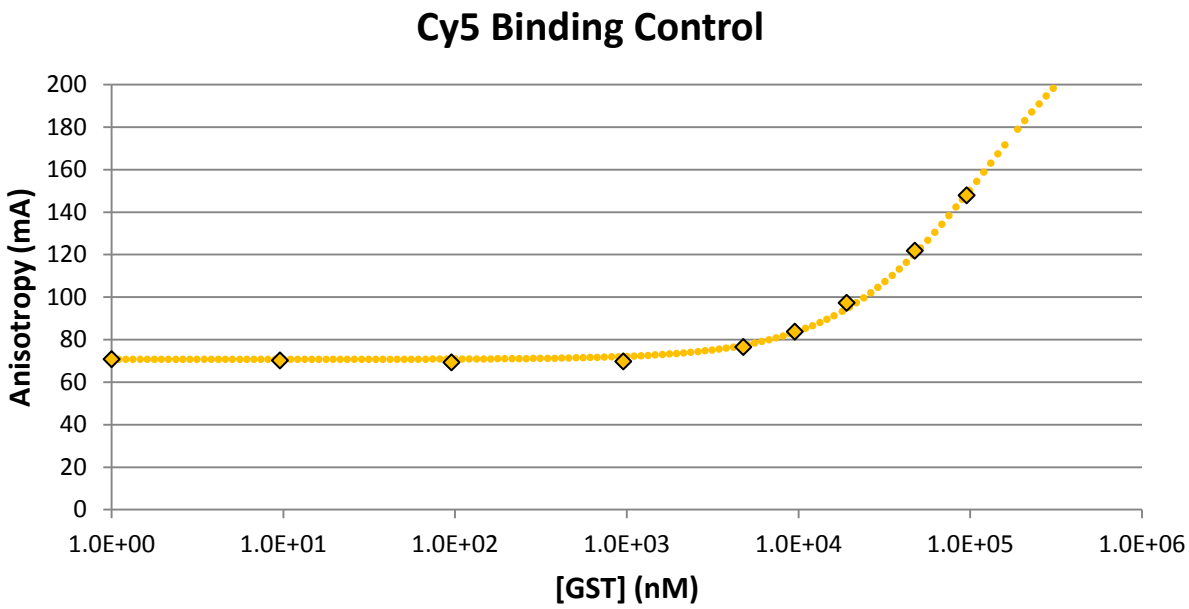

Figure 2.17: Fluorescence anisotropy binding curve of Cy5 to GST used as a control. A high concentration of Cy5 was used (500µM) which might contribute to the fact that any binding was observed. Non-specific interactions between Cy5 and the capillary will contribute to a decrease in free rotation and increase the observed anisotropy. Since a high concentration of Cy5 was used this effect should be stronger. The K_d was approximated to 125µM with non-cooperative biding (n=1) assuming the maximum anisotropy, needed for curve fitting, is the same as for Cy5-GST. This affinity is, however, very low compared to the other ligands suggesting that the effect of the dye interacting with the capillary is negligible.

interaction of Cy5 to the capillary restricting the rotation of the dye and therefore causing the anisotropy and K_d to artifactually increase. However, a non-specific interaction with the capillary should be independent of the enzyme concentration. The observed anisotropy is therefore more likely a result of a non-specific interaction between the dye and GST that does not affect the enzymatic rate of the enzyme. Cy5 has no inhibitory effect on the CDNB assay suggesting that the obtained K_d from the polarization experiment must be a result of other experimental factors than binding to the active site of GST. Since the combined effect of these factors is still very low, generating a high K_d representing a low affinity, these factors can only have a very small effect on the results obtained for the higher affinity ligands.

In one polarization experiment Cy5-GSH and CDNB was added together with GST in a capillary and a small shift in the binding curve was observed over time. This suggests the production of a higher affinity ligand, the Cy5-GS-DNB conjugate (**Figure 2.18**). If the reaction is incubated for 20h this shift becomes greater suggesting production of a conjugate with tighter binding. The observed K_d for Cy5-GSH is 52µM, 42µM after CDNB addition, and 20µM 20h after CDNB addition.

The K_d of Cy5-P2-GSH was determined to be 19.1µM suggesting the longer linker is increasing the affinity for labeled GSH. This supports previous results in which GST conjugated Cy5-P2-GSH at a higher rate than Cy5-GSH, suggesting that the longer linker favors catalysis.

To test the specificity of the binding a displacement experiment was done. If Cy5-GS-hex binds the same site as GS-hex, the addition of GS-hex to Cy5-GS-hex bound to GST should compete off the labeled ligand and decrease the anisotropy. At 500nM Cy5-GS-hex and 21.1µM GST essentially all Cy5-GS-hex is bound to the enzyme. GS-hex was added until no decrease in

anisotropy could be seen and a binding curve constructed. From the binding curve the K_d of GS-hex could be determined to 280nM. The result suggests that the labeled ligand can bind the same site as the non-labeled ligand (**Figure 2.19**).

2.10 - Characterization of Ligand Binding by FCS

FCS was used as an additional method to confirm that Cy5-labeled ligands bind GST. Cy5-GS-hex at 30nM was used together with increasing concentrations of GST to test if the diffusion time changed as ligand binds the enzyme. Non-specifically labeled Cy5-GST was used as a control simulating the condition where all ligand is bound to GST. The non-specifically labeled Cy5-GST was produced by reacting Cy5-NHS with GST at a 2:1 ratio in bicarbonate buffer (pH 8.0) followed by extensive washing to remove any residual free dye.

The Carl Zeiss LSM-510 META MP ConfoCor 3 Confocal Microscope in the Molecular Biosensor and Imaging Center (MBIC) was used for the experiment. A 40x C-Apochromat 1.2W objective was used together with the 633nm laser line for excitation. Data was analyzed with Zen 2011 (Carl Zeiss AG).

The diffusion time of Cy5-adduct (Cy5-GS-hex) increased upon the addition of GST and the correlation curve is very similar to the curve of a non-specifically Cy5-labeled GST (**Figure 2.20**) suggesting that most ligand is binding to the enzyme.

TIR-FCS has also been used to try to find multiple binding states when one ligand binds an immobilized enzyme. These experiments were done on the same TIRF setup as our single-molecule binding kinetics experiments that will be discussed further in chapter 3. Using FCS on this setup has not yet been able to reveal the existence of multiple binding states.

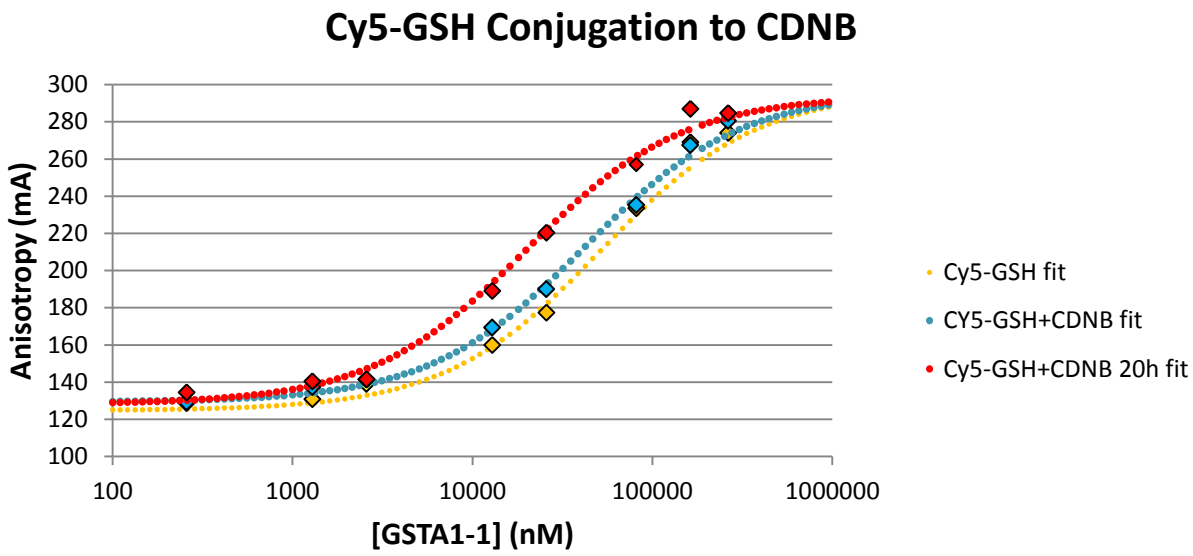

Figure 2.18: Binding curve of Cy5-GSH, Cy5-GSH with CDNB, and Cy5-GSH with CDNB after 20h. Both [Cy5-GSH] and [CDNB] are 500nM. There is only a slight shift in K_d with the addition of CDNB. If the reaction is incubated for 20h this shift becomes greater suggesting production of a conjugate with tighter binding. The curves have been fitted to the same max anisotropy with non-cooperative binding (n=1). Even if the real max anisotropy differs from the fixed one the same trend with a shift in K_d should be observed. An additional data point at a GST concentration higher than 14.5mg/ml would have been desirable, but was not possible to produce without risking protein aggregation and precipitation. The observed K_ds are 52µM, 42µM and 20µM.

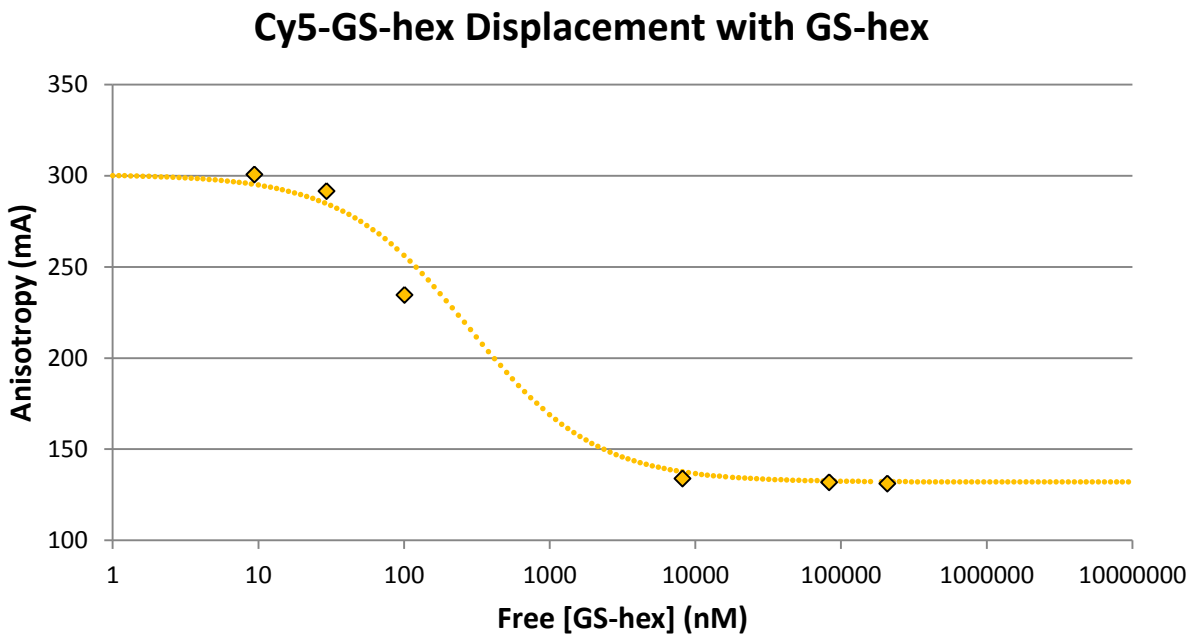

Figure 2.19: The fluorescence anisotropy experimental setup can be tested by displacing Cy5-GS-hex with GS-hex. This experiment would test for specific binding and obtain binding constant for GS-hex. A concentration of Cy5-GS-hex (500nM) and GST (21.1µM) was chosen where all Cy5-GS-hex is bound to the enzyme. GS-hex was added until no decrease in anisotropy could be seen and a binding curve constructed. A binding curve was constructed from where a K_d of GS-hex (280nM) could be extracted.

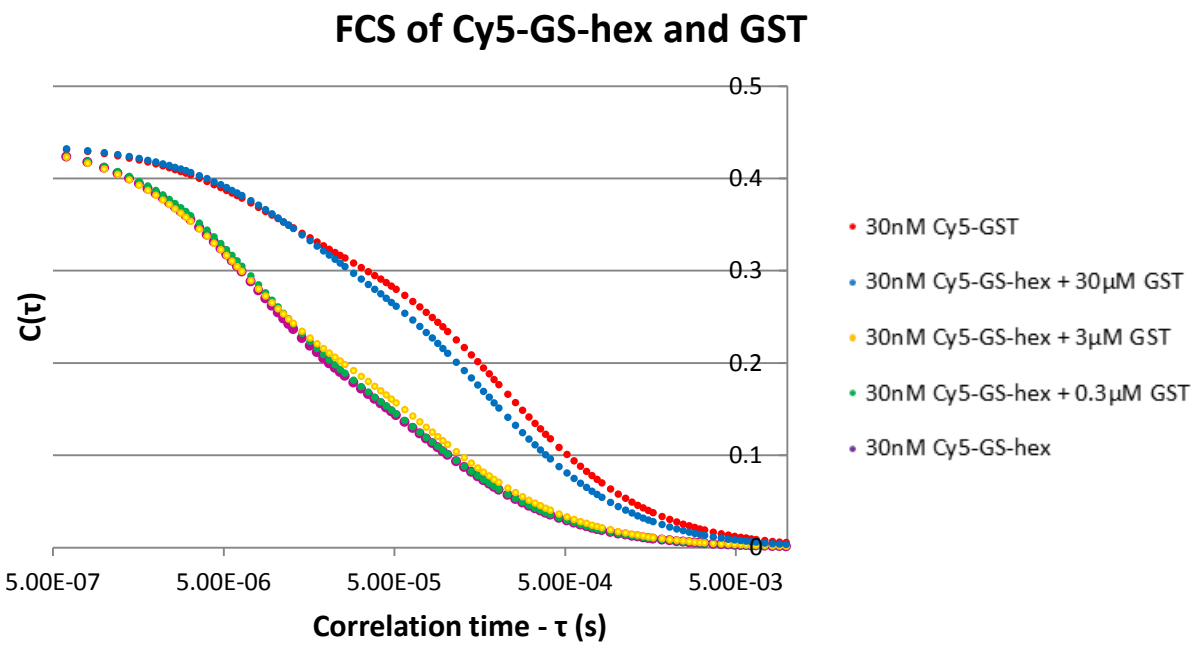

Figure 2.20: Normalized and fitted FCS-data of Cy5-adduct (Cy5-GS-hex) biding GST. The diffusion time of the Cy5-adduct increases as GST is added suggesting binding to the enzyme. The correlation curve of Cy5-adduct with the highest concentration of GST is similar to that of Cy5-GST which further implies that the ligand binds the enzyme.

2.11 – Conclusions

To study single molecule binding events to GSTA1-1 we aimed to use fluorescent ligands. A biotinylated GSTA1-1 that could be immobilized in a single molecule experiment was successfully expressed and purified. The GSH conjugates of the fluorogenic substrates were found to be quenched when bound to the enzyme. Instead known high affinity ligands of GSTA1-1 were labeled on the N-terminal with Cy3 or Cy5.

After some initial binding experiments the affinity of the fluorescent ligands were improved by modifications to the chemical structure of the ligand. A longer and less hydrophobic linker was introduced, and a bis-ligand with two ligand linked to one dye was constructed. Both alterations show improved affinity, particularly the bis-ligands.

One of the fluorescently labeled ligands is GSH, one of GSTs substrates. GST is capable of conjugating the labeled GSH to CDNB even if addition of the dye slows down the catalytic rate of the enzyme.

The affinities of the fluorescently labeled substrates, GSH-conjugates and bis-ligands were evaluated by inhibition of the CDNB assay. Most of the ligands maintain high affinity even after being fluorescently tagged and are well suited for single molecule imaging experiments. In addition to inhibition of the CDNB assay fluorescence polarization and FCS were used to confirm binding to GSTA1-1. The status of all ligands studied is listed in **Table 2.3**.

The numerical binding constants obtained from the fluorescence polarization experiments do not match up with the binding constants calculated from the IC50s obtained from the inhibition assay. Only a few ligands have been analyzed using fluorescence polarization. The method was primarily used to ensure that labeled GSH still bind GST. This was

also confirmed by GSTs ability to catalyze the conjugation of a labeled GSH in the CDNB assay. Non-specific binding to the capillary does not seems to be an issue since BSA blocked capillaries do not affect the obtained anisotropy, and emptied capillaries are basically non-fluorescent. Some of the discrepancy might lay in the k_ds obtained from the CDNB assay.

In the next chapter the binding of a single fluorescent ligand to an immobilized GST dimer has been studied in an attempt to identify multiple conformations of the enzyme.

Table 2.3: All GSTA1-1 substrates and ligands evaluated.

Ligand	K_d	**Method**	**Status**
GSH	3.9 μM	Literature[19]	Substrate
GS-hex	70 nM	Literature[25]	Most common inhibitor
GS-EA	1.8 μM	Literature[28]	Ligand, addition reaction product
CDNB	62 μM (K_M)	Literature[33]	Substrate
Cy5	152 μM	Fluorescence Polarization	Fluorescent Label
Cy5-GSH	52 μM	Fluorescence Polarization	Catalytically active
Cy5-P2-GSH	19.1 μM	Fluorescence Polarization	Catalytically active
Cy5-GS-hex	4.7 μM	Fluorescence Polarization	Inhibits CDNB assay
Cy5-GS-hex	68 nM	Inhibition Assay	Inhibits CDNB assay
Cy5-P2-GS-hex	41 nM	Inhibition Assay	Inhibits CDNB assay
Cy5-$(GS\text{-}hex)_2$	8.2 nM	Inhibition Assay	Inhibits CDNB assay
Cy3-GS-hex	65 nM	Inhibition Assay	Inhibits CDNB assay
Cy3-$(GS\text{-}hex)_2$	4.2 nM	Inhibition Assay	Inhibits CDNB assay
Cy5-GS-DNB	3.8 nM	Inhibition Assay	Inhibits CDNB assay
Cy5-P2-GS-DNB	13 nM	Inhibition Assay	Inhibits CDNB assay
Cy5-$(GS\text{-}DNB)_2$	16 nM	Inhibition Assay	Inhibits CDNB assay
Cy5-GS-EA	X	X	Never successfully labeled/purified
P4-GS-hex	X	Inhibition Assay	Inhibits, unknown concentration
Bromobimane	X	X	Discarded, High Background
NBD	X	Inhibition Assay	Discarded, Quenching
GS-NBD	X	Inhibition Assay	Discarded, Quenching

Chapter 3 – Single-Molecule Binding Kinetics of Fluorescent Ligands to hGSTA1-1

3.1 - Introduction

In the previous chapters the fluorescently tagged ligands have been shown to bind GST with high affinity and stay fluorescent upon binding. This next chapter will show how the ligands can be employed to study the biding properties of a single ligand to a single enzyme. Since the ligands differ in their structure they will likely express different binding properties. The binding kinetics reveals information about the binding states of the enzyme which is related to the conformational states of the enzyme. To facilitate such an experiment the fluorescent tag has to become stationary during a binding event. This was made feasible by immobilizing GST on a fused silica surface and having a pool of rapidly diffusing fluorescent ligand in solution that only becomes detectable as it binds to the immobilized enzyme. Fluorescent ligand in solution will only have a small contribution to background fluorescence since TIRF microscopy is used and only molecules in the evanescent field, in the very thin region close to the surface with immobilized enzyme, are being excited.

3.2 - Functionalizing fused silica slides

To be able to immobilize GST the fused silica slide first has to be properly functionalized. Since slides are being reused extensive cleaning is necessary before a two-step functionalization process can start. In the first step amines are introduced on the surface of the slide, and in the second step a biotin is covalently linked to the amine.

To clean the slides they are first soaked in a 50% mixture of acetone and methanol over-night. The next day residual tape and glue are removed with a razorblade and the slides are

washed in LiquiNOX until visually clean. Following is a 10min sonication in 5% LiquiNOX. Slides are washed in water and then cleaned in warm Piranha solution for 30min. The slides are washed in water and sonicated in acetone for 15min followed by 15min in methanol and 30min in 1M potassium hydroxide. Cover glasses are treated as well but excluded from steps including strong acid or base.

The cleaned fused silica slides and cover glasses were incubated in 3-aminopropyltriethoxysilane (APTES) (100µl in 10ml MeOH and 500µl acetic acid) for 30min. This covers the slides with primary amines. The APES treated slides and cover glasses are then sandwiched after addition of 75µl methyl-polyethylene glycol-succinimidyl valerate (mPEG-SVA) (100mg/ml) and biotin-polyethylene glycol-succinimidyl valerate (bio-PEG-SVA) (5mg/ml). This will covalently link the succinimidyl valerate to the amine and thereby biotin to the surface. Biotinylated slides are washed in distilled water, dried, and stored in -80°C freezer in Ar until used.

A flow chamber was constructed by drilling two holes in the slide to which tubing was attached and fixed with epoxy. Double sided tape was used to form a channel between the holes on the other side of the slide, and the channel was closed by a cover glass.[97] The dimensions of the typical channel are 37x5x0.1mm. Epoxy was used to seal the gaps in between the tape **(Figure 3.1)**. The flow chamber was incubated with 0.1mg/ml NeutrAvidin for 10min. The biotinylated GST was then able to bind the immobilized NeutrAvidin and fluorescent ligands were added to the flow chamber.

The N-terminal of GSTA1-1 had previously been biotinylated and the enzyme dimer should carry two biotins. As mentioned previously the enzyme is fully biotinylated and it is

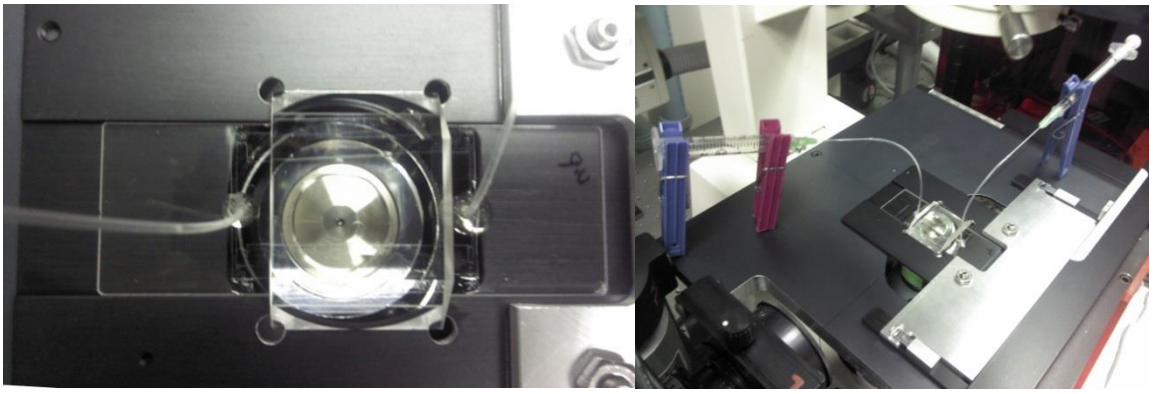

Figure 3.1: The setup of the flow chamber on the stage of the TIRF microscope with the inlet and outlet tubing, the double sided tape forming the chamber, and the prism pictured.

therefore likely that the enzyme is immobilized through both biotins. The two biotins can bind the same or different NeutrAvidins, but due to the larger distance between the biotins than between the biotin binding sites on NeutrAvidin immobilization to two different NeutrAvidins is more likely. Even if C-terminal and active sites are spatially separated from the N-terminal biotinylation site, dual immobilization might put stress on the enzyme, which could possibly affect its dynamics and alter the properties of the enzyme. Data will be presented that shows the immobilized enzyme is active.

3.3 - Occupancy calculation

To estimate the expected number of single molecule binding events in the field of view the density of immobilized GSTA1-1 and the binding constant of the ligand to the enzyme needs to be calculated and determined. To attain close-packing of GST on the inner surfaces of the flow chamber, an enzyme concentration of 570nM is required, corresponding to 97pmoles of immobilized enzyme. With a binding constant of 100nM we would expect an occupancy of 1900 molecules within the field of view at any time. The binding constant (K_d) depends on the concentration of ligand (*[L]*), the concentration of binding sites (*[S]*) and the concentration of the complex between the ligand and active site (*[C]*) (Equation 3.1). The occupancy, which is the same as the concentration of complex between ligand and binding site, can be calculated by solving a quadratic equation (Equation 3.2).

$$K_d = \frac{[Ligand][Sites]}{[Complex]} = \frac{([L]_0 - [C])([S]_0 - [C])}{[C]} \qquad \text{(Eq. 3.1)}$$

$$[C] = \frac{[L]_0+[S]_0+K_d}{2}\left(1 - \sqrt{1 - \frac{4[L]_0[S]_0}{([L]_0+[S]_0+K_d)^2}}\right) \quad \text{(Eq. 3.2)}$$

If the GST packing is less tight than what is theoretically possible, which might be more realistic, a smaller number of molecules should be seen. The concentration of bio-PEG-NHS (0.8µmoles) and NeutrAvidin (0.6 µmoles) are used in great excess and should not limit the amount of GST immobilized.

In any single frame of the single molecule binding kinetics time laps movies hundreds of binding events are observed suggesting an occupancy slightly lower that what is theoretically possible. The number of binding events observed is directly proportional to the concentration of fluorescent ligand used suggesting that the binding is specific.

3.4 - Test of Immobilization

For the single molecule experiments to work all steps of the functionalization and immobilization process have to work efficiently and as expected. In the functionalization process APTES has to react with the fused silica slide and the bio-PEG-SVA has to react with the amine. Next, NeutrAvidin has to bind the immobilized biotin and the biotin of biotinylated GSTA1-1 has to bind NeutrAvidin. Only once GSTA1-1 has been properly analyzed can a fluorescent ligand be added and its binding characteristics to the enzyme analyzed (**Figure 3.2**). The binding specificity of the ligand also has to be evaluated.

The binding specificity of GST to the biotinylated and NeutrAvidin treated fused silica slide was evaluated by excluding biotin, or excluding both NeutrAvidin and biotin from the immobilization process. By excluding biotin the number of Cy5-GST (**chapter 2.10**) immobilized

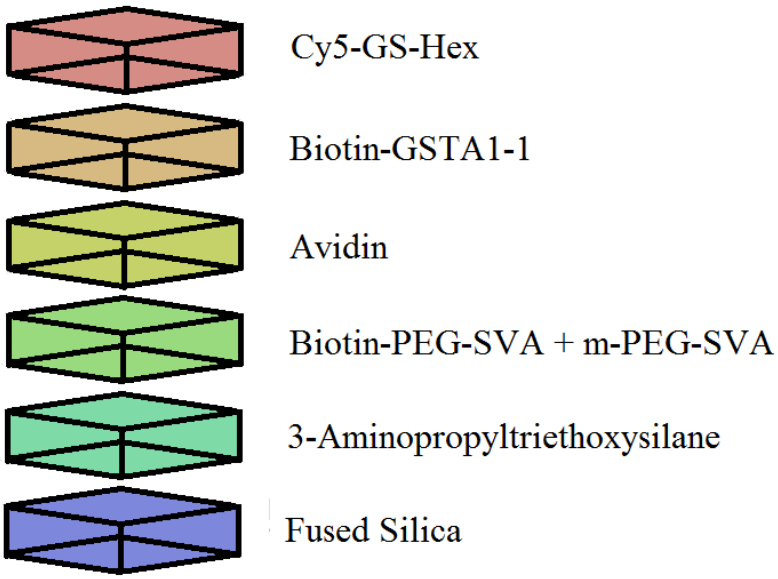

Figure 3.2: The different layers of the functionalized fused silica slide enabling immobilization of GSTA1-1 which will bind the fluorescent ligands.

is reduced dramatically which suggests that biotin is necessary for specific immobilization and that NeutrAvidin is not binding non-specifically to the surface which would immobilize Cy5-GST **(Figure 3.3, Table 3.1)**. If NeutrAvidin is excluded as well almost no Cy5-GST is immobilized. The very few non-specific binding events that are observed are likely due to non-specific interactions of Cy5-GST to the surface **(Figure 3.3, Table 3.1)**.

If no GST is immobilized to the functionalized fused silica slide and fluorescent ligand is added to the flow chamber only very few binding events are observed. If the concentration of the labeled ligand is increased a higher background glow can be observed but only very few single molecule binding events suggesting that almost all ligand binding is specific. If the experiments are repeated with immobilized GST single molecule binding events once again appear (**Figure 3.4**).

To confirm the binding specificity of a labeled ligand to GST Cy5-P2-GS-DNB was added to the flow chamber with and without enzyme immobilized. Very low non-specific binding is observed for Cy5-P2-GS-DNB when no GST has been immobilized (**Figure 3.5**). The same result was obtained for all fluorescently labeled GSH-conjugates. The only molecules showing non-specific interactions to the flow chamber were the labeled substrates Cy5-GSH and Cy5-P2-GSH. Their binding properties will be discussed later in this chapter.

Another way to test for specific binding to the active site of the enzyme is to outcompete the binding of the fluorescent ligand with a high concentration of non-labeled ligand. Very few binding events of Cy5-GS-hex binding to GST were observed when a high concentration of GS-hex is added (**Figure 3.6**).

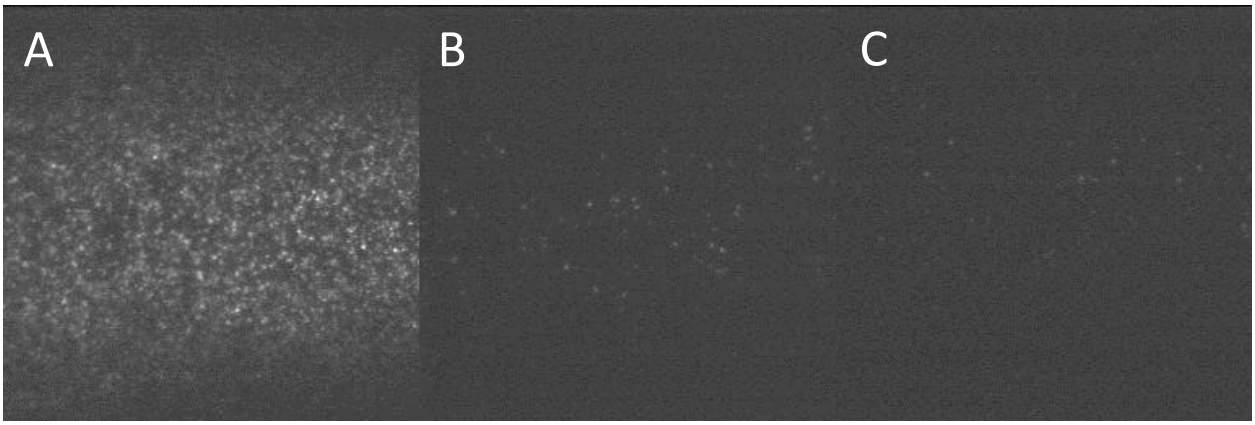

Figure 3.3: Biotinylated and Avidin treated surface with 1nM Cy5-Bio-GSTA1-1 (**A**), non-biotinylated but Avidin treated surface with 1nM Cy5-Bio-GSTA1-1 (**B**), non-biotinylated surface without Avidin with 1nM Cy5-Bio-GSTA1-1 (**C**). Biotin is necessary for immobilization and Avidin alone will not immobilize biotinylated GST. This suggests that Avidin is, as intended, necessary to link GST to the functionalized surface.

Table 3.1: Outline of the different surface treatments in figure 3.3.

Treatment	**A**	**B**	**C**
APTES	YES	YES	YES
Metyl-PEG-SVA	YES	YES	YES
Biotin-PEG-SVA	YES	NO	NO
Avidin	YES	YES	NO
Cy5-Bio-GSTA1-1	YES	YES	YES

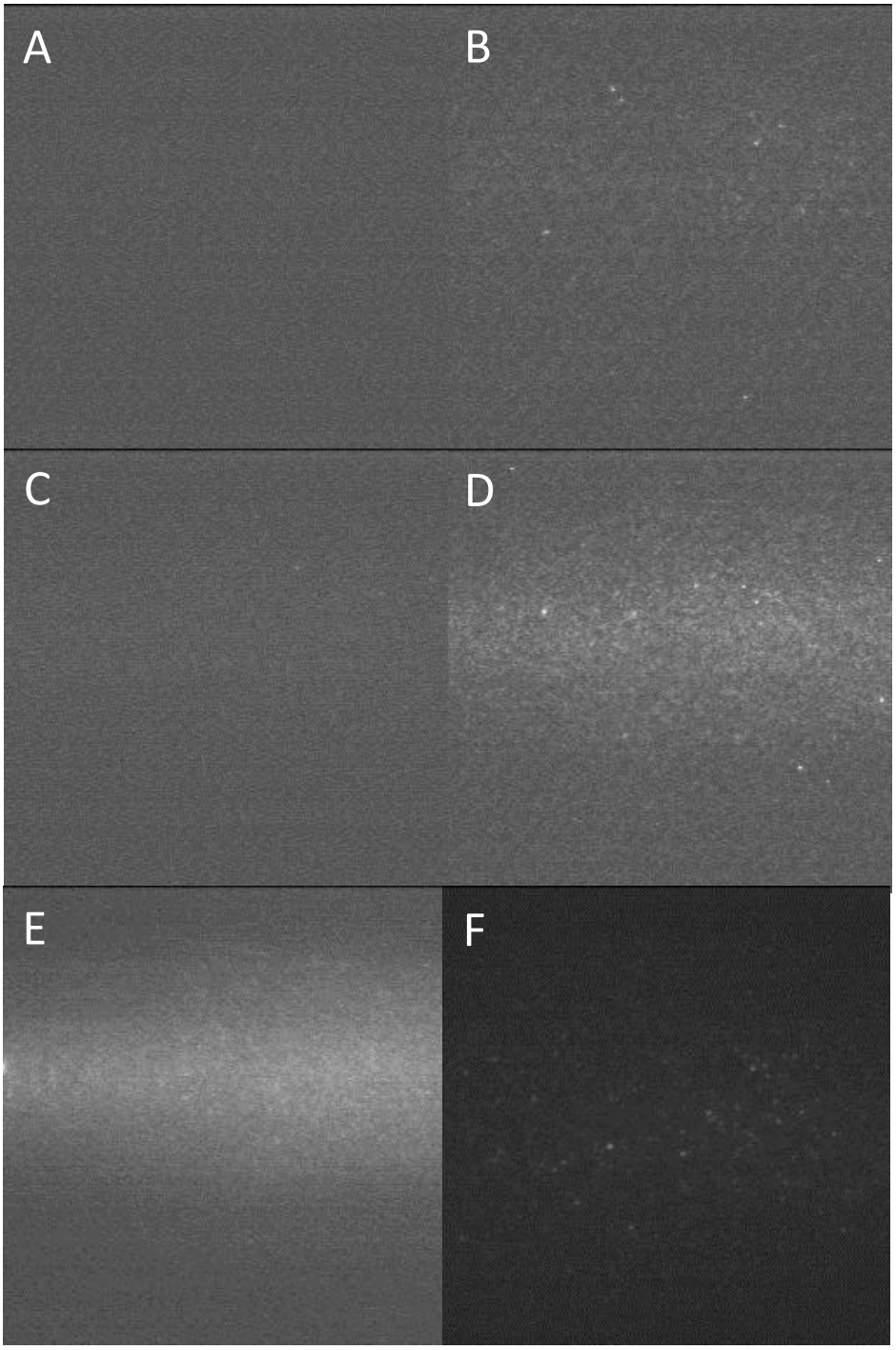

Figure 3.4. Single molecule data from biotin and Avidin treated surfaces with and without immobilized GST. No GST with 0.1nM Cy5-GS-hex (**A**), no GST with 0.1nM Cy5-GS-hex and high intensifier gain (**B**), no GST with 0.5nM Cy5-GS-hex (**C**), no GST with 0.5nM Cy5-GS-hex and high intensifier gain (**D**), no GST with 6.7nM Cy5-GS-hex (**E**), immobilized GST with 0.5nM Cy5-GS-hex (**F**). GST has to be present to observe single molecule binding events suggesting specific binding of the labeled ligands.

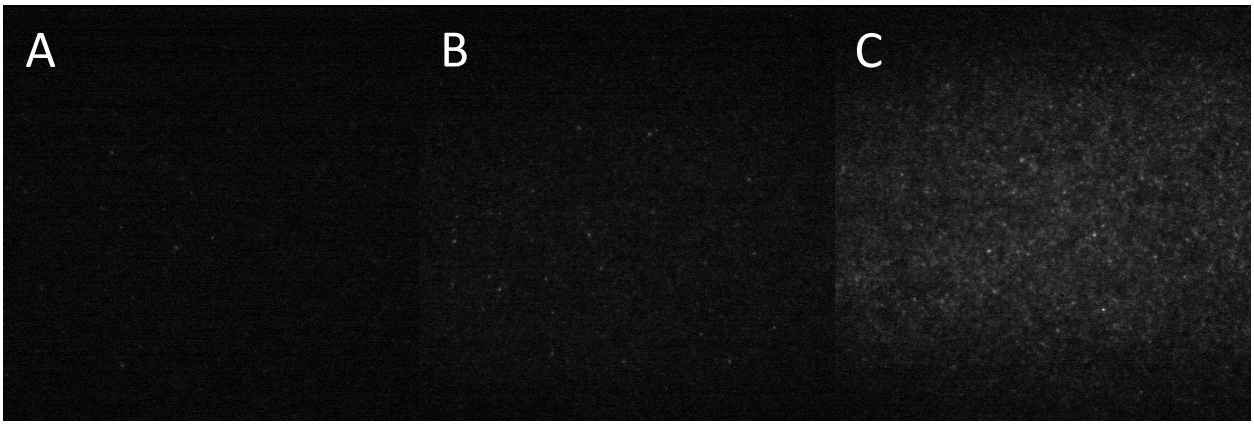

Figure 3.5: Specificity of Cy5-GS-DNB binding to immobilized GST. Imaging buffer (**A**), 450pM Cy5-P2-GS-DNB without immobilized GST (**B**), 450pM Cy5-P2-GS-DNB with immobilized GST (**C**). Cy5-P2-GS-DNB is not binding to the surface without immobilized GST.

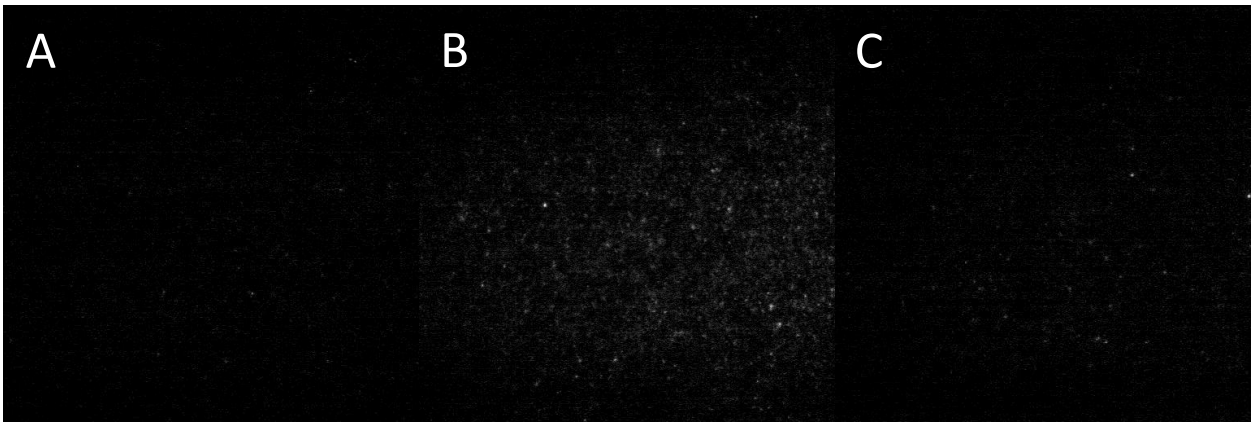

Figure 3.6: Specificity of Cy5-GS-hex binding to immobilized GST. Imaging buffer (**A**), 425pM Cy5-GS-hex (**B**), 425pM Cy5-GS-hex with 5µM GS-hex (**C**). The binding of Cy5-GS-hex must be specific to the active site of GST since it can be competed off with a high concentration GS-hex.

To better visualize the decrease in the number of binding events the average occupancy time histogram of Cy5-P2-GS-DNB with and without GST, and Cy5-GS-hex with and without GS-hex were plotted (**Figure 3.7 and 3.8**).

3.5 - CDNB Assay in Flow Chamber

To verify that GST is immobilized in the flow chamber and maintains its activity while immobilized a number of experiments have been performed. As an initial test the flow chamber with immobilized GST was mounted in the beam path of an Agilent Tachnologies Cary 60 UV-Vis spectrophotometer, GSH and CDNB was added, and the change in absorbance at 340nm showing the formation of the conjugate measured. Immobilized GST is capable of catalyzing the conjugation. A control chamber was also tested without GST immobilized to obtain the non-catalyzed rate. The non-catalyzed rate is very slow (**Figure 3.9**). This is suggesting that all steps of functionalization and enzyme immobilization are working as expected. Only about 10% of the activity observed when performing the CDNB assay in a cuvette is observed. The path length of the flow chamber is approximately 100µm which is 100-times shorter than the 10mm path length of the cuvette. The reason why 10% of the activity is observed, and not 1% as would be expected, is because higher substrate concentrations are used. Both GSH and CDNB are used at 1mM. A tenfold increase in substrate concentration does not necessarily result in a tenfold increase in activity even if this happened to be the case this time. The immobilized enzyme concentration in the flow chamber is also higher than in the cuvette assay which will contribute to a higher rate.

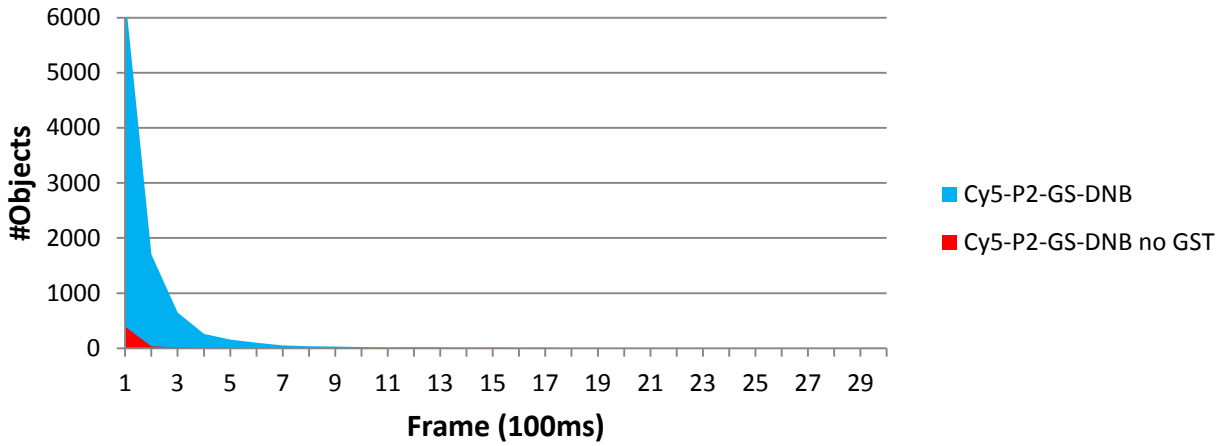

Figure 3.7: Number of binding events and the length of the binding events of Cy5-P2-GS-DNB with and without GST. Very few binding events are detected without the presence of GST.

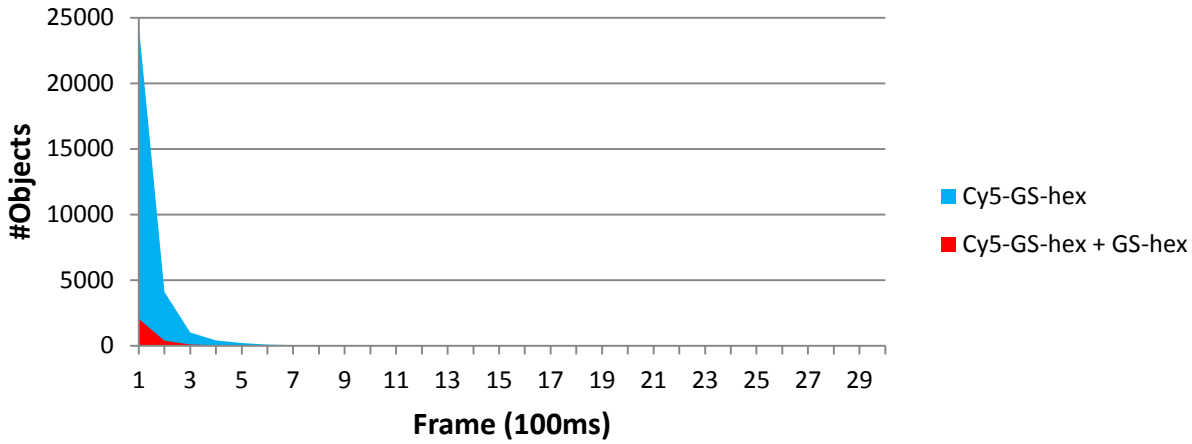

Figure 3.8: Number of binding events and the length of the binding events of Cy5-GS-hex with and without GS-hex. Very few binding events are detected if a high concentration of the competitive inhibitor GS-hex is added to the sample suggesting specific binding of Cy5-GS-hex to the active site.

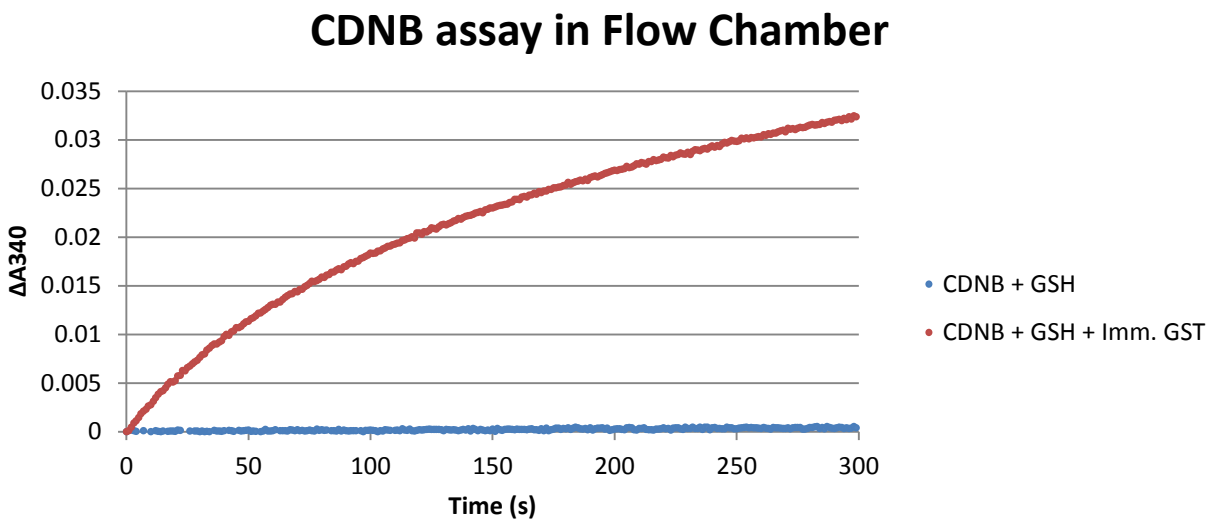

Figure 3.9: CDNB assay in flow chamber with and without immobilized GST. The non-catalytic rate is very low compared to the GST catalyzed rate. This shows that GST is still active when immobilized. CDNB and GSH were used at 1mM concentration. This is the concentration traditionally used but higher than what I have used in most assays. Path length is approximately 100µm.

In another test GST was labeled with Cy5 and immobilized. Labeled GST shows a carpet of fluorescence in a single molecule TIRF experiment in which single molecules only become visible after bleaching due to extensive exposure. Labeled ligand doesn't bleach but immobilized labeled GST does. To visualized single labeled immobilized Cy5-GSTs the labeled enzyme has to be spatially separated on the surface. Diluting the enzyme will not work since that would only result in a higher concentration of immobilized enzyme at the inlet of the flow chamber. By instead diluting Cy5-GST with non-labeled GST the dye was spatially separated enough to detect single immobilized enzymes.

3.6 - TIRF Imaging

Multiple TIRF microscopes capable of single-molecule imaging have been used throughout my thesis research, but the vast majority of experiments were performed on a home built prism-type TIRF system. It consists of a Zeiss Axiovert 135 TV microscope with a 40x C-Apochromat 1.2W Korr objective, a 2.5x Optivar, with a 632.8nm long pass filter (633R Semrock) blocking the laser light. A Hamamatsu C4742-98 camera with a 6.7µm CCD element (1280x1024), of which 1024x1024 is used, was installed on the trinocular port with a C-mount tube on a Zeiss 60mm interface. A VideoScope VS4-1845 image intensifier with a microchannel plate detector was also used. To speed up the camera as well as minimize the readout time 2x2 binning (512/512) and 100ms exposure in burst mode (QED InVivo) giving 9.8ips was used. Excitation with 3.92mW HeNe laser (633nm) focused through a 160mm f.l. achromat into the prism generates an intensity of 5.5kW/cm^2 in the evanescent field. The 45° fused silica prism

sets up an angle of incidence of 73.97° and thereby a 112.6 nm attenuation length for the evanescent field (Equation 1.3).

At Nyquist sampling the airy disc is 4.88 pixels. The diameter of the airy disc using this setup is 66.1 µm which is corresponding to 9.9 pixels. Since 2x binning was used the airy disc is instead 4.9 pixels which is very close to Nyquist sampling. This is also what we observed in the single-molecule imaging data. Most single molecule images are about 5 pixels in diameter.

To prevent bleaching a Glucose Oxidase and Catalase deoxygenation system was added to the imaging buffer (25mM HEPES, 125mM KCl, pH 7.3) together with a combination of the antioxidants Trolox (0.2mM) and Ascorbate (1mM). Both antioxidants bind and inhibit GST at high concentrations and have to be used at low concentrations. Dextrose (0.8%) was also added to the imaging buffer. Glucose oxidase is oxidizing glucose and water to gluconic acid and hydrogen peroxidase, and catalase is reducing hydrogen peroxide to water and oxygen. Half of an O_2 is removed per cycle which rapidly reduces the oxygen concentration in a sample and helps prevent bleaching.

During imaging data was collected from three regions of each sample and the average rates are used to calculate the average occupancy time.

3.7 - Antioxidant GST affinity

The flow chamber has to be kept free from fluorescent contaminations during functionalization and assembly, but it is also crucial to ensure that none of the components of the imaging buffer are interfering with the binding of a ligand. Initially none of the buffer

components affected the activity of GST, but as the buffer composition was altered less binding events were observed.

In addition to a deoxygenation system the antioxidant Trolox was added to the imaging buffer. Trolox is a Vitamin E analogue that is commonly used in single-molecule applications due to its antibleaching and antiblinking (triplet state quenching) properties.[98] Trolox was initially used successfully at what was thought to be 2mM. Trolox water solubility is approximately 4mM. A saturated solution was stirred overnight and filtered in the morning generating a 4mM stock solution. One way of increasing the solubility is by adjusting the pH to 9 and back to 7. This enabled preparation of a 20mM stock solution that was diluted 10-fold in the imaging buffer. This however resulted in very poor SM-data where much fewer binding events were observed. It turned out the old 4mM stock that was assumed to be saturated contained much less than 4mM Trolox. Adding Trolox to the CDNB assay revealed that it has an inhibitory effect on the enzyme at concentrations above 1mM (**Figure 3.10**). Using 2mM Trolox from the pH adjusted stock will thereby prevent biding. GST has been shown to have enhanced CDNB activity during Vitamin E deficiency suggesting that Vitamin E has an inhibitory effect on GST.[99] The concentration of Trolox was therefore lowered and Ascorbate, which also has antibleaching properties, was added to the imaging buffer.[67] Since ascorbate also shows some inhibitory effect on GST it has to be used at low concentration as well (**Figure 3.10**), but in combination with Trolox should still help prevent photobleaching. The decrease in the number of binding events of a fluorescent ligand caused by competition with Trolox further proves that the binding of a labeled ligand to GST is specific.

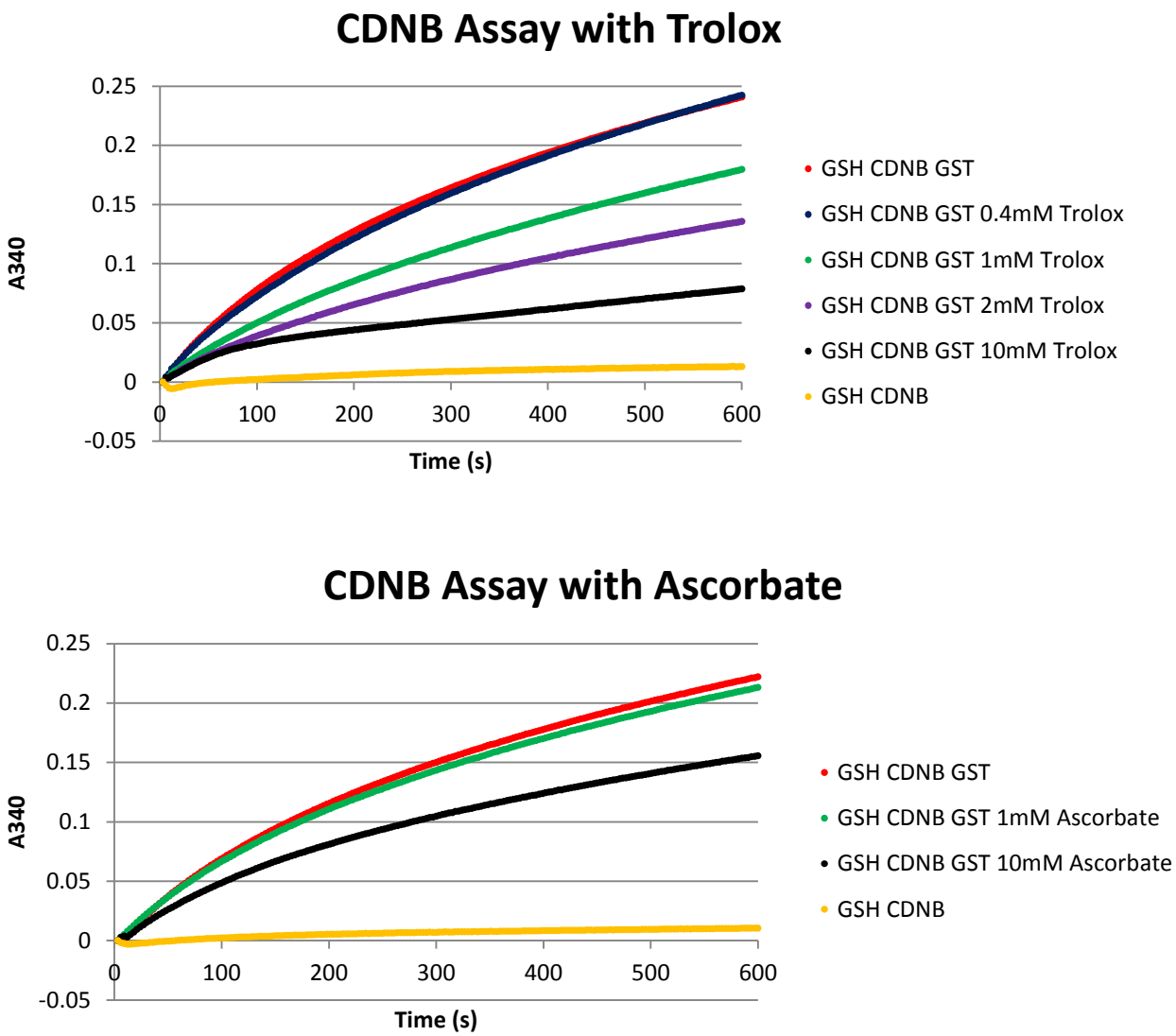

Figure 3.10: The inhibitory effect of Trolox and Ascorbate on the CDNB assay. High concentration (2mM) of Trolox is commonly added as an antioxidant to the imaging buffer in single molecule experiments. This is inhibiting the CDNB assay by 50%. Ascorbate is also inhibiting the CDNB assay but higher concentrations than Trolox are required to see an inhibitory effect. The concentration of GSH and CDNB is 100µM.

The effect of adding Trolox or Ascorbate to the imaging buffer with and without GOC present was evaluated by studying the bleaching rate of immobilized Cy5-GST with TIRF microscopy. GOC slows down the bleaching rate and addition of either antioxidant further reduces the rate of bleaching (**Figure 3.11**).

The molecular structures of Trolox and Ascorbate are quite similar to known substrates of GST and that they would have affinity for the enzyme does not seem unlikely **(Figure 3.12)**. The affinity of the antioxidants may be a result of GSTs ligandin activity and transport of antioxidants might be one the enzyme's many functions.

Even if GST is capable of binding Trolox it is unable to conjugate it to GSH. This is quite expected since Trolox does not contain any obvious conjugation sites for either addition or substitution reactions. Equimolar amounts of trolox and GSH were incubated with GSTA1-1 at room temperature over night, but no GS-Trolox conjugates were detected using MS.

3.8 - Average Occupancy Time

To be able to carry out single molecule kinetic experiments an estimate of the time the inhibitor will occupy the immobilized enzyme is necessary to make sure that these events are experimentally accessible. The inverse of the dissociation rate constant of a ligand is the average occupancy time (τ). The dissociation rate constant of GS-EA for rat GSTA1-1 is approximately $25s^{-1}$ at pH 7 which generates an average occupancy time of 40ms.[100] The dissociation rate constant for GS-DNB to rat Mu class GST is approximately $28s^{-1}$ giving a 36ms average occupancy time.[101] These events should be accessible with our experimental setup,

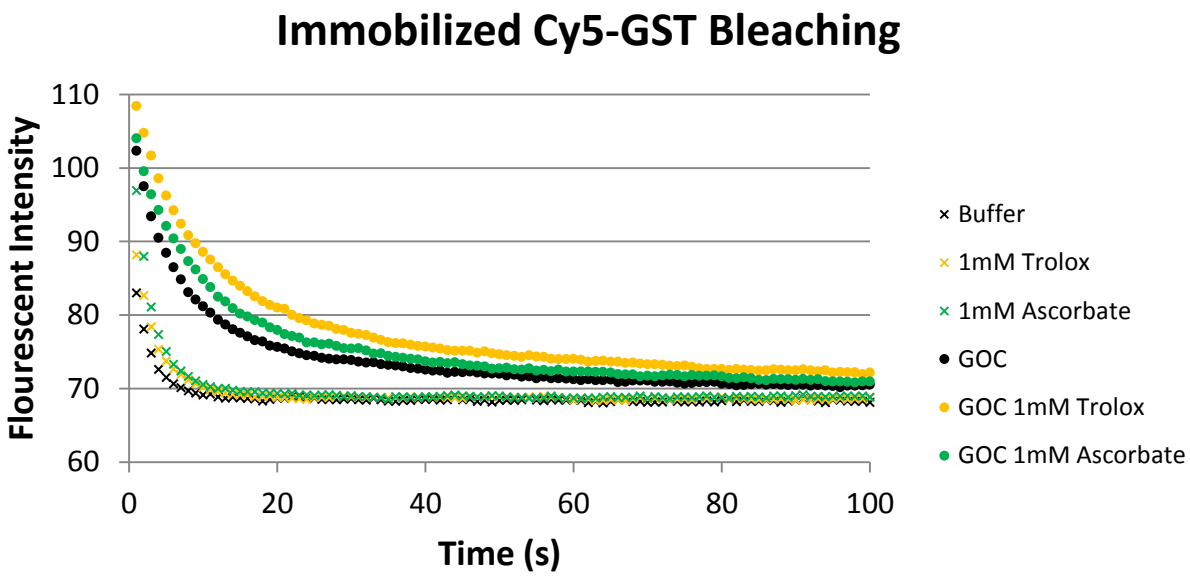

Figure 3.11: The effect of GOC and antioxidants on Cy5-GST bleaching. Average intensity from singe molecule data of immobilized Cy5-GST in flow chamber. Addition of GOC decreases the bleaching rate and addition of either antioxidant further decrease the rate.

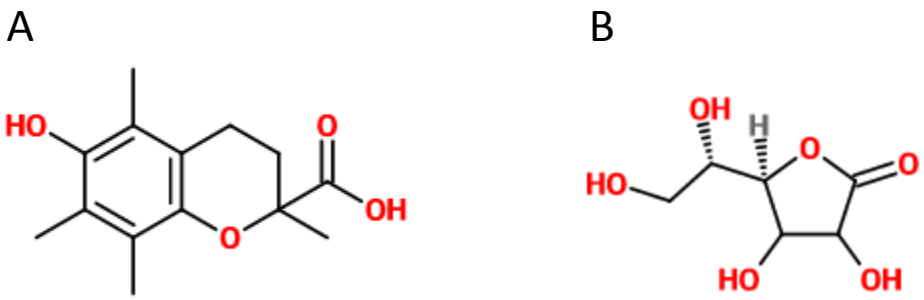

Figure 3.12: Structure of the antioxidants Trolox (**A**) and Ascorbate (**B**) which are added to the imaging buffer to prevent dye oxidation and quench triplet state dyes. The structures are fairly similar to many of the more characterized ligands of GSTA1-1 (Figure 1.X) and affinity towards the active site of the enzyme does not seem unreasonable.

though we are close to the cameras fps limit. No dissociation rate constant for s-hexyl glutathione has been found in literature.

There might be physiological parameters such as ionic strength, pH, polarity and viscosity of the solvent that affect dynamics and binding of the inhibitor. Temperature and pressure are also likely to affect binding rates but are more difficult to regulate on the stage of our microscope. Different conditions will be screened to determine their impact on inhibitor binding.

3.9 - Exposure time

To detect single molecule binding events of fluorescent ligands, such events have to be accessible with the experimental setup and the CCD camera used. Short enough exposure has to be used to ensure that the binding events are captured (approx. 50ms). However, the intensity of the image will decrease with a decreased exposure time, and using a too short exposure time might decrease the amount of photons collected to the extent where a single molecule binding event is indistinguishable from the fluorescent background. The readout time of the chip also becomes more significant as shorter exposure times are used. If a 25ms exposure is used and the readout time is 30ms most of the data would be lost. To speed up the readout time the data can be binned. Spatial resolution will be lost by binning the data but that will not affect the single molecule binding data as long as the fluorescent objects are spatially separated enough to be detected as different objects. After careful evaluation of different exposure times, binning, and the resulting readout time the standard exposure time was set to 100ms simply because of the shortest fraction of readout time (**Table 3.2**). The 100ms exposure

Table 3.2: Readout time at different exposure time and binning using the Hamamatsu C4742-98 camera. At 2x binning 100ms exposure gives 9.8fps, 50ms exposure gives 10fps and 25ms exposure gives 10fps. A framerate faster than 10fps cannot be obtained unless a subarray of pixels is being used. Although what looks like single molecules can be observed in subarray stacks, the 128x128 pixel array did not result in a histogram containing any long lived objects. The % Readout time column display how long the readout time is in comparison to the exposure time in percent. A low % Readout time is desired to record as much data as possible.

Binning	Resolution	Subarray (pixels)	Exp. Time (ms)	Framerate (ips)	Readout time (ms/frame)	% Readout time
4	256x256	none	50	18	5.555555556	11.11111111
4	256x256	none	25	18	30.55555556	122.2222222
2	512x512	none	100	9.8	2.040816327	2.040816327
2	512x512	none	50	10	50	100
2	512x512	none	25	10	75	300
2	512x512	256x256	50	15	16.66666667	33.33333333
2	512x512	256x256	25	15	41.66666667	166.6666667
2	512x512	128x128	50	19	2.631578947	5.263157895
2	512x512	128x128	25	28	10.71428571	42.85714286

was compared with 50ms exposure time to ensure that shorter events were not failing to be detected, but no difference in the histogram of average occupancy times could be observed (**Figure 3.13**).

An estimation of the average occupancy times expected was discussed in previous section. The specific activity of GSTA1-1 can also be used to approximate the maximum average occupancy time of a non-labeled ligand. The specific activity of GSTA1-1 with CDNB is 45μmoles*mg^{-1}*min^{-1}. This translates to a turnover number of 20.8s^{-1} which corresponds to an average occupancy time of 48ms. In this calculation the average occupancy time corresponds to GSH and CDNB binding, conjugating, and GS-DNB dissociating which might be slightly different from binding and dissociating of a ligand without catalytic turnover. The fastest average occupancy times observed for the labeled ligands are generally around 50ms, which suggests that the labeling is not impairing binding too much and that the imaging setup worked as expected.

In most experiments the shortest average occupancy time calculated is shorter than the exposure time used. Since the average occupancy time is not very sensitive to the exposure time, where a 50ms exposure generates the same average occupancy time as a 100ms exposure, this is not considered a concern (**Figure 3.13**).

3.10 - Data Analysis

The binding time of every fluorescent ligand has to be extracted from the single molecule data before subpopulations can be detected. The data has to be processed to ensure

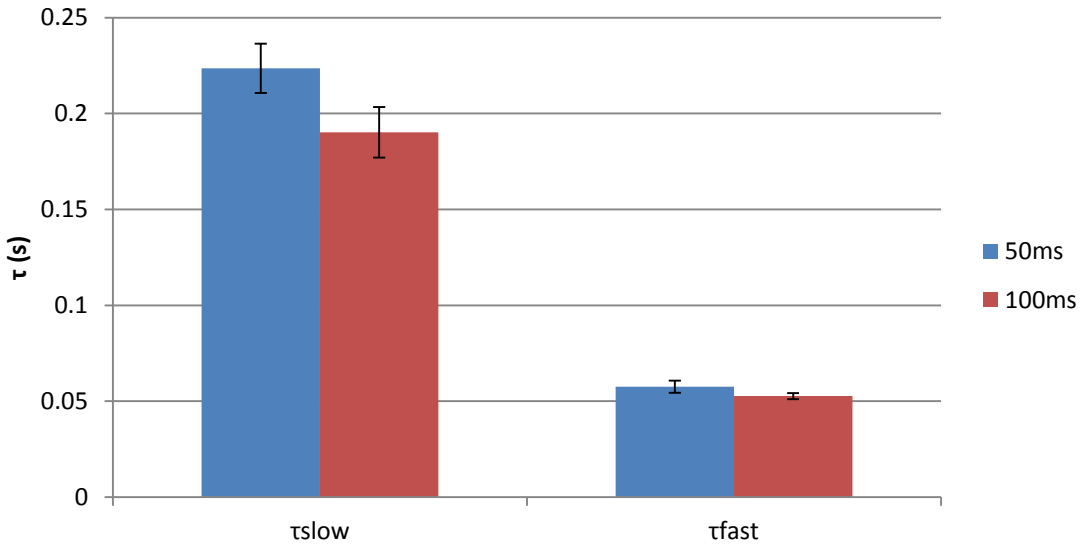

Figure 3.13: Average occupancy time of Cy5-GS-hex binding to immobilized GSTA1-1 with 50ms and 100ms exposure. A sum of two exponentials was used to fit the data generating a fast and a slow average occupancy time for each exposure time. Most binding events are represented by the fast average occupancy times. No big difference in average occupancy time can be seen using a shorter exposure, particularly not for the fast τ, suggesting that we do not fail to detect events faster than the exposure time.

that no binding events are excluded but also to prevent non-binding events from being analyzed as false-positives.

Stacks of images are analyzed using the Fiji image processing package. The 3D Object Counter plugin connects features in adjacent images and calculates the dimensions of these objects. By plotting the depth of each object, representing the residency time, the time a fluorescent ligand stays bound to an immobilized GST, in a histogram the distribution of residancy times for all enzyme bound inhibitors can be analyzed.

If the observed binding events are a result of a ligand binding one conformation of GST the histogram of occupancy times should decay exponentially. If there are *n* binding states the histogram should be a combination of *n* exponential decays. From the exponential curve the amplitude (α, the number of binding events for each occupancy time) and the off-rate (k) can be obtained. The inverse of the off-rate is the average occupancy time (τ), the average time a ligand stays bound to an immobilized enzyme.

$$y = \alpha e^{-kt} \qquad \text{(Eq. 3.3)}$$

$$y = \alpha e^{-t/\tau} \qquad \text{(Eq. 3.4)}$$

$$y = \alpha_1 e^{-t/\tau_1} + \alpha_2 e^{-t/\tau_2} + \alpha_3 e^{-t/\tau_3} \qquad \text{(Eq. 3.5)}$$

An exponential curve was fitted to the histogram using Excels solver function (Microsoft Office) by minimizing the sum of squares. A single exponential generated a good fit of the

majority of objects, but many long lived objects were not well fitted. A combination of two exponentials includes the more long lived objects in the fit, and a combination of three exponentials includes even more of them (**Figure 3.14**).

Even if a sum of exponentials seem to fit the data better than a single exponential the difference can sometimes be quite subtle. The longer binding events are more rare than the shorter binding events and enough data has to be collected to represent binding events of all lengths. For a particular example where Cy5-GS-hex was binding GST a single exponential can be fitted to describe 90.1% of all binding events, and a sum of two exponentials was fitted to describe 99.9% of all binding events. If 100000s of binding events are detected even a small fraction represent 1000s of events, which should be enough for statistical analysis (**Figure 3.15**). Going from a monoexponential to a sum of two exponential does not only include more long lived objects, it also fit the short lived objects better resulting in an overall better fit.

3.11 - Evaluating Fitted Data

There are multiple ways to evaluate how well a fitted curve describes the histogram of occupancy times data. Tests can be done to compare different fitting methods and to quantify how well the fit describes the data.

Generally three stacks of images were collected from three different regions of a sample. A histogram of occupancy times was generated for all of them and the average occupancy time extracted. The mean and standard deviation of the different data sets were then calculated. By comparing the average occupancy time for different inhibitors, different

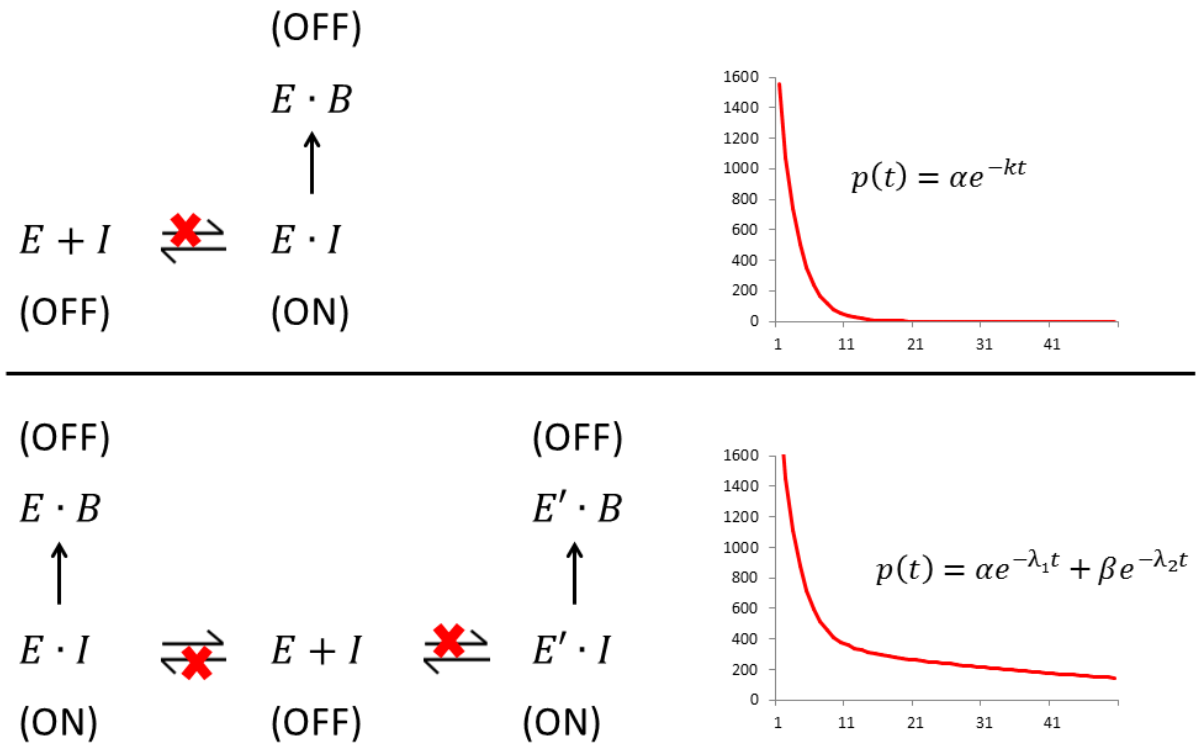

Figure 3.14: Curve fitting based on multiple binding states. One binding state will follow a single exponential while multiple binding states can be described by a sum of multiple exponentials. The measured occupancy times are the time from which a fluorescent ligand binds to an immobilized GST until it dissociates. The k_{on} will therefore not affect the occupancy time but the k_{off} will. The calculated k_{off} will be the sum of k_d and k_b (bleaching rate). By measuring k_b the k_d can be calculated.

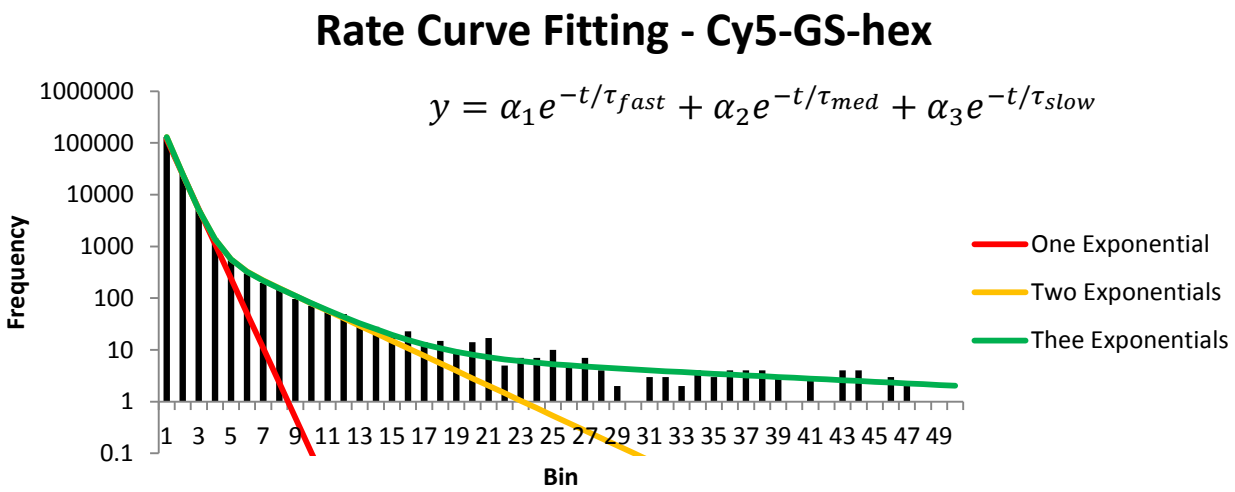

Figure 3.15: Fit of a monoexponential, a sum of two exponentials, and a sum of three exponentials to the histogram of average occupancy times of Cy5-GS-hex. The Y-axis is exponential. In this experiment a single exponential can be fitted to about 90.1% of all occupancy times, a sum of two exponentials to 99.9% of all occupancy times, and a sum of three exponentials to 100% of all occupancy times. As long as many binding events are recorded, in this case more than 150000, even the more rare events, represented by the second exponential, would have occurred enough time to generate good binding statistics. In this case adding a third exponential only includes a few additional objects to the fit and the existence of a third very rare state can be questioned.

conditions, or different GST mutants, information about different binding states can be obtained **(Figure 3.16 and 3.17, Table 3 and 4)**.

To prove the existence of multiple binding states it has to be statistically validated that a sum of exponentials generates a better fit than a single exponential. A primitive measure of the quality of the fit is to compare the sum of squares between the exponential and biexponential fit. The sum of squares always decreases going from an exponential fit to a biexponential fit. Since adding more parameters to a fit generally improves it comparing the sum of squares from a single exponential to the sum of squares from a biexponential fit might not be the best measure for determining the quality of the fit. To better evaluate the fit an F-test was performed. To calculate F the sum of squares (*SS*) and the degrees of freedom (*df*) for each fit was needed (Equation 3.6).

$$F = \frac{(SS_1 - SS_2)/(df_1 - df_2)}{SS_2/df_2} \qquad \text{(Eq. 3.6)}$$

When comparing a single exponential with a sum of two exponentials the F is always bigger than the P-value suggesting the second model has a better fit. For all ligands studied increasing the number of exponentials improved the fit.

The fact that the data was better fitted to a sum of exponentials instead of a single exponential suggests the existence of multiple binding states. This is true for all labeled GSTA1-1 ligands tested. Multiple average occupancy times can thereby also be extracted and compared between different ligands and different mutant enzymes.

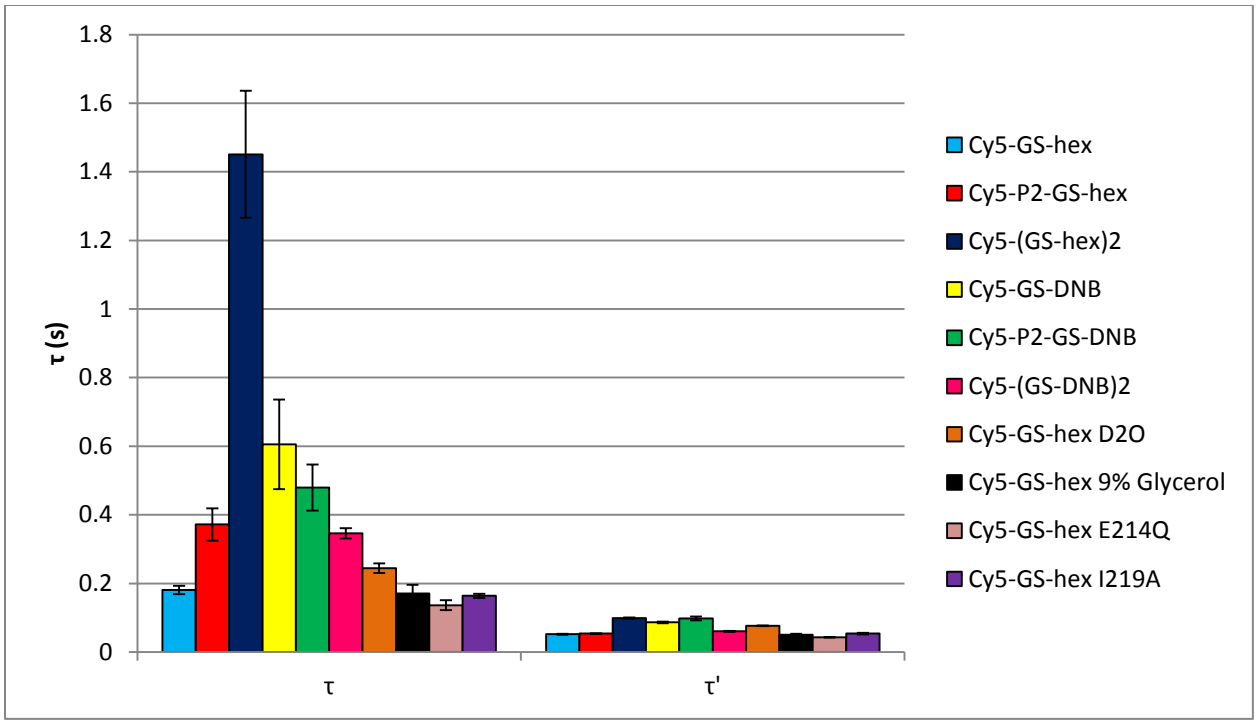

Figure 3.16: Fast and slow average occupancy time of different ligands and mutants enzyme.

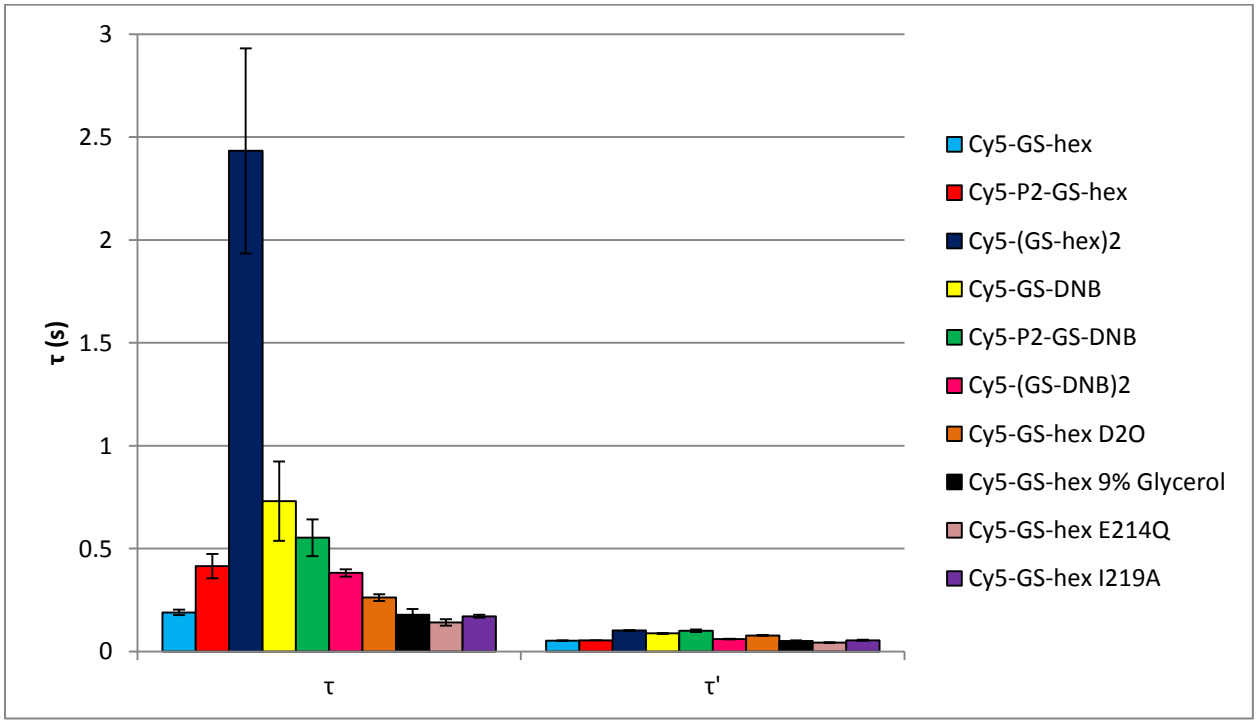

Figure 3.17: Fast and slow average occupancy time of different ligands and mutants enzyme where the bleaching rate has been subtracted.

Table 3.3: Off-rates and calculated average occupancy times for different ligands, mutant enzyme and imaging conditions. A frame rate of 9.8 generates an unit of the off rate of $0.102s^{-1}$.

	k_{off}	τ	k_{off}'	τ'
Cy5-GS-hex	0.565996	0.180823	1.966478	0.051921
Cy5-GS-hex 2	0.620862	0.166134	1.945583	0.052841
Cy5-P2-GS-hex	0.277095	0.371967	1.895511	0.053836
Cy5-$(GS\text{-}hex)_2$	0.071136	1.450922	1.027957	0.09929
Cy5-GS-DNB	0.17333	0.605483	1.180833	0.086448
Cy5-P2-GS-DNB	0.215478	0.479388	1.043687	0.097989
Cy5-$(GS\text{-}DNB)_2$	0.295248	0.346034	1.688491	0.060459
Cy5-GS-hex D2O	0.386292	0.244774	1.513351	0.076629
Cy5-GS-hex 9% Glycerol	0.606279	0.170639	2.044538	0.050049
Cy5-GS-hex 9% Glycerol 2	0.51489	0.199833	2.055848	0.049637
Cy5-GS-hex E214Q	0.754824	0.136537	2.380287	0.042892
Cy5-GS-hex I219A	0.623306	0.163874	1.888617	0.054093

Table 3.4: Off-rates and calculated average occupancy times for different ligands, mutant enzyme and imaging conditions. A frame rate of 9.8 generates a unit of the off rate of $0.102s^{-1}$. Adjusted for bleaching.

	k_{off}	τ	k_{off}'	τ'
Cy5-GS-hex	0.5381	0.190256	1.938582	0.052669
Cy5-GS-hex 2	0.592966	0.174125	1.917687	0.053621
Cy5-P2-GS-hex	0.249199	0.414638	1.867615	0.05464
Cy5-$(GS\text{-}hex)_2$	0.043239	2.432646	1.00006	0.102061
Cy5-GS-DNB	0.145433	0.731098	1.152937	0.088542
Cy5-P2-GS-DNB	0.187582	0.552951	1.015791	0.100693
Cy5-$(GS\text{-}DNB)_2$	0.267352	0.382244	1.660595	0.061475
Cy5-GS-hex D2O	0.358396	0.262371	1.485454	0.078268
Cy5-GS-hex 9% Glycerol	0.578383	0.17912	2.016641	0.050745
Cy5-GS-hex 9% Glycerol 2	0.486993	0.211481	2.027951	0.05032
Cy5-GS-hex E214Q	0.726928	0.141883	2.35239	0.043401
Cy5-GS-hex I219A	0.59541	0.171568	1.860721	0.054906

Another way to evaluate the reproducibility of the data is by assigning a confidence interval to the histogram of occupancy times fit. The mean of the fits can be used to calculate the standard deviation, and from there the confidence interval. The upper and lower limits of the confidence interval can be used to calculate how well the fit represents the data.

A biexponential fit to the average occupancy time histogram falls within the limits of the confidence interval until longer average occupancy times (**Figure 3.18**). This is expected since a biexponential fit generally does not include the more rare long lived objects. A triexponential fit would include more long lived objects and more data points would be contained within the limits of the confidence interval, but since the most long lived objects are very rare they are generally excluded from the data analysis by using a biexponential fit. Only a 100s out of 100000s of objects lay outside the confidence interval. Collecting more data sets from the same sample might be able to decrease the standard deviation and improve the fit.

3.12 - Single Molecule Dissociation Rate

In a single molecule experiment the time it takes for a bound molecule to dissociate, also known as the dissociation rate constant (k_{off}), was recoded, while the rate at which single molecules were appearing, the binding rate constant (k_{on}), was not. The order of the k_{off}s for the different ligands does not necessarily have to follow the same order as the K_ds since the k_{on} also affects the K_d. A particular ligand can have a moderate K_d and slow k_{off} as long as k_{on} is slow as well (Equation 3.7). Despite this, the highest affinity ligands are in general also expressing the longest average occupancy times.

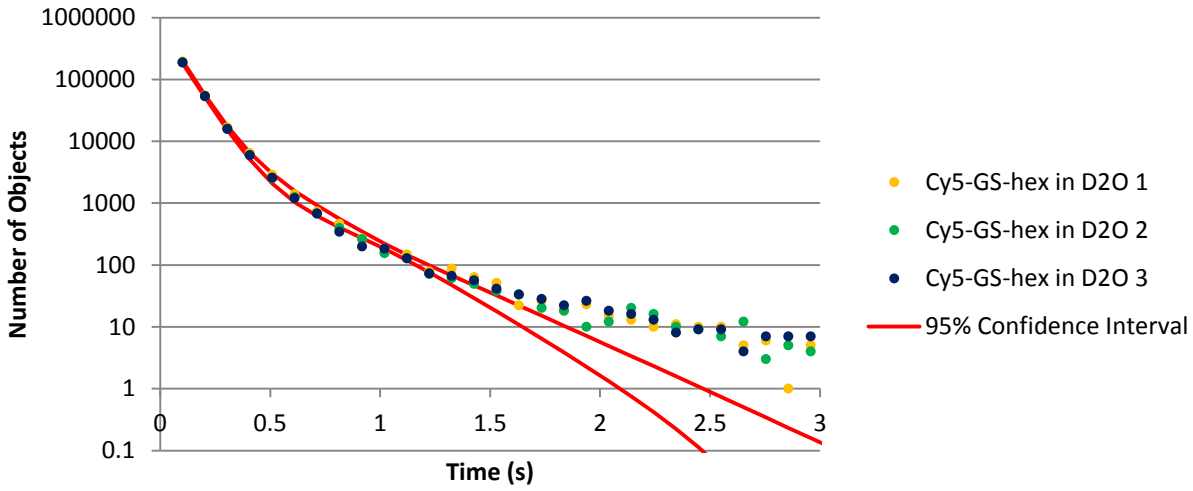

Figure 3.18: Average occupancy times of Cy5-GS-hex binding to GST in D_2O compared to the confidence interval of a biexponential fit from three data sets. More long lived objects do not fall within the confidence interval which is expected since they are not well fitted. These objects are very rare and intentionally excluded from the fit.

$$K_d = \frac{k_{off}}{k_{on}} \quad \text{(Eq. 3.7)}$$

Fitting to a sum of three exponentials generates three average occupancy times but the slowest average occupancy time generally only have an amplitude of 10s to 100s of objects. Since the specificity of these more rate binding events are hard to evaluate a sum of two exponentials is instead generally used. This might group multiple states binding states in to averages of fewer states.

3.13 - Bleaching

A dye molecule immobilized in the high intensity of the evanescent field will eventually contract non-reversible photo damage and bleach. The bleaching rate might not be significant compared to the short time frame of a binding event, and even if it is it can be corrected for.

The average occupancy time of a ligand (τ) is the result of the time a ligand binds an immobilized enzyme and the time it takes for a bound ligand to bleach. Multiple different observations, however, suggest that the bleaching should only contribute very little to the average occupancy time. First, no bleaching was observed in a sample in which fluorescently labeled ligand binds GST, as the ligand was probably not occupying the enzyme long enough to bleach. Even if some rare long binding events might result in bleaching the pool of ligand was so great that a few bleached molecules did not significantly affect the concentration of fluorescent ligand and the fluorescent intensity. Second, an immobilized non-specifically Cy5-labeled GST bleached eventually, but on a timescale much longer than that of the average occupancy time of a ligand. While the average occupancy time for a ligand is in the tens to hundreds of

milliseconds range, the average bleaching time for immobilized Cy5 with GOC deoxygenation system, 1mM ascorbate, and 0.2mM Trolox is approximately 3.7s. The average bleaching time was thereby almost one hundred times slower than the average occupancy time for most ligands, and bleaching was therefore unlikely to occur. Third, attenuating the laser to lower power should affect the bleaching rate but not the average occupancy time. No change in the average occupancy time was observed with lower laser power, suggesting that bleaching has no effect.

The conclusion of these observations is that the Cy5-bleaching rate (k_b) is slow compared to the off-rate (k_{off}) of most ligands studied, and the majority of the ligands are not occupying immobilized GST long enough to bleach. The observed k_{off} can therefore be considered the same as the dissociation rate constant (k_d). If ligands with longer occupancy times are being used the bleaching rate has to be taken in to consideration (**Figure 3.17**).

$$k_{off} = k_d + k_b \qquad \text{(Eq. 3.8)}$$

3.14 - k_{off} and τ of Ligands

Many of the fluorescent ligands have similar average occupancy times but some of them stand out. Since Cy5-GS-hex is the best characterized ligand it will be used as a reference and be compared to the other ligands. The longest average occupancy time does not necessarily result in the highest affinity (k_d) since the k_{on} also comes in to play. To generalize the results the bis-inhibitors show very high average occupancy times, particularly Cy5-(GS-hex)$_2$. Introducing the P2-linker increased the τ for Cy5-P2-GS-hex but not for Cy5-P2-GS-DNB if compared to the

shorter linker ligands. A higher GSTA1-1 catalyzed CDNB conjugation rate is observed for Cy5-P2-GSH than for Cy5-GSH so this result is unexpected. GSTA1-1 should favor binding the adduct with the longer linker. The k_d is decreasing with introduction of the P2 linker but only a small change in τ can be observed suggesting that the k_{on} of Cy5-P2-GS-DNB increases significantly more than for Cy5-P2-GS-hex.

The ligands k_{off} and the τ (**Table 3.3 & 3.4**) can be compared to the K_d (**Table 2.3**). The average occupancy times are also graphically represented for comparison of different ligands (**Figure 3.16**). The higher affinity ligands, such as Cy5-$(GS\text{-}hex)_2$ bind long enough where bleaching becomes significant. The average occupancy time has been recalculated to compensate for bleaching and the biggest increase is observed for the ligands with the longest τ (**Figure 3.17**). The data is presented both before and after correction for bleaching.

In the controls of the single molecule imaging experiments, when only imaging buffer or fluorescent ligand without GST is imaged, a few fluorescent objects can be observed. None of these contaminating objects or non-specific binding events have long occupancy times. This suggests that the longer binding events observed in a sample with ligand and GST present are in fact a result of specific binding to the enzyme (**Figure 3.19**).

The average occupancy times are calculated from the average of at least three different regions of the sample and are fairly reproducible. The reproducibility of the average occupancy times are also good even if the same experiment is repeated on a different day (**Figure 3.20**).

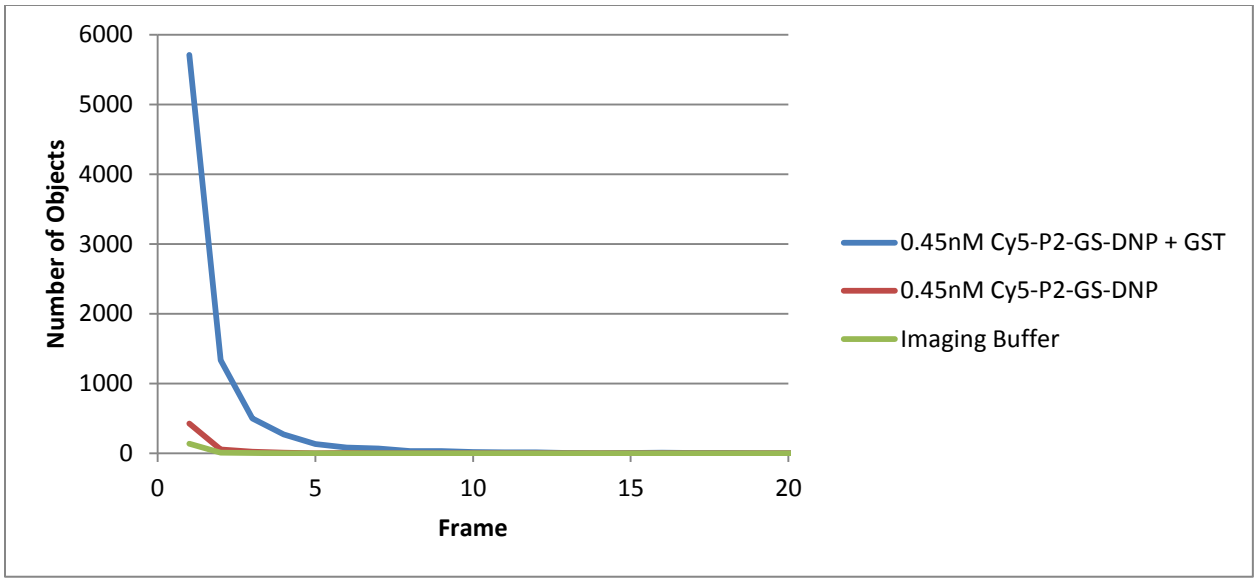

Figure 3.19: Number of objects identified in a sample with the fluorescent ligand Cy5-P2-GS-DNB and immobilized GST, with only Cy5-P2-GS-DNB, and in imaging buffer without any fluorescent ligand. In this particular experiment a high threshold of 120 counts was used resulting in the lower number of fluorescent objects.

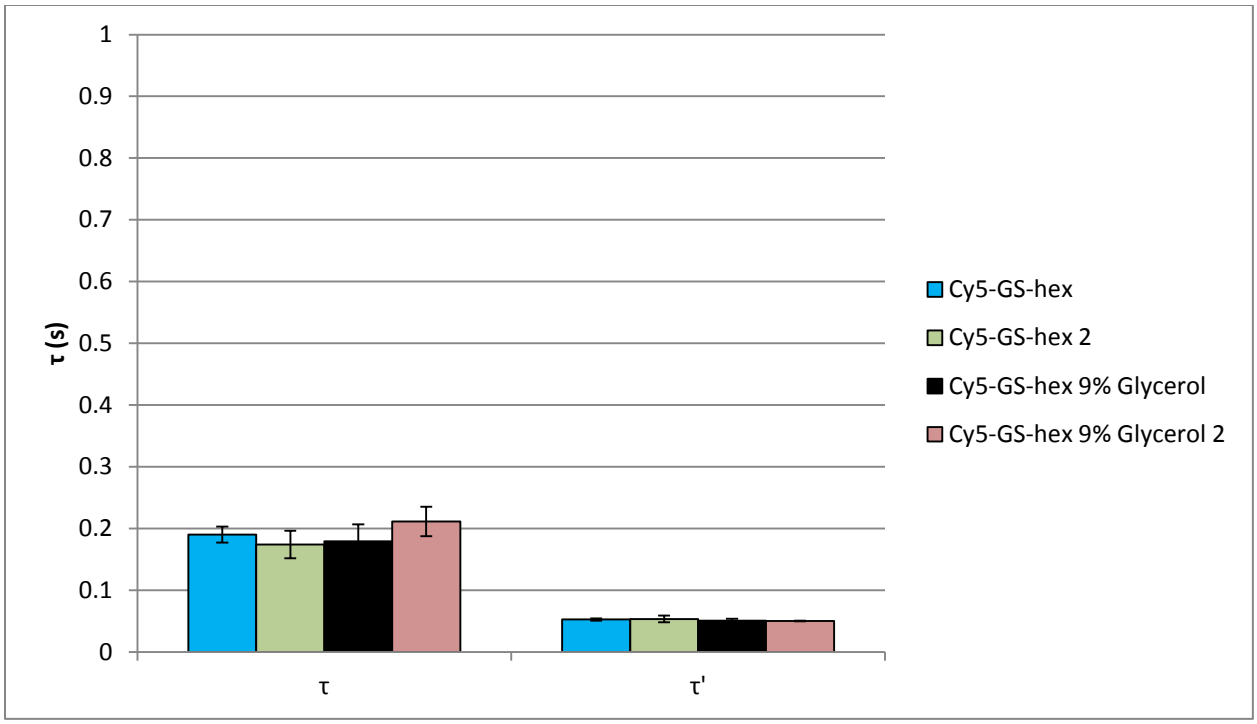

Figure 3.20: Reproducibility of average occupancy time of Cy5-GS-hex in water and 9% glycerol. The experiments were done on different days. The τ's has been adjusted for bleaching.

3.15 - Construction of GST Mutants

The effect of mutating residues in the active site of GSTA1-1 has already been evaluated by various labs, but there are only a few studies addressing what effects a mutation might have on the dynamics of the enzyme. [23,24,30,31] Since dynamics and catalysis seem to be closely related, affecting the catalysis might be a result of altered dynamics.[49] Mutations with strong effects on catalysis but not on substrate affinity would make good candidates for dynamic studies and were therefore constructed and expressed. Ile219 plays a role in the stability and positioning of the C-terminal region,[25] and Glu214 forms an electrostatic reaction with Arg217 stabilizing the helix. I219A and E214Q are therefore believed to alter the dynamics of the C-terminal helix. A Y9F mutant was constructed to generate a catalytically inactive enzyme that could be used as a control and a G223/C224 mutant was created for maleimide labeling with a FRET pair. A lysine to glutamate substitution in the AviTag was also generated as a non-biotinylatable control.

Site directed mutagenesis was used to create the mutants. Primers with the desired mutation were designed and mutant DNA was amplified in a PCR reaction. Template DNA was digested with DpnI (New England Biolabs) followed by heat shock transformation in to *E.coli.* A plasmid mini-prep (Thermo Scientific) was preformed from a single transformant and a sample of the purified DNA was sent for sequencing (Genewiz).

The average occupancy times of the mutant enzymes are indistinguishable from wild-type enzyme. However, the activities of some of the mutants are greatly affected by the mutation. The decrease in activity of the previously studied I219A mutation has been confirmed (**Figure 3.21**).[25,27,102] This verifies the importance the residue in the stability of the region.

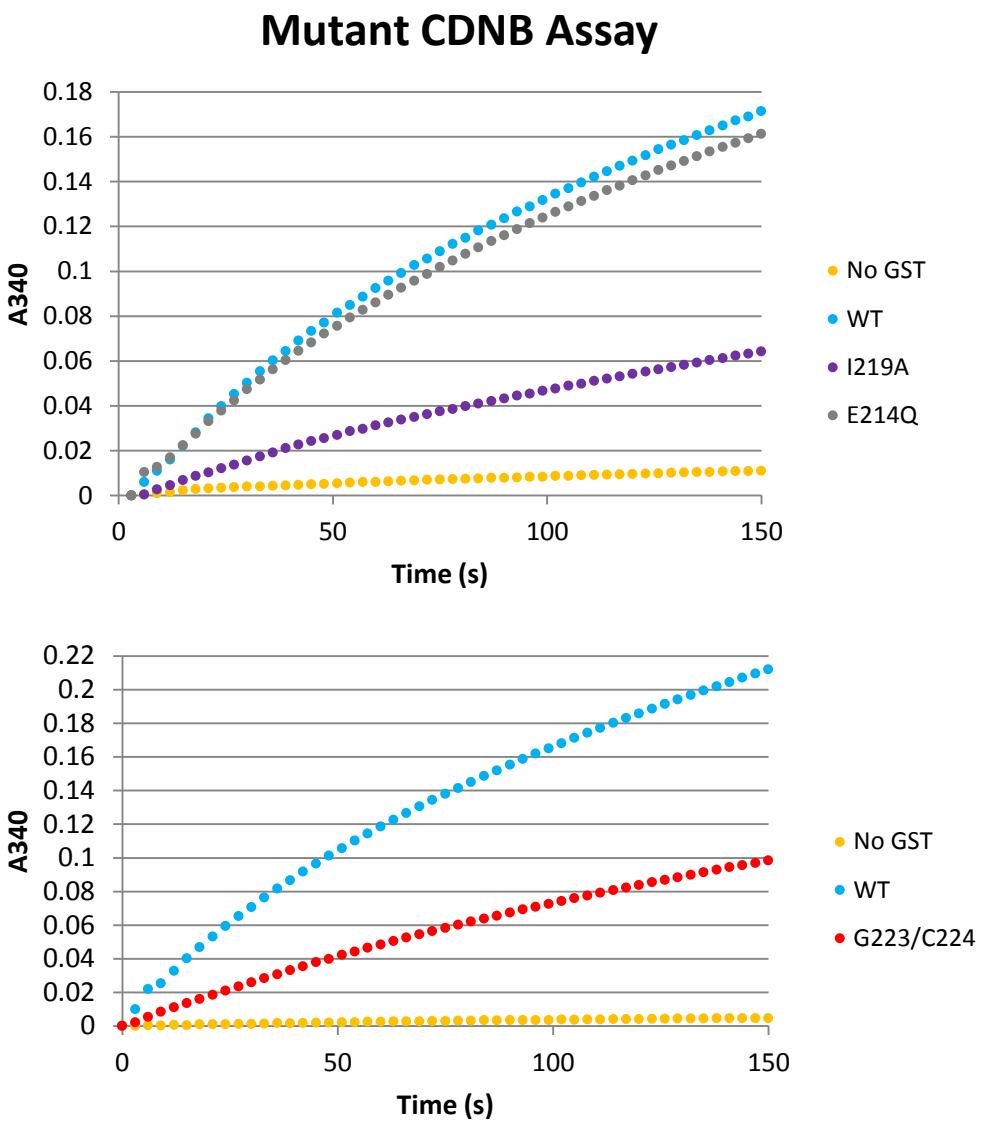

Figure 3.21: Activity of GSTA1-1 mutants. The inhibition assay with the different mutants were done on different days and are therefore presented in different plots. The I219A and G223/C224 mutants show decreased activity while the E214Q mutant does not.

Unexpectedly the novel E214Q mutation did not show any decrease in enzymatic rate (**Figure 3.21**). It is possible that disrupting the electrostatic interaction in the mutant is not significant enough to disrupt the helix and affect the activity of the enzyme. It is possible that the mutation disrupts the helix, but a rigid stable helix might not be necessary for localization and activity. It is possible that the mutation will affect other activities of the enzyme but not the CDNB assay.

The G223/C224 mutation created to enable fluorescent labeling for FRET studies and spin labeling for DEER experiments has altered activity as well. The catalytic rate of the mutant is about half of the wild-type enzyme (**Figure 3.21**). This is a bit surprising since a glycine linker was introduced to separate the cysteine from the active site. It is possible that the mutation is interfering with anchoring of the helix which is necessary for activity. Mutating residues at the C-terminal has shown to reduce the activity by preventing anchoring of the helix, and it seems like introducing additional residues have a similar effect on the activity. It is likely that the fluorescently or spin labeled enzyme is even less active.

The G223/C224 mutant does not bind the S-hexylglutathione resin as well as wild-type enzyme which suggest that the observed decrease in activity is at least partially a result of decreased affinity for the substrates (**Figure 3.22**).

The dramatic effect of mutations in the C-terminal proves how important the region is for the activity of the enzyme. The mutations show that helix anchoring points are important for the activity of the enzyme, but also that the sequence of the helix might not be as important as expected.

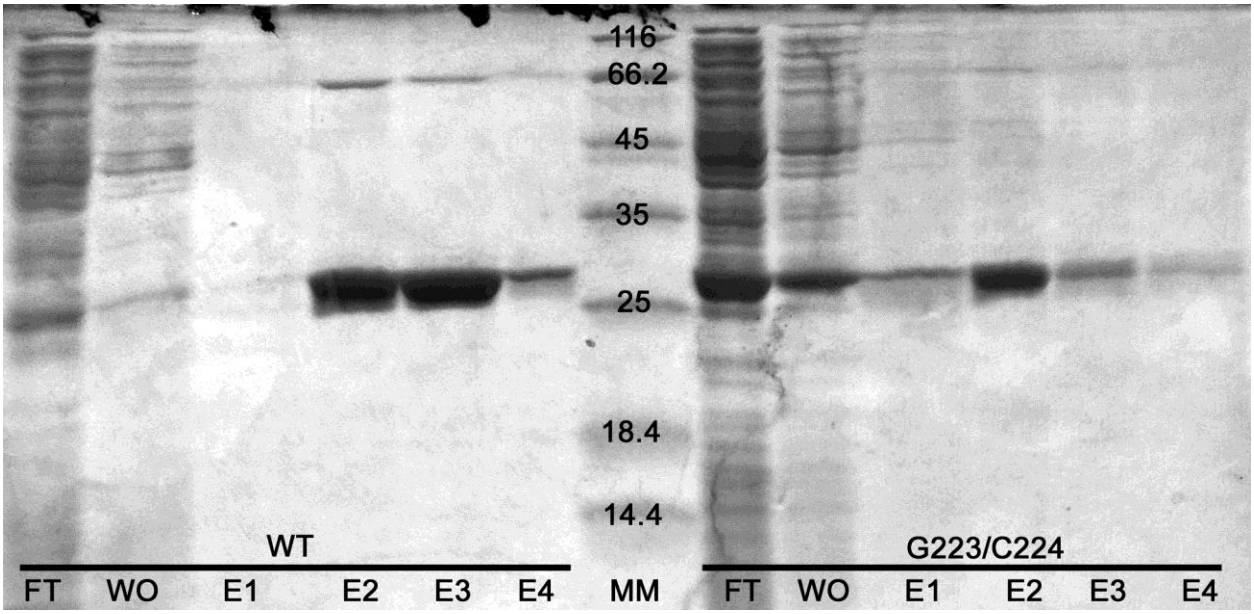

Figure 3.22: SDS-PAGE gel of GST purification fractions. Flow Through (FT), Wash Out (WO), and Elution Fractions (E1-E4) for wild-type GSTA1-1 and the G223/C224 mutation. The protein ladder is marked MM.

The mutant CDNB activity assays were done months apart with different batches of GSTA1-1 and substrates which might explain the small difference in the activity of the wild type enzyme.

3.16 - Shifting the Population of Binding States

Multiple binding states can be found through fitting a multi-exponential decay curve to the occupancy time histograms. Finding multiple binding states would suggest a heterogeneous population of enzyme. The majority of the number of binding events can be described by the fastest decay constant, the shortest average occupancy time. If there are multiple conformations there must be a chemical equilibrium between them that can be altered by changing the properties of the sample.

The disorder-to-order transition of the enzyme is triggered by ligand binding and the frequency of this transition must depend on the physiological properties of the sample. Hypothetically parameters such as temperature, ionic strength, pH, and viscosity could affect the ordering of the enzyme. One of the easiest properties to manipulate in the flow chamber at the stage of a microscope is the viscosity of the sample. In biology, this is commonly done by adding glycerol to the sample. Unfortunately glycerol has a different refractive index than water and glycerol addition to a sample would result in an increase in the depth of the evanescent field. A deeper evanescent field would result in a higher fluorescent background since more non-bound ligand diffusing in the sample would be detected. An alternative to using glycerol would be to use heavy water (D_2O). D_2O has a higher viscosity than water but still a quite similar refractive index and would be a suitable solvent for a single molecule experiment. D_2O

has less of a quenching effect than water and should therefore increase the fluorescence of a sample which would be an additional desirable feature.

Both glycerol and D_2O was used to increase the viscosity of the buffer. Glycerol is much more viscous than D_2O so 9% was used to match the viscosities. At 9% glycerol the refractive index is only slightly increased which should only have a marginable effect on the fluorescent background if any (**Table 3.5**). Imaging buffer with, dextrose, Trolox and ascorbate was lyophilized to replace water with D_2O. Only 1µl GOC is added per ml of D_2O imaging buffer causing a negligible dilution factor of the D_2O.

In a series of single molecule experiment the viscosity of the buffer was increased with either D_2O or glycerol and the average occupancy time calculated. In a biexponential model D_2O increased both the fast and slow average occupancy time while 9% glycerol had no effect on the average occupancy time (**Figure 3.17**). The fluorescence intensity increased in the D_2O sample due to less quenching and as a result more single molecules were detected.

3.17 - Non-Specific Binding of Cy5-GSH

In contrast to most labeled ligands Cy5-GSH is binding non-specifically to the flow chamber and is bleaching. No fluorescence recovery after photobleaching is observed indicating that the interaction is non-reversible. S-Cy5-GSH is not binding non-specifically suggesting that the free thiol of GSH is the main reason for the non-specific interaction of N-Cy5-GSH. In an attempt to block thiol reactive sites and the non-specific binding, the flow chamber was pre-treated with 1mM betamecaptoethanol (BME). The BME treatment was preventing most of the non-specific binding, but also the specific binding. It is unlikely that BME is forming disulfides

Table 3.5: Physical properties of water and heavy water at 20°C, *n* of fused silica is 1.457[103].

	Refractive index (*n*)	Viscosity (η), cP	Evanescent Depth (z_0), nm
Water	1.333[104]	1.002[105]	117.7
Heavy Water	1.327[104]	1.2467[105]	112.8
Glycerol	1.474[106]	1410[106]	-
9% Glycerol	1.344[106]	1.299[106]	128.4

with Cy5-GSH unless a large fraction of Cy5-GSH has been reduced to Cy5-GSSG-Cy5. Only the reduced form can be detected with mass spectrometry so the formation of a Cy5-GS-BME disulfide is unlikely. What might be more probable is that BME somehow disrupts the functionalized surface and in that sense prevents both specific and non-specific binding.

A more gentle approach to prevent the non-specific binding is to simply block the thiol reactive sites with non-labeled GSH. Since we know that the thiol of GSH is non-specifically and non-reversibly interacting with an unknown target in the flow chamber this should block all non-specific binding. By adding 1mM GSH to the flow chamber and incubating for 30min after immobilization of GST some of the non-specific binding could be prevented. Objects are still binding and bleaching, but new molecules from the buffer are constantly binding, which prevents the field of view from going completely dark. All Cy5-GSH still cannot be completely washed out of the flow chamber and if no Cy5-GSH is in the bulk solution all objects bleach completely.

A sum of two exponentials generates the best fit to the Cy5-GSH histogram of binding times, and two k_{off} are obtained. The two k_{off} will be a combination of k_b and k_d (**Eq. 3.6**). The k_b can be obtained from the bleaching of Cy5-GSH that has not been washed out from the flow chamber, and k_d can be calculated. Since there are two observed dissociation rate constants for Cy5-GSH k_b has to be subtracted from both of them. The bleaching rate of immobilized Cy5-GSH is $0.028s^{-1}$ and has been subtracted from the rates used to calculate the average occupancy times of the samples described in the next section.

3.18 - GST Conjugation of Cy5-GSH and CDNB

In contrast to all of the fluorescently labeled ligands Cy5-GSH is binding non-specifically to the flow chamber. The non-specific and non-reversible binding of Cy5-GSH results in bleaching, but the bleaching can be corrected for and the binding of the ligand to GST can still be studied. To study GSTs' catalytic function at the single molecule level the conjugation of Cy5-GSH to CDNB by immobilized enzyme was studied.

In a single molecule experiment the average occupancy times of Cy5-GSH was determined to 0.145s and 1.19s. Addition of 1mM CDNB dramatically increased the fluorescent intensity of the sample and the fluorescent threshold subtracted before single-molecule analysis had to be increased from 100 counts to 140 counts. Still, the average occupancy times increased to 0.203s and 6.74s. Even though the threshold was increased by 40 counts 33.4% more objects were observed after CDNB addition. The addition of CDNB alone had no effect on the fluorescence. The explanation is likely a result of GST conjugating Cy5-GSH and CDNB into the higher affinity Cy5-GS-DNB which has a higher occupancy time.

If the concentration of CDNB added to the Cy5-GSH sample is lowered from 1mM to 50µM a more subtle effect is expected. When the lower concentration of CDNB is used the average occupancy time changes from 0.130s and 0.873s to 0.128s and 0.930s. While this was only a slight change, the number of objects observed after CDNB addition increased by 26.8%. The same sample was imaged 1h after CDNB addition and the average occupancy time had increased slightly to 0.143s and 0.995s suggesting production of a higher affinity conjugate. The number of objects in the sample had increased by 55.6% compared to the sample without the

CDNB. Thus, adding GS-hex drastically decreases the number of objects by competing with binding of Cy5-GSH and Cy5-GS-DNB.

3.19 - Number of Binding Events vs. Concentration of Ligand & Average Occupancy Time

One way of testing the performance of the single-molecule TIRF imaging system is to investigate how the concentration of ligand used scale with the number of binding events detected. If the same types of binding events are detected at different ligand concentrations the number of observed binding events should have a linear correlation to the concentration of ligand used. This is only true if there are enough unoccupied active sites available in the flow chamber to accommodate the higher concentration of ligand.

It turns out the imaging system and image processing procedure performs well in the concentration range used. Cy5-GS-hex at 106pM, 212pM, and 425pM show a linear relationship between concentration and the number of objects detected. A very small variance in the number of objects detected in duplicate samples was observed **(Figure 3.23)**.

Varying the concentration of ligand should not affect the average occupancy time as long as single molecule binding events are well resolved and do not overlap. The average occupancy time was calculated from the same samples that were used to show the linear relationship between ligand concentration and number of binding events detected. Only a very slight shift towards longer average occupancy time was observed when the concentration of Cy5-GS-hex was increased from 106pM to 425pM. The shift was only visible for the slower of the two average occupancy times obtained from a fit with two exponentials, which was calculated from much fewer single molecule binding events than the faster average occupancy

time. This observation could be explained by some binding events overlapping when higher concentration of ligand is used resulting in a longer occupancy time. Both samples of the duplicates are presented to display the small shift in average occupancy time between samples **(Figure 3.24)**.

3.20 - Effect of Threshold

During the detection of the 3D-objects a threshold has to be set to avoid background fluctuations in fluorescence from being detected as single molecule binding events. The camera has a dark count of about 73 and a threshold is usually set slightly above that to remove some of the fluorescent background. The level of the threshold affected the number of objects detected but not the distribution of the objects detected. This means that long and short binding events are equally bright **(Figure 3.25)**.

If a sum of three exponentials is fitted to the histogram of occupancy times of Cy5-GS-DNB binding to immobilized GSTA1-1 using two different thresholds the same average occupancy times are obtained **(Figure 3.26)**. This indicates that the threshold setting has no effect on the average occupancy times.

3.21 - Conclusion

The fluorescent ligands that were constructed have been employed to detect and characterize different binding states to GSTA1-1 which should be related to conformational substrates of the enzyme. To accomplish this GST was immobilized to a functionalized surface though an N-terminal biotin. It has also been verified that immobilized GSTA1-1 is active. A

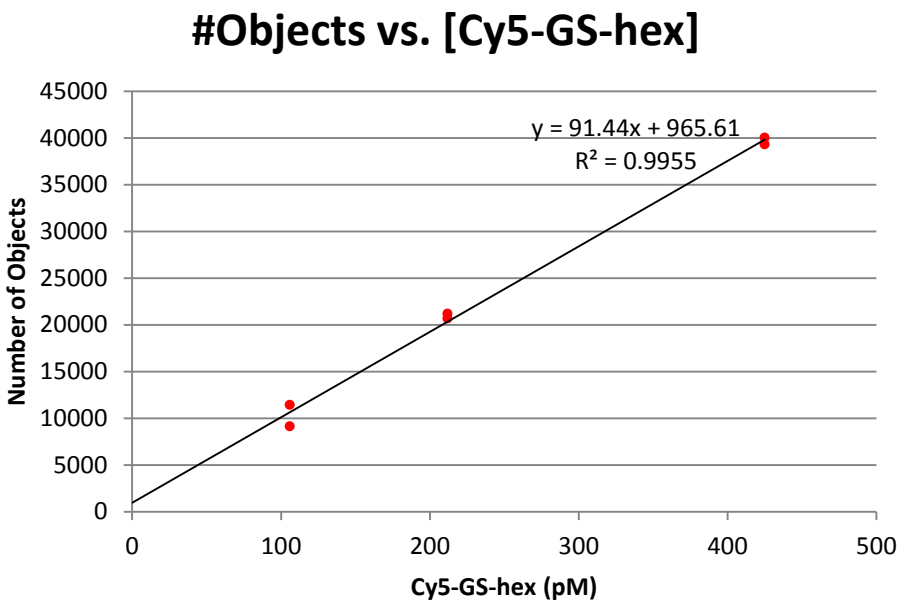

Figure 3.23: The number of objects detected has a linear relationship to the ligand concentration. The number of objects detected is very reproducible. Both data points of duplicate samples are presented.

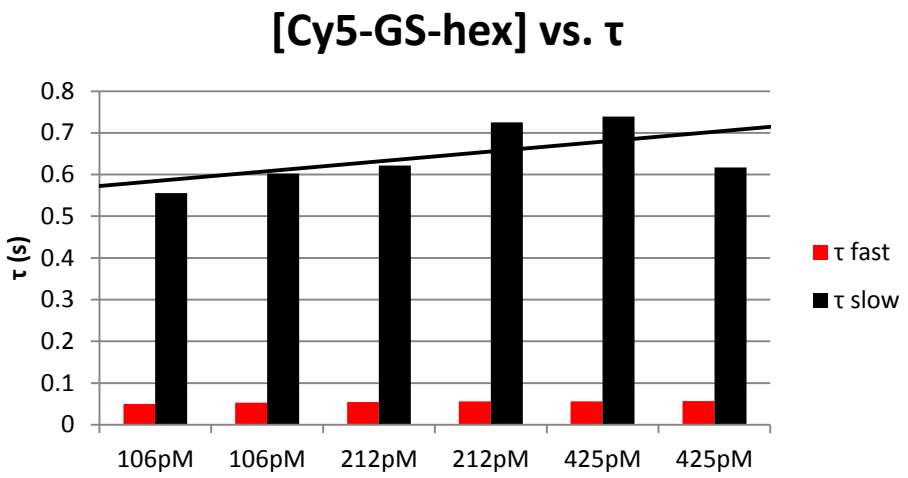

Figure 3.24: The effect of Cy5-GS-hex concentration on average occupancy time. A trend line was added to display the small increase in the long average occupancy time with higher ligand concentration.

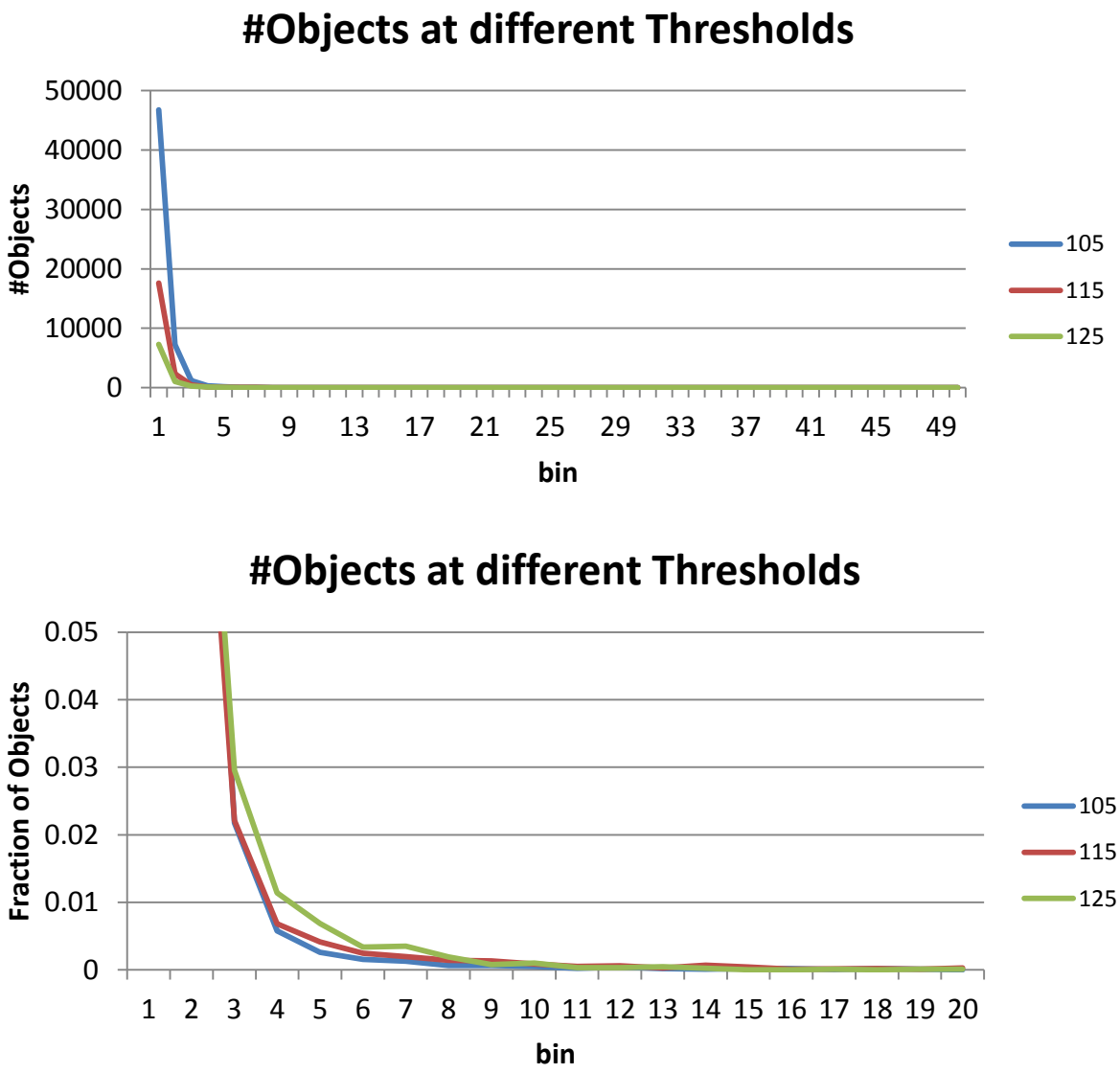

Figure 3.25: The thresholds effect on the average occupancy time. Each bin represents a frame of 100ms exposure. Only a very slight shift towards longer average occupancy times can be observed with a higher threshold suggesting that the longer binding events are only slightly brighter.

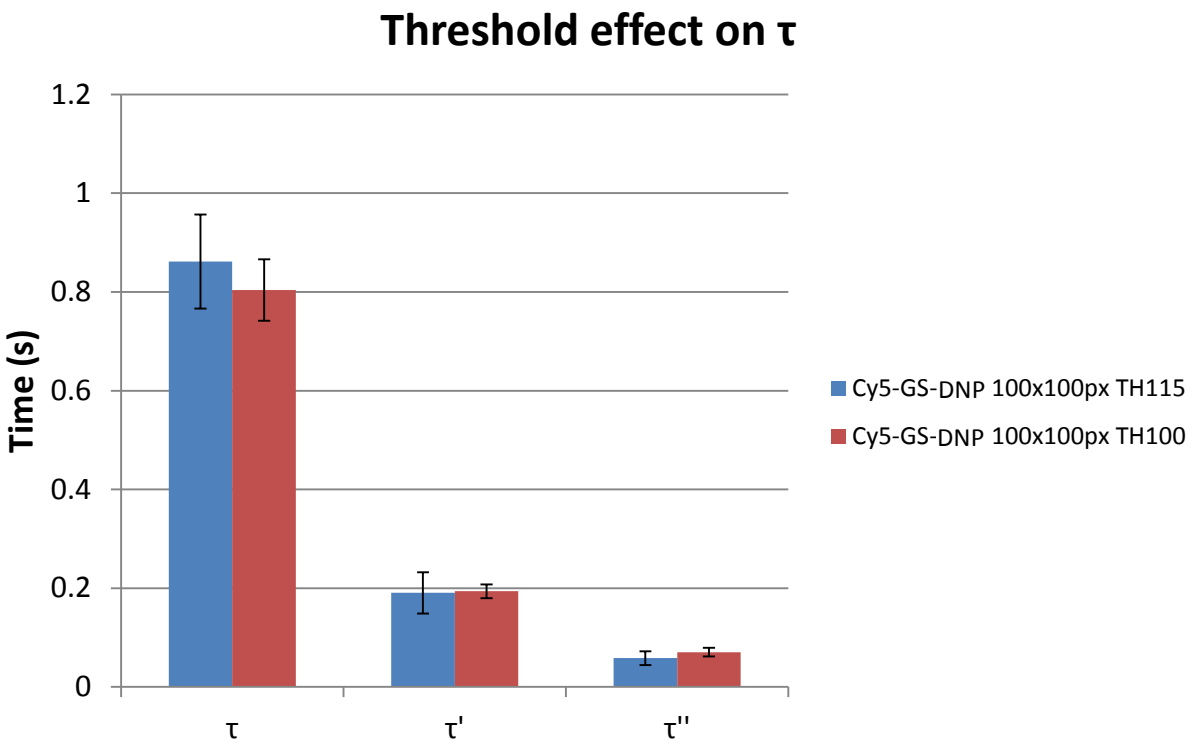

Figure 3.26: The thresholds effect on average occupancy time for Cy5-GS-DNB. For a fit with a sum of three exponentials a higher threshold does not affect the average occupancy time. The slow average occupancy time is similar to what was obtained when Cy5-GSH was incubated with CDNB forming Cy5-GS-DNB.

histogram of occupancy times for a particular ligand and imaging condition was constructed to which a sum of exponentials was fitted. The fitted curve was used to obtain the average occupancy times for the ligand. The fact that a sum of exponentials generates the best fit to the histogram of occupancy times suggests the existence of multiple binding states.

In addition to characterizing the binding kinetics of the fluorescent ligands to GST the enzyme is capable of conjugating a fluorescently tagged GSH to CDNB. This enabled us to image a single turnover event of an enzyme. The fluorescent product, Cy5-GS-DNB, also has affinity for the enzyme and it can be hard separating a Cy5-GSH or Cy5-GS-DNB binding event from a Cy5-GSH binding and conjugation event. The enzymatic rate with labeled GSH is much slower than that of GSH suggesting that having a linker sticking out of the active site negatively affect the catalytic capabilities of the enzyme.

The fluorescently tagged ligands are binding immobilized GSTA1-1 specifically and to the active site. When the ligands are bound to GST in the high intensity of the evanescent field they will slowly bleach. The bleaching becomes more significant for higher affinity ligands with longer average occupancy times. By calculating the bleaching rate of the dye the average occupancy time can be corrected for bleaching.

The effect of different microscope settings and data analysis parameters on the average occupancy time has been thoroughly evaluated. The exposure time and threshold used during the single molecule imaging has very limited effect on the average exposure time. The concentration of ligand used determines the number of objects detected, but it does not affect the average occupancy time.

To further characterize the heterogeneity of the enzyme the conformation of the active site during ligand binding will be studied using FRET and DEER. The experiments will be setup to study the difference in distance between the C-terminals and might reveal more conformational states than the previously reported disorder-to-order transition upon ligand binding.

Chapter 4 - Conformational Dynamics of GSTA1-1 Active Site

4.1 - Introduction

In addition to characterizing the binding kinetics of the fluorescent ligands we were also interested in the dynamics of the active site, particularly the C-terminal helix, as a ligand binds to the enzyme. Single molecule FRET studies could reveal the distribution of conformations of the helix. FRET would not necessarily reveal the existence of multiple conformers, like the single molecule binding kinetics experiments described in chapter 2, but could be employed to determine the distribution of helix conformations when different ligands are bound to the enzyme. The GSTA1-1 G223/C224 mutant was labeled with the FRET-pair Cy3 and Cy5. The rate of energy transfer should change as the helix localizes, and it might be possible to identify the asymmetric state where one C-terminal is disordered and the other one localized.

To confirm the FRET results DEER was used. The same GSTA1-1 G223/C224 mutant can be spin labeled with MTSL to introduce unpaired electrons into the enzymes structure. The labeled enzyme can be used to determine the distance distribution between the two labeling sites with and without ligand present.

4.2 - GSTA1-1 Labeling for FRET

The thiol of cysteines is commonly used to specifically label proteins and there are various reactive groups that under certain conditions will conjugate a label to the residue. To ensure specific labeling the number and location of cysteines in the protein might have to be altered.

In order to specifically label GSTA1-1 a mutant with a C-terminal cysteine was constructed. This cysteine was specifically labeled with a fluorescent tag using the thiol reactive maleimide form of the dye. To separate the label slightly from the active site, so as to avoid altering the activity of the enzyme, a glycine linker was introduced as well. The distance between the alpha carbons of the most C-terminal residue in each monomer (F222) can be used to approximate the distance between the two labels. In the X-ray crystal structure of GSTA1-1 with GS-hex bound (PDB entry 1K3L) and the helix is localized this distance is 27.1Å. The addition of two amino acids and a label might increase or decrease this distance slightly depending on the conformation of the additional residues. This is too far apart to form disulfides between the C-terminals in the dimer. The formation of disulfides between different enzymes is possible but TCEP was added in excess during labeling to reduce any disulfides present. It is reasonable to hypothesize that when the C-terminal is non-localized and unstructured this distance will increase. The FRET pair Cy3 and Cy5 has an R_0 of 60Å and should be suitable for this application. The GSTA1-1 G223/C224 mutant was labeled with 10-fold excess sulfo-Cy3-maleimide as well as 10-fold excess sulfo-Cy5-maleimide in 25mM HEPES pH 7.3. This generated a mixed population of enzyme labeled with both Cy3 and Cy5 as well as enzymes labeled with just Cy3 or Cy5. This is not necessarily an issue since energy transfer will only be observed for enzymes labeled with Cy3 and Cy5. Three different FRET states are expected; one for when both C-terminals are disordered, one for when one C-terminal is ordered as a helix and the other C-terminal disordered, and one for when both C-terminals are ordered as helices. The localization of the helices should be triggered by addition of ligand and a change in the distribution of FRET states should be observed (**Figure 4.1**).

FRET State 1:

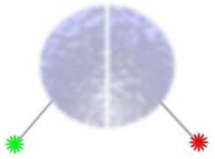

FRET State 2:

FRET State 3:

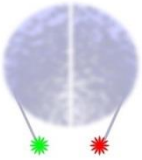

Figure 4.1: The expected FRET states of labeled G223/C224 GSTA1-1. State 1 represents the unlighted form of the enzyme where the distance between donor and acceptor should be the longest and the energy transfer rate the slowest. State 2 represents the semi-ligated form of the enzyme where one helix will be localized. State 3 represents the conformation where ligand is bound to both active sites and both helices are localized.

Single color FRET can potentially also be used to look at different states of the enzyme. A GSTA1-1 labeled solely with Cy3 or Cy5 should display different fluorescent intensities as the conformation of the enzyme changes. Since the two dyes are within FRET distance and close enough for energy transfer quenching of the fluorescence is also possible. The Cy5-emission could be quenched when both helices are localized and increase in two steps when unstructured.

PIFE has been observed for a Cy5-labeled ligand binding GST suggesting that the quantum yield of the dye increases in proximity to the active site. Assuming that the same is true for Cy3 it would result in more efficient energy transfer and brighter Cy5-signal for Cy3/Cy5-GST and more efficient quenching for Cy3-GST and Cy5-GST.

4.3 - Labeled GST Species

If the thiols of the GSTA1-1 G223/C224 mutant are labeled with a 10-fold excess of equal amounts of Cy3-maleimide and Cy5-maleimide the result will be a mixed population of labeled enzyme. Since the reactive dye is used in excess it can be assumed that all cysteines have been labeled. The end result, however, will be a mixed population of enzyme, some will have one Cy3 and one Cy5, some will have two Cy3, and some will have two Cy5. The distribution of the different populations can be described by a binomial expansion (**Equation 4.1 and 4.2**).

$$(p+q)^2 = 1 \qquad \text{(Eq. 4.1)}$$

$$p^2 + 2pq + q^2 = 1 \quad \text{(Eq. 4.2)}$$

The ratio between the two dyes can be determined by absorbance and the distribution of the different populations calculated. The result is that 67.5% of the dye in the Cy3/Cy5-GST sample is Cy3 and 32.5% is Cy5. This is giving the following fractions of the labeled species; 45.5% Cy3/Cy3-GST, 43.9% Cy3/Cy5-GST, and 10.6% Cy5/Cy5-GST (**Table 4.1**). The absorbance of Cy5 at 550nm and the resulting fluorescence has been corrected for.

The calculated dye concentration matches up fairly well with the protein concentration, but this is not supposed to be the case. The dye concentration should be twice the protein concentration. This anomaly could be the result of a non-efficient labeling reaction where only half of the cysteines present have been labeled. Interestingly this was not the case. The reason for the observed low ratio of labeling turned out to be the absorbance of the cyanine dyes at 280nm. The protein concentration was determined using 280nm absorbance and the dye contributing to the absorbance was thereby artificially decreasing the labeling ratio of dye per protein. Even if the absorbance of the cyanine dyes at 280nm seems to be at baseline compared to their high peak absorbance this is not the case. Despite the fact that the peak absorbance of the dyes is much higher than that of the protein, the absorbance of the dye and the protein at 280nm are quite similar. Once this was taken into consideration the dye to protein ratio turned out to be 2.6. The reason for a labeling ratio higher than 2 could be the presence of some residual dye in solution, and some non-specific labeling of amines.

Using 10-fold excess dye during labeling might seem wasteful, but if we use less dye in the labeling reaction we risk ending up with a fraction of non-labeled enzyme. The fraction of

Table 4.1: Relative concentration of Cy3 and Cy5 in Cy3/Cy5-GST as well as the calculated concentrations of the different labeled species following a binomial distribution.

Cy3 in Cy3/Cy5-GST	67.5%
Cy5 in Cy3/Cy5-GST	32.5%
Cy3/Cy3-GST	45.5%
Cy3/Cy5-GST	43.9%
Cy5/Cy5-GST	10.6%

each species would then be described by trinomial expansion (**Equation 4.3 & 4.4**). Non-labeled GST is not an issue in our fluorescence experiments as long as the immobilized GST density is high, but having a larger population of enzyme where energy transfer cannot occur will decrease the number of events that can be observed.

$$(p + q + r)^2 = 1 \qquad \text{(Eq. 4.3)}$$

$$p^2 + q^2 + qr^2 + 2pq + 2qr + 2rp = 1 \qquad \text{(Eq. 4.4)}$$

If GST is as tightly packed on the biotinylated slide as we predict immobilizing labeled enzyme would merely generate a strong fluorescent glow since the resolution limit is below the spatial separation of the immobilized dyes. This has previously been observed in our lab for singly non-specifically labeled Cy5-GST. If the labeled enzyme is diluted in imaging buffer it would only get immobilized close to the injection site of the chamber but it would not generate a controllable dilution of fluorescent GST on the surface. To be able to separate Cy3/Cy5-GST and evenly immobilize it on the surface it was cut with non-labeled GST 3000-fold.

To better understand how the properties of the dye are affected by conjugation to GST a singly labeled GST was also made. This was accomplished by minimal labeling where the GST monomer was used in 10-fold excess to the dye. The result is a predominantly singly labeled GST. Most enzymes will lack a label but that does not matter since we can calculate the fraction that has been labeled form the dye absorbance. This labeled species is referred to as CyX-GST-min. Since the doubly labeled GST has to be cut with non-labeled enzyme to be spatially

separated in a single molecule experiment it does not matter that some GST in the Cy3-GST-min sample lack a fluorescent tag. The fluorescence of CyX/CyX-GST is weaker than that of CyX-GST-min, when normalized to absorbance, suggesting that some quenching does occur in the doubly labeled enzyme (**Figure 4.2**).

It could be possible that the labeling of GST is cooperative and that even when enzyme is used in excess to reactive dye most enzymes are labeled with two dyes. The labeling can be analyzed by looking at the bleaching pattern of a single immobilized labeled enzyme. The bleaching of Cy3-GST-min occurs in a one step process where all of the fluorescent intensity is lost. The bleaching of Cy3/Cy3-GST occurs in a one-step or a two-step process (**Figure 4.3**). The reason that some one-step bleaching can be observed even for Cy3/Cy3-GST could be that one dye is quenched and not fluorescent, that the bleaching of the two dyes sometimes is cooperative or simultaneous, or that some enzyme dimers have only one conjugated dye. Since no two-step bleaching events were observed for immobilized Cy3-GST-min most enzymes are expected to be singly labeled. This could be analyzed further using MS.

4.4 - Dye Quenching

It is possible that the region around the active site will be very crowded in the G223/C224 mutant, where additional amino acids have been added, when both cysteines have been labeled with a large fluorescent dye, and when GS-hex is bound. This could potentially quench the fluorescence of the dyes by their close proximity, or by the environment of the active site. It cannot be excluded that GS-hex is contributing to quenching by directly interacting with the dye and not by initiating a conformational change of the active site. No

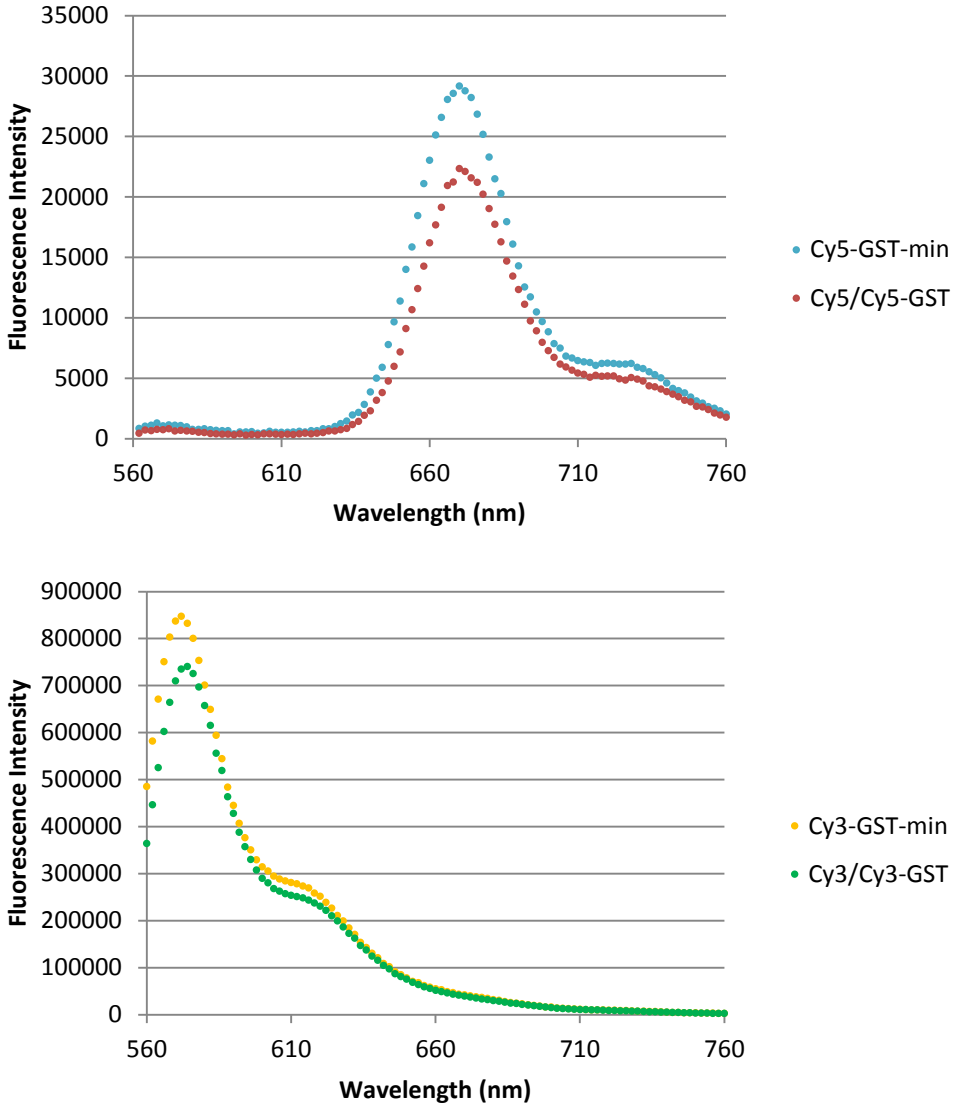

Figure 4.2: Emission of singly labeled (CyX-GST-min) and double labeled (CyX/CyX-GST) GST with 550nm excitation. The emission data has been scaled to the absorption data to correct for differences in concentration between the samples. The fluorescence of singly labeled enzyme is brighter suggesting that some quenching occurs in the doubly labeled enzyme.

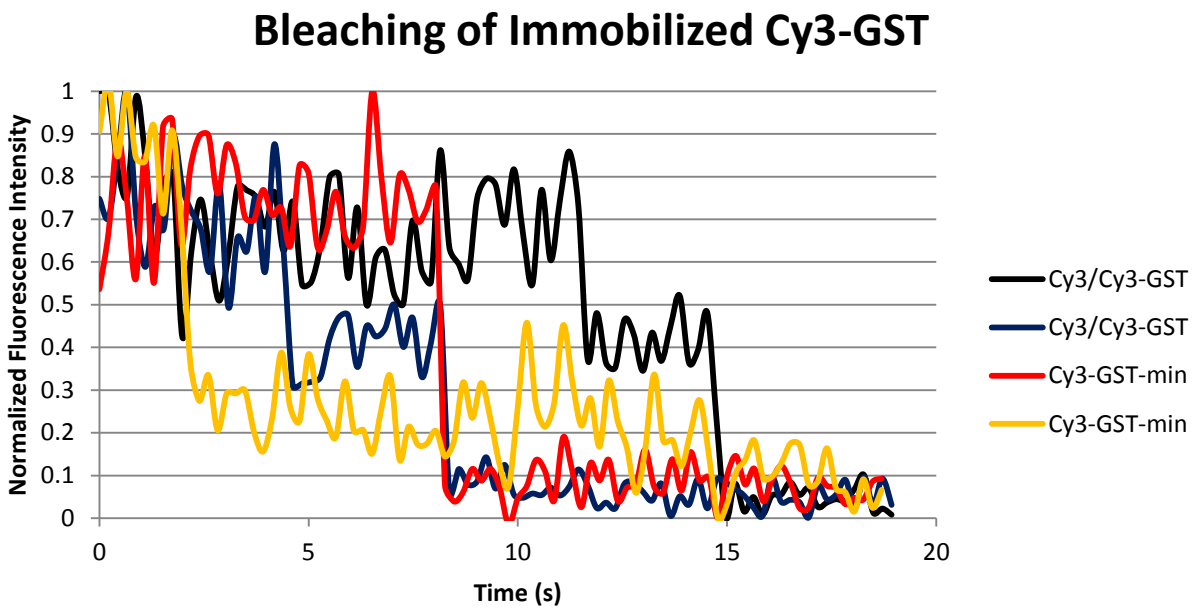

Figure 4.3: Bleaching pattern of Cy3-GST-min and Cy3/Cy3-GST. Immobilized doubly labeled Cy3/Cy3-GST bleach in a two-step or one-step process while immobilized Cy3-GST-min only bleach in a one-step process. This suggests that the minimal labeling of GST results in a singly labeled enzyme.

decrease in the fluorescence was observed when GS-hex is added to Cy3 or Cy5 in solution, but the environment close to the active site might be different from that in solution.

When GS-hex is added to Cy3/Cy5-GST a decrease in donor fluorescence is observed. The proposed reason is an increase in energy transfer between the dyes as the C-terminal helices localize and the distance between the dyes decreased. The decrease in fluorescence with GS-hex addition is also observed for Cy3/Cy3-GST and Cy5/Cy5-GST. This was probably a result of non-radiative energy transfer between the dyes resulting in quenching of the fluorescence. A fraction of the GST in the Cy3/Cy5-GST sample will be labeled with two Cy3 or two Cy5. The Cy3/Cy3-GST and Cy5/Cy5-GST controls can be used to subtract the emission from those species from the emission spectra of the Cy3/Cy5-GST sample, thereby getting the emission spectra from Cy3/Cy5-GST alone, with and without GS-hex (**Figure 4.4**).

The Cy3-GST-min show less quenching with the addition of GS-hex than Cy3/Cy3-GST does, suggesting that the observed decrease in fluorescence is caused by energy transfer (**Figure 4.5**). The emission intensity of Cy3/Cy3-GST decreases with 37% when GS-hex is added while the emission intensity of Cy3-GST-min decreases with 6%. This supports dye quenching. It is possible that the GS-hex somehow induces quenching more in a doubly labeled enzyme since the area around the active site is more crowded.

4.5 - Ensemble FRET

Before attempting to perform a single-molecule FRET experiment the labeled GST can be tested for occurrence of FRET in an ensemble experiment. If energy transfer can be detected and a change in energy transfer can be observed with the addition of a ligand we might be able

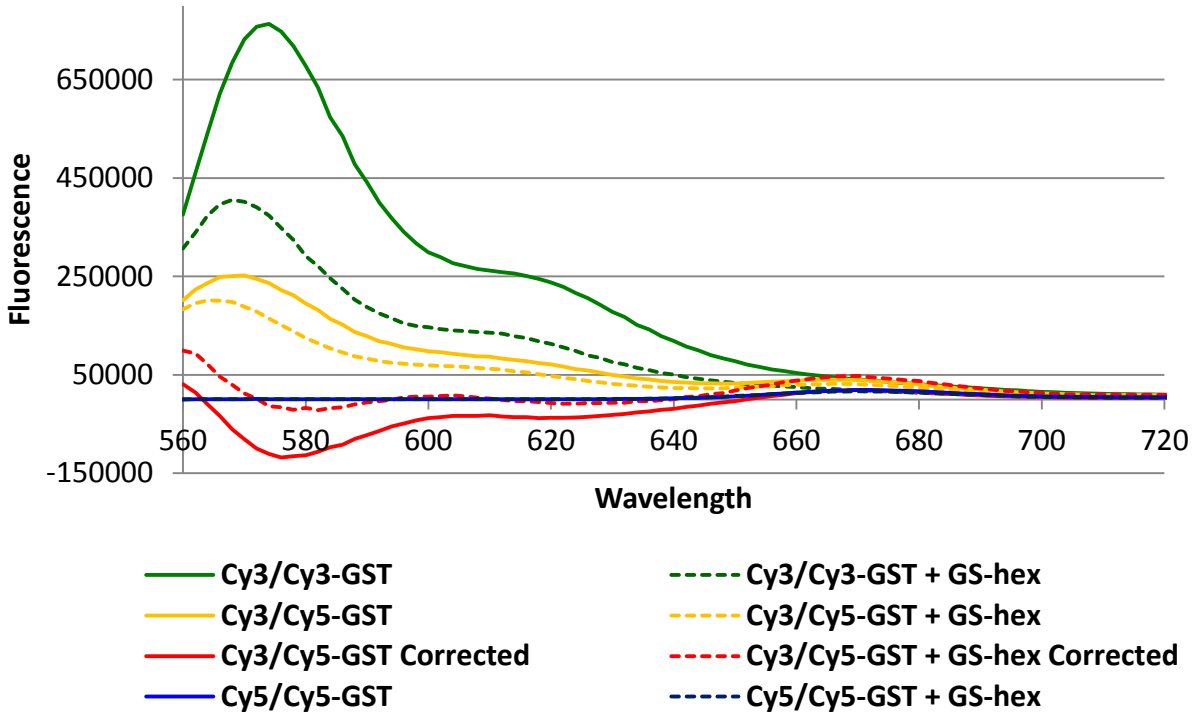

Figure 4.4: Ensemble FRET test of Cy3/Cy5-GST. The fluorescence emission spectra of Cy3/Cy5-GST at 550nm excitation with and without GS-hex present. The contribution from Cy3/Cy3-GST and Cy5/Cy5-GST has been corrected for. Negative values are obtained for the corrected Cy3/Cy5-GST emission which suggests that something is inaccurate in the correction. The peak shift during ligand binding could be one contributing factor.

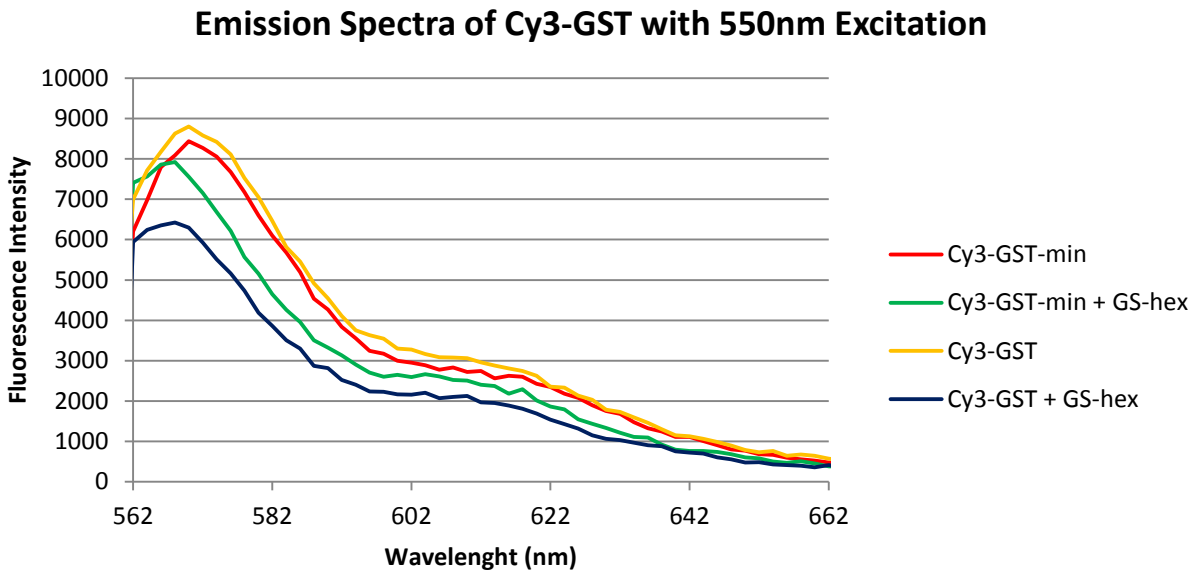

Figure 4.5: Quenching of Cy3-GST and Cy3-GST-min with the addition of 25µM GS-hex. The decrease in fluorescent intensity upon addition of GS-hex is greater for Cy3-GST than for Cy3-GST-min suggesting that the dyes of the fully labeled GST do quench when a ligand is bound. A blue shift in emission can be observed with GS-hex addition. The addition of GS-hex must therefore affect the environment of the dye in the active site.

to characterize different FRET states in a single molecule experiment. The ensemble FRET experiments were done in a 96-well plate by collecting the emission spectra using a Tecan Safire2 Fluorescence Plate Reader.

The ensemble FRET experiments are somewhat complicated by the complexity of the Cy3/Cy5-GST sample. The sample does not only contain Cy3/Cy5-GST but also Cy3/Cy3-GST and Cy5/Cy5-GST, and the spectra collected from the sample will be a combination from all species. However, the fraction of Cy3 to Cy5 in the sample can be calculated and from that the concentration of each species. By collecting the spectra of Cy3/Cy3-GST and Cy5/Cy5-GST and subtracting them form the Cy3/Cy5-GST sample the contribution from Cy3/Cy5-GST only can be calculated (**Figure 4.4**). The emission is scaled by the peak absorbance and the low absorbance of Cy5 at 550nm is included in the correction. The same experiment can be repeated in the presence of a ligand and the change in FRET efficiency calculated. The FRET efficiencies can then be used to calculate the distance between the donor and acceptor dye.

Unfortunately the calculated spectrum of Cy3/Cy5-GST has negative values at the Cy3 peak emission, while positive values at Cy5 peak emission (**Figure 4.4**). This could be a result of an error in the conversion from the emission spectrum of mixed species to the spectrum of Cy3/Cy5-GST. The Cy3 emission of Cy3/Cy3-GST is about three times as intensive as Cy3/Cy5-GST which is resulting in the negative values after correction. Since the spectra has been normalized and 67.5% of the dye in the Cy3/Cy5-GST sample is Cy3, a 1.5:1 ratio in intensity between Cy3/Cy3-GST and Cy3/Cy5-GST sample is expected if no dye interaction resulting in energy transfer or quenching is occurring. One obvious reason for the lower intensity in the Cy3/Cy5-GST sample could be energy transfer. Even if energy transfer is occurring the Cy3

emission in the calculated Cy3/Cy5-GST spectra should certainly never be negative. Until the unexpected results can be explained and the issue with negative emission resolved it is impossible to calculate the FRET efficiency and distance between donor and acceptor. The fluorescence intensity of all labeled species decrease in the presence of GS-hex which changes all the spectra used to calculate the Cy3/Cy5 emission spectrum. The emission is also blue shifted once GS-hex is added. None of these observations could explain the negative emission for Cy3/Cy5-GST.

There are orientations of the dyes that are more efficient for energy transfer. It is possible that in a disordered C-terminal the dye is capable of rotating freely, similar to a dye in solution. When one helix or both helices localizes this might occur in an orientation non-favorable for energy transfer, decreasing the FRET efficiency although the dyes are closer in distance than when the helices are disordered. To evaluate the behavior of a C-terminal dye fluorescence polarization can be used. Different rotational diffusion coefficients should be obtained if the dye act similarly to a free dye in solution without ligand present, or if they act more like a dye immobilized on the protein when the helix is localized. If the localization restricts the rotation of the dye this could affect the observed energy transfer.

4.6 - SM-FRET

With the inconclusive results from the ensemble FRET experiments it seems reasonable to attempt single molecule FRET experiments. The ensemble FRET experiments are complicated by the multiple number of fluorescent species in the sample. In a single-molecule experiment

only immobilized Cy3/Cy5-GSTs that show both Cy3 and Cy5 emission can be selected. A two channel system is needed to be able to simultaneously detect Cy3 and Cy5 emission.

Single-Molecule imaging was done using a Nikon Eclipse Ti microscope, a Photometrics Evolve 512 EMCCD Camera, a Photometrics DV2 beam splitter with a 640nm dichroic reflector, a HQ600/50m and a ET700/75m filter, a Nikon 60x Plan Apo objective, and the Nikon NIS Elements software. The system is equipped with a 640nm red laser and a 532nm green laser. The same type of flow chamber as in the regular TIRF experiments can be used but since the Nikon Eclipse Ti setup is a through the objective TIRF system the evanescent field will be at the cover-glass buffer interface and not the fused silica slide buffer interface. Data analysis was done in imageJ.

In a single molecule FRET experiment the green laser is used to excite the Cy3 of Cy3/Cy5-GST. Energy transfer would result in the appearance of red emission in the Cy5 channel. To obtain the FRET efficiency and identify different conformations of the active site the fluorescence from both Cy3 and Cy5 of a single molecule has to be recorded. The emission from the two channels should be anti-correlated where the donor emission decrease and the acceptor emission increase upon energy transfer.

To validate that the Cy3 and Cy5 of immobilized Cy3/Cy5-GST are fluorescent both red and green light was used to excite the labeled enzyme. If the fluorescence from the Cy3 (green) and Cy5 (red) channels are overlaid objects can be observed that are emitting photons of both wavelengths (yellow) (**Figure 4.6**). Four frames using 100ms exposure from each channel was used for the overlay. If the transition between different FRET states is fast a shorter exposure time might be needed.

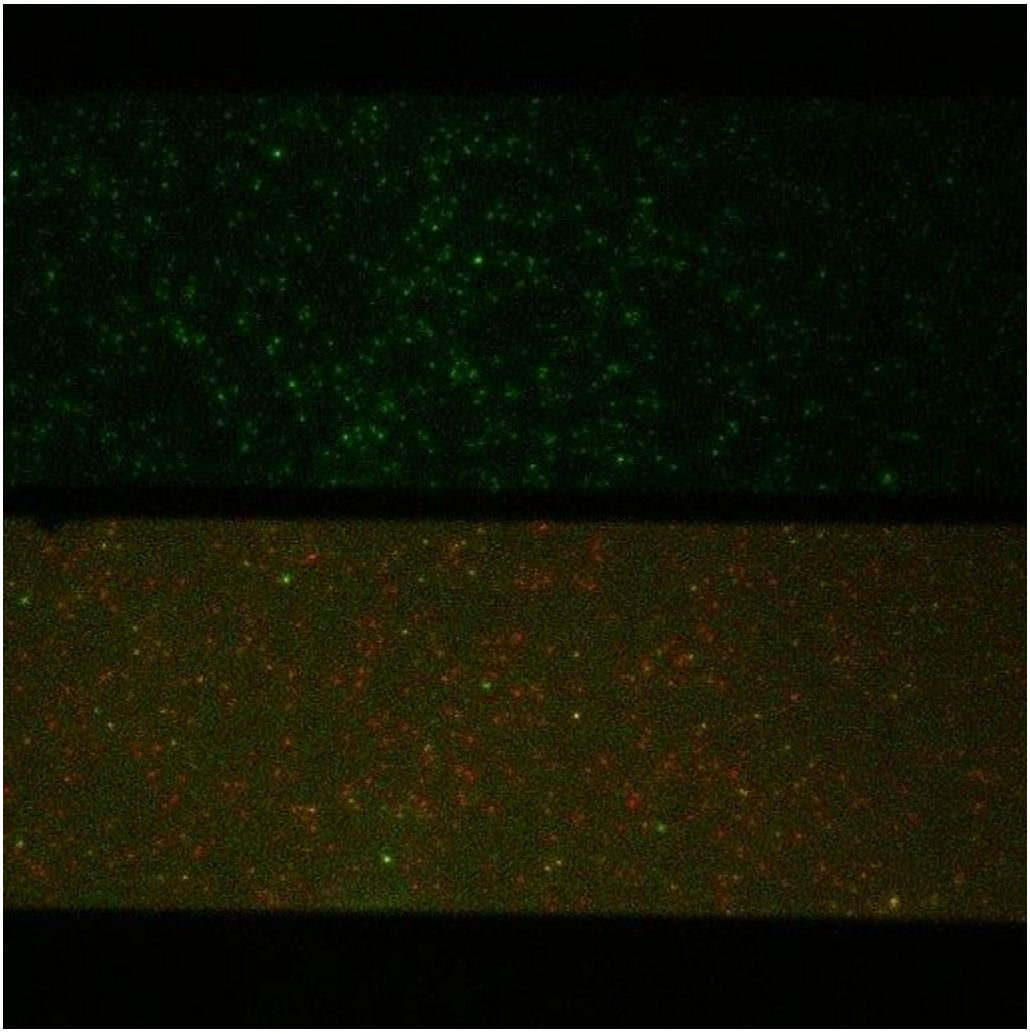

Figure 4.6: Overlay of Cy3 emission (top) and Cy5 emission (bottom) using 532nm (green) and 640nm (red) excitation. Some overlap can be seen in the Cy5 channel suggesting that some of the objects accepting Cy3 emission can also be excited using a 640nm laser. Notice the absence of Cy3 emission using 640nm excitation.

To detect an enzyme where energy transfer between Cy3 and Cy5 occurs the emission from Cy3 has to be overlaid with the emission from Cy5 using only Cy3 excitation (532nm). Ten frames using 100ms exposure were combined and overlaid. Some of the objects can be observed in both channels (**Figure 4.7**). Cy5 can be excited by 532nm light but the resulting fluorescence would be very dim. The few objects observed with both Cy3 and Cy5 emission is therefore likely the result FRET.

Although both Cy3 and Cy5 emission is observed for immobilized Cy3/Cy5-GST only very few two-channel fluorescence time trajectories have been observed where the intensity of the two channels are anti-correlated. One of the main reasons for this is bleaching. By conjugating the label to GST, which is immobilized in the evanescent field, instead of the ligand, which is diffusing in solution when not bound to an immobilized GST, the dye will bleach much faster.

A higher laser intensity can be used with the single molecule FRET-TIRF setup, enabling the use of shorter exposure time, and thereby the analysis of faster events, but a higher laser intensity is also resulting in faster bleaching. The bleaching of immobilized Cy5-GST on the prism TIRF system is slower, at least initially. This was tested by studying bleaching of the same Cy5/Cy5-GST sample on both setups (**Figure 4.8**). This must be a result of a higher intensity evanescent field.

4.7 – GSTA1-1 Labeling for DEER

An alternative method to FRET where the distance distribution between two labeled residues in a protein can be studied is DEER. DEER is not an optical method but a type of spectroscopy used to study the spin of unpaired electrons.

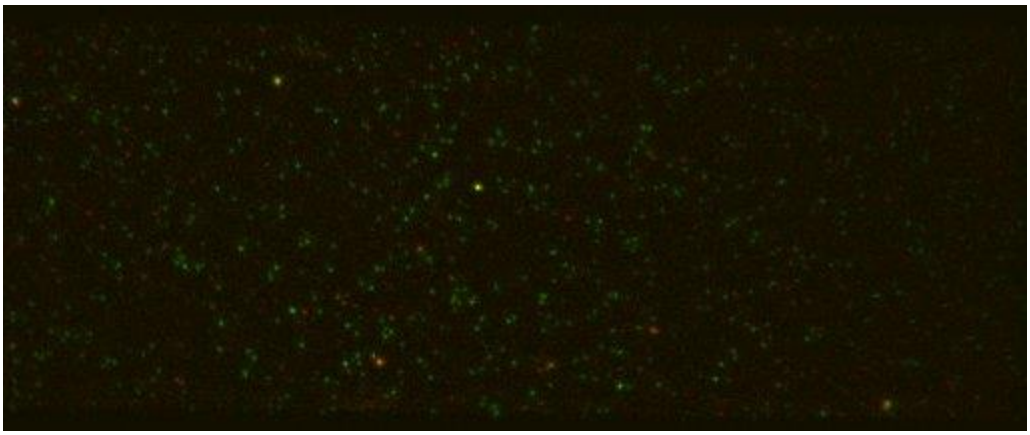

Figure 4.7: Overlay of Cy3 emission (green) and Cy5 emission (red) from Cy3/Cy5-GST using 532nm excitation. Ten frames (100ms) were combined before the overlay to capture both donor and acceptor fluorescence. Some objects can be seen in both channels (yellow).

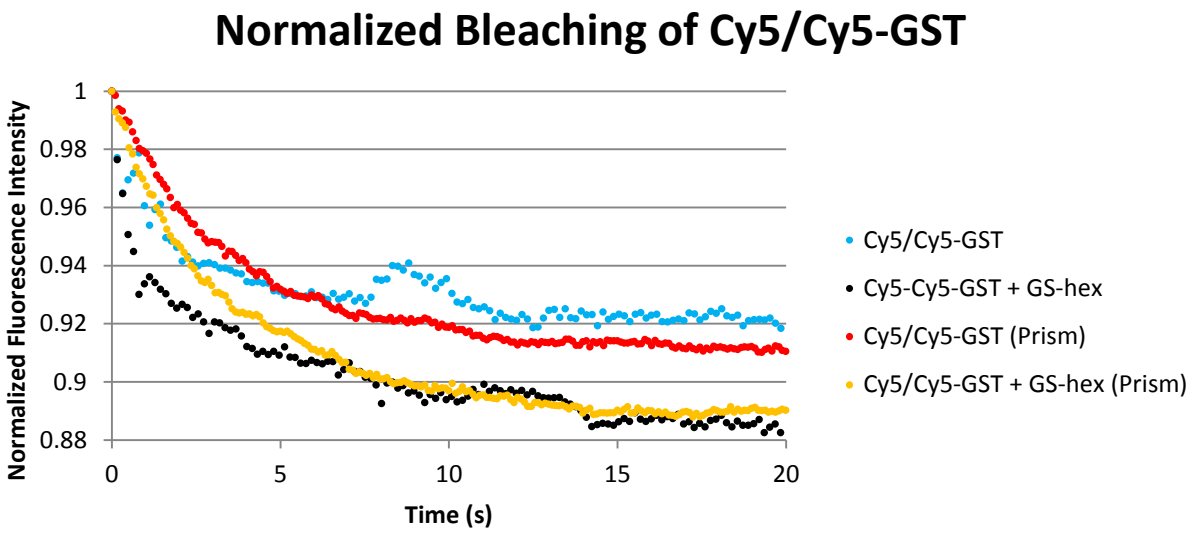

Figure 4.8: Normalized fluorescent intensity of Cy5/Cy5-GST immobilized in the flow chamber imaged with both the Nikon Eclipse Ti setup and the prism TIRF setup. Each bleaching curve is the average intensity from two measurements.

One way of introducing an unpaired electron into a protein structure is by MTSL (*S*-(1-oxyl-2,2,5,5-tetramethyl-2,5-dihydro-1H-pyrrol-3-yl)methyl methanesulfonothioate) labeling. The label is specific to cysteines and introduces a nitroxide paramagnetic spin label into the protein structure. As discussed previously a protein can be mutated to introduce cysteines at specific sites of interest. In the labeling reaction MTSL is conjugated to the cysteine through a disulfide producing a sulfinic acid leaving group.

The G223/C224 GSTA1-1 mutant was labeled with a 10-fold excess MTSL at pH 7.8 and the reaction was incubated at 4˚C over night. The protein has to be extensively washed after labeling to ensure that all unreacted label is removed. A Continuous Wave (CW) spectra revealed that the labeling had been successful with a good label to dimer ratio.

The DEER spectra was collected for MTSL labeled G223/C224 mutant without any ligand, with GS-hex, and with GSH. The distance between the two labels in the non-ligated mutant was determined to 30Å. Unexpectedly the distance between the two labeled C-terminals does not change upon addition of GS-hex but does decrease to approximately 26Å when GSH is added. These distances fit well with what can be observed in the X-ray crystal structure.

It is still unexpected that the addition of GS-hex is not localizing the helix since this has been reported previously by X-ray crystallography. However, it would explain why almost no energy transfer events were observed with the addition of GS-hex.

4.8 – Nitroxide Quenching

With the somewhat non-conclusive results from the FRET experiments in mind additional methods are necessary to study the conformation of the active site with and without

a ligand present. Once again the weakness of one method can be converted in to an advantage and applied to approach the problem from a different angle. To avoid issues related to how the orientation of the dyes affect the transfer efficiency in a FRET experiment one cysteine of the dimer can be labeled with a dye, and the other cysteine labeled with a distance dependent quencher of fluorescence.

Some molecules with an unpaired electron are good quenchers of exited state fluorophores. The effect of the unpaired electron is distance dependent and is believed to occur through electron transfer mechanism.[107] The unpaired electron introduced by MTSL labeling of the G223/C224 GSTA1-1 mutants is capable of quenching a fluorescent dye. Similarly to the energy transfer in a FRET experiment the quenching is effective in the 30-80Å range.[108] One advantage of this method compared to FRET is that the quenching can be disrupted by reducing the label. The addition of ascorbic acid will reduce the nitroxide which would leave the label diamagnetic, thereby disrupting the quenching.

For the quench-labeled GST to work it is important that only one cysteine is labeled in the CyX-GST-min samples. It could be possible, even if unlikely, that there is a cooperative effect to the labeling of the enzyme. This can be evaluated by mass spectrometry.

The fluorescence of Cy3/NO-GST is not as bright as the fluorescence of Cy3-GST-min. The decrease in intensity could possibly be a result of intermolecular quenching. However, the decrease in fluorescent intensity when GS-hex is added is only slightly greater for Cy3/NO-GST that for Cy3-GST-min. The decrease in fluorescent intensity also seems to depend on what ligand is being added. The fluorescence intensity of Cy3-GST-min decrease with 29.2% with GS-hex addition while the fluorescence of Cy3/NO-GST decrease with 31.7% with GS-hex addition.

When GSH is added the fluorescence intensity of Cy3-GST-min decrease with 5.9% and the fluorescence intensity of Cy3/NO-GST decrease with 11.5%. This result is consistent with the DEER studies in that GSH seems to localize the helix better than GS-hex. The emission peak shift that can be observed with GS-hex addition is less pronounced upon GSH addition. It is possible that the quenching probe is working but that it is not very sensitive for this particular application. It is also possible that the mutant has altered dynamics that will not allow the Cy3 to move close enough to the nitroxide to quench fully, or that the nitroxide itself is restricting the dynamics of the helix (**Figure 4.9**). It is also possible that our system is not very sensitive to the quenching due to the conformation or environment at the labeling site.

The maleimide labeling of GST does not seem to be cooperative due to the observed one-step bleaching process discussed in the chapter 3. It is therefore unlikely that all Cy3-GST-min has two dyes and not a dye and a nitroxide. If this was the case only intermolecular quenching would be observed and there would be no difference in fluorescence upon ligand addition.

4.9 – Fluorescence Polarization

Fluorescent polarization can be used as an additional method to study the conformation of the active site and the C-terminal helix. The method can be used to test if the helix localizes when GS-hex is added as observed in the X-ray crystal structure (PDB entry 1K3L).[11] C-terminal localization was not observed in the DEER experiment. If the helix localizes the radius of the labeled protein will decrease and therefore also the rotational diffusion coefficient of the protein. This would result in a decrease in the fluorescence anisotropy.

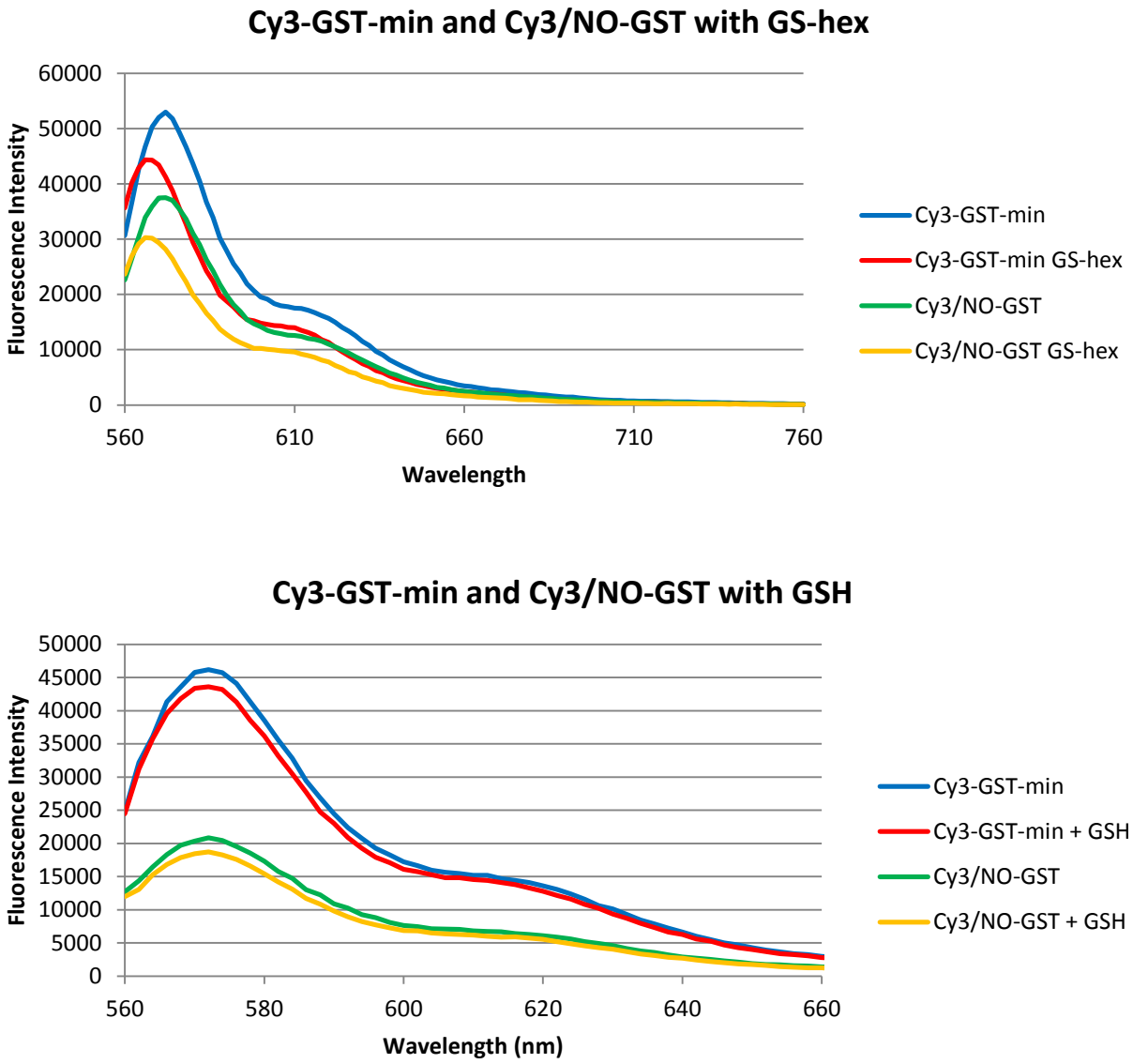

Figure 4.9: Quenching of Cy3/NO-GST upon addition of GS-hex or GSH. Cy3/NO-GST is less fluorescent than Cy3-GST-min and the decrease upon addition of ligand is also slightly altered. The fluorescence intensity of Cy3-GST-min decrease with 29.2% with GS-hex addition while the fluorescence of Cy3/NO-GST decrease with 31.7%. When GSH is added the fluorescence intensity of Cy3-GST-min decrease with 5.9% and the fluorescence intensity of Cy3/NO-GST decrease with 11.5%. The emission peak shift that can be observed with GS-hex addition is less pronounced upon GSH addition. The concentrations of Cy3/NO-GST are different in the two experiments.

No change in anisotropy was observed when GS-hex was added to Cy3-GST-min which suggests that the ligand is not triggering localization of the helix. This could explain why no energy transfer events can be observed in a FRET experiment when GS-hex is added to immobilized Cy3/Cy5-GST. Somewhat unexpectedly no decrease in anisotropy was observed upon GSH addition either. This suggests that a C-terminal labeled with a Cy3 will not localize and could explain the quite uninterpretable FRET data. The ligands were added at a concentration 100-fold greater than their k_d to ensure binding. The unlabeled G223/C224 mutant shows activity in the CDNB assay and is capable of binding labeled ligand, but a fluorescently or spin labeled mutant might have altered activities. The anisotropy of Cy3-(GS-hex)$_2$ increases when binding to GST. The increase is the same for both WT GSTA1-and the G223/C224 mutant suggesting that the mutation is not severely affecting ligand binding (**Figure 4.10**).

Cy3-GST-max surprisingly shows the lowest anisotropy. One explanation could be that energy transfer between the two dyes scrambles the polarization. However, the anisotropy does not change with addition of GS-hex which once again suggests that GS-hex binding is not enough to trigger localization of the helix (**Figure 4.10**).

The residues at the end of the C-terminal helix have been reported to be involved in anchoring of the helix of the active site of the enzyme, particularly Ile219[25], Phe220[12], Arg221[30], and Phe222[12]. Introduction of the two additional residues Gly223 and Cys224 might interrupt the interactions between these residues and residues in the active site, thereby preventing localization of the helix. The introduction of the large dye might also interfere with localization. The Cyanine dyes are large and can interfere with the dynamics of the helix because of that, but

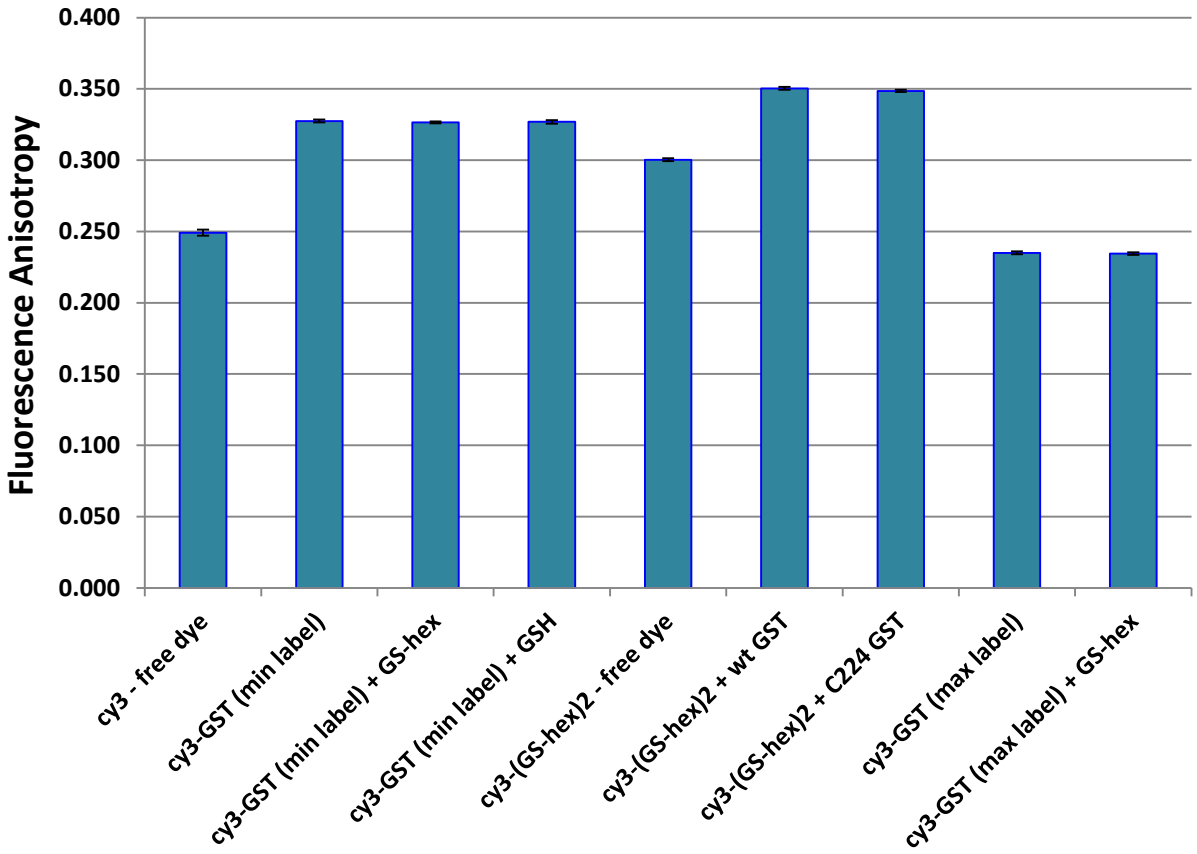

Figure 4.10: The anisotropy of Cy3-labeled GST obtained from fluorescent polarization experiments. Cy3-GST has higher anisotropy than Cy3 just as expected. Ligand binding to Cy3-GST does not decrease the anisotropy suggesting that the C-terminal helix cannot localize. The anisotropy of the large Cy3-(GS-hex)$_2$ ligand binding to both wild type and C224 mutant GST is increases the anisotropy showing that the mutant is not preventing binding of a ligand. The excited-state lifetime for Cy3 is shorter than for Cy5 which results in a higher anisotropy for Cy3.

they also carry a net negative charge. There is an electrostatic interaction between Arg221 and Asp42 that helps localizing the helix that could potentially be disrupted by the conjugation of the dye.[30]

If the labeling of the C-terminal is interfering with localization of the helix it would be possible to construct an additional mutant with an alternative labeling site. Residues in the helix that are not involved in anchoring the C-terminal over the active site could be potential targets for mutation. The side of the helix facing the solvent consists of only charged residues and mutating these residues might interfere with the stability of the helix. Previous experiments show that the E214Q mutant has approximately the same activity in the CDNB assay as wild type enzyme. This glutamate is therefore a potential candidate that can be substituted for a cysteine and spin or fluorescently labeled (**Figure 4.11**). Another residue in the helix that could be targeted for mutagenesis is S212. The serine is fairly exposed and also lacks a charge. Substituting it for a cysteine should therefore not disrupt helix (**Figure 4.11**).

4.10 - Conclusion

The GSTA1-1 G223/C224 mutant was labeled with both Cy3 and Cy5 generating an enzyme with the FRET pair conjugated to the C-terminal. The labeling is expected to follow a binomial distribution and the concentration of all labeled species can be calculated from the relative concentrations of the dyes. As controls the same mutant was labeled with just Cy3 or Cy5 at high and low concentration generating a fully labeled GST and a sparsely labeled GST. The fluorescence of the fully labeled enzyme is lower than that of the singly labeled enzyme suggesting quenching.

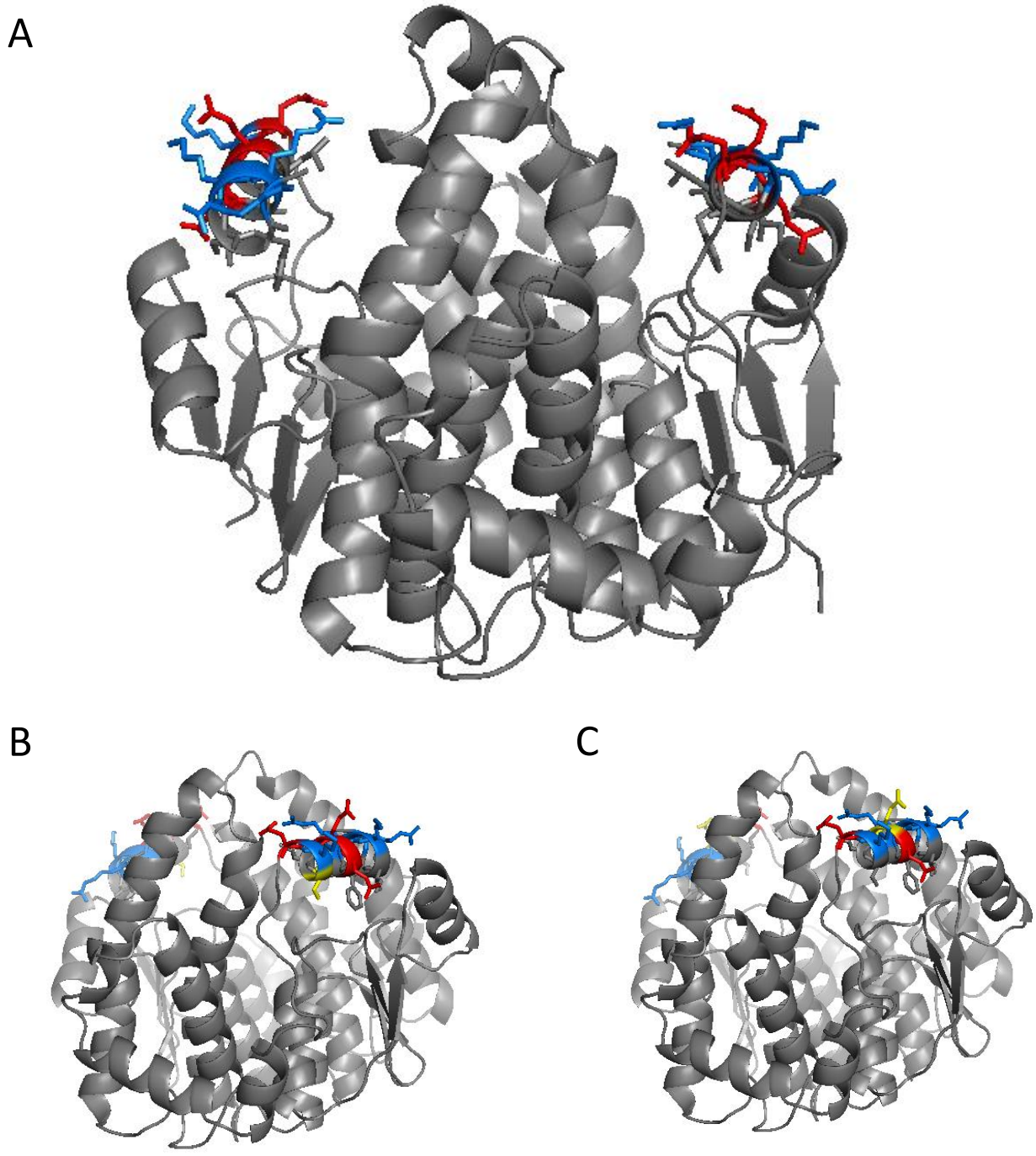

Figure 4.11: Charged residues in the C-terminal α-helix of GSTA1-1. Positively charged residues are labeled in blue and negatively charged residues in red. The side of the helix facing the solution when localized consists almost exclusively of charged residues (**A**). Serine 212 is somewhat exposed and might be targeted for mutagenesis and labeling (**B**). Glutamate 214 is charged but mutation to a glutamine did not change the activity of the enzyme in the CDNB assay (**C**). Substituting and labeling at this position might therefore not affect the activity of the enzyme or localization of the helix.

By comparing the donor and acceptor peak with and without GS-hex in the ensemble FRET experiment energy transfer seems to occur. While the donor intensity decreased upon GS-hex addition the acceptor intensity stays about the same. The donor decrease is much greater than the acceptor decrease, and there is therefore a fairly large change in donor-acceptor emission ratio.

In a single molecule FRET experiment no energy transfer events were observed. This might be due to transitions on timescales that were not available with our experimental setup or due to the fast bleaching of the immobilized dye. Alternative approaches had to be developed and a quench-labeled GST is currently being studied. DEER experiments are also being conducted together with Dr. Sunil Kumar Saxena at University of Pittsburgh. Preliminary results suggest that GSH is localizing the helix of the MTSL labeled G223/C224 mutant while GS-hex is not. It is possible that the helix of a labeled mutant is not able to localize due to alterations in the structure of the active site when introducing additional residues or when labeling the enzyme. An alternative labeling site will be used to confirm or refute the data.

As an alternative to labeling with a FRET pair the enzyme was also labeled to quench the fluorescence of a dye at one C-terminal once the helices localize by introducing an unpaired electron at the other C-terminal. Introducing an unpaired electron decreases the fluorescence intensity of a singly labeled GST. However, the fractional decrease in fluorescence upon addition of a ligand is only slightly greater for a singly labeled GST with an unpaired electron than for singly labeled GST without an unpaired electron.

It is possible that the location of the label in the G223/C224 mutant is interfering with localization of the C-terminal, and that alternative labeling sites are needed. Two residues that

are surface exposed and could be substituted with cysteines are Serine 212 and Glutamate 214. These mutants will be analyzed with DEER before FRET experiments are conducted to ensure that the helix localizes and that energy transfer between the dyes is possible.

Chapter 5 – Future Direction

5.1 - Introduction

I have in my PhD thesis explored and characterized many interesting properties of GSTA1-1. A variety of different biophysical methods has been applied to study both the binding kinetics of different ligands and the dynamics of the enzymes' active site. We have gained an understanding of the multispecificity of the enzyme and determined how to best label the enzyme or ligand for a particular application. Even though new discoveries were made and old results were confirmed some questions remain unanswered due to lack of time or relativeness to my research aims. Many of these questions have emerged as a result of my own research experience and I hope that in the future someone will be able to pursue them. Considering the multifunctionality of GSTs, further characterization should be of biomedical, pharmacological, environmental, and thereby also commercial interest.

5.2 - Antioxidants

In addition to binding and catalyzing GSH GST also has affinity for the antioxidants Ascorbate and Trolox. GST is known for its ligandin activity and functions as a transport protein for steroids, carcinogens and anionic xenobiotics.[22] It would be possible that another function of GST is to bind and transport antioxidants. GSTs affinity and activity with the antioxidant GSH has been well characterized, but other antioxidants less so. The binding constant of Trolox and ascorbate to GSTA1-1 can be estimated from my CDNB inhibition assay (**Figure 3.10**) and should be in the low micromolar range for Trolox and high micromolar range for ascorbate. The higher hydrophobicity of Trolox could explain the proposed higher affinity for the H-site.

5.3 - GST Bis-Ligands

My experiments show that bis-ligands have the highest affinity for GST of all the ligands tested. Judging from the obtained binding constants it seems like one bifunctional ligand is a more efficient inhibitor of the CDNB assay than two monofuctional ligands. GST has been reported to show cooperative behavior in some reactions but it is unknown if both active sites have the same conformation at the same time. One interesting experiment to do would be to test if a GS-DNB-Cy5-GS-hex ligand acts different from Cy5-GS-hex and/or Cy5-GS-DNB, or the bisfunctional form of the inhibitors.

5.4 - Ligand Linker

My research has shown that GST is capable of binding a GSH with an N-terminal tag. It is possible and likely that there are other linkers that will have less of an effect on the ligand affinity than the P2-linker. How crucial the length and chemical composition of the linker is could be evaluated further. The gamma bond between cysteine and glutamate in GSH is non typical for peptides, however, the reaction between the amine and an NHS-ester result in a peptide bond. It would be interesting to test if a ligand with an additional N-terminal amino acid would still bind the enzyme. If this is the case GST could potentially be used to specifically modify the cysteine of small peptides.

5.5 - Addition Reactions

As mentioned in an earlier chapter GSTA1-1 is also able to catalyze addition reactions. One of the substrates for an addition reaction is ethacrynic acid (EA). GSTA1-1 is capable of

binding two EA[109] but only one active site is active at the time[34]. After conjugation of EA to GSH GST generates a racemic mixture of product, but this is not the case for all GST classes. Out of the two diastereoisomers A and B GSTP1-1 produces 100% diastereoisomer A, GSTA1-1 produces 66% A, and GSTA2-2 produces 50% A.[91] It seems like GSTA1-1 somewhat favors one diastereoisomer. It is possible that GSTA1-1 can produce both diastereoisomers, but only A if a ligand is already bound. That would however result in 75% A and 25% B which is not the case. Another possible explanation is that A can be produced in both sites while B can only be produced in one site. This would result in a 67% A and 33% B diastereoisomer which seems to be accurate. It could be possible that the active site only accepts two A diastereoisomers but not two B diastereoisomers.

However, if the proposed one site reactivity of GSTA1-1 in addition reactions is actually accurate[34] the enzyme must favor production of diastereoisomer A. This could be as simple as slightly more favorable interactions of the substrates, product, or transition state.

5.6 – GSTA1-1-Complex

There is a protein co-purifying with GST that is approximately 65kDa in size. The contaminating protein only leaves a faint band on an SDS-PAGE gel and is only visible when very high concentrations of protein are loaded on to the gel. Since the band can be visualized in the S-hexylglutathione-agarose resin purified samples contaminating protein must be quite abundant in the cell and have affinity for the resin. Interestingly I have not been able to get rid of the band with size exclusion chromatography or ion exchange chromatography, only slightly shift it compared to the elution peak of GST (**Figure 5.1**). If the contamination was a GST

aggregate I would suspect a less defined band on the SDS-PAGE gel. It is possible that GSTA1-1 forms a complex with another protein but still maintains its affinity towards GS-hex. Another explanation is that a small fraction of GSTA1 interacts and forms a dimer or trimer with non-characteristic migration properties. MS could be used to determine the identity of the contaminating protein. The band is a little bit too big to represent the GSTA1-1 dimer at 55.5kDa (**Figure 3.21**). The presence of a contaminating protein at very low concentration is not any major concern since the protein lack the Avitag and is very unlikely to be biotinlylated. The risk of finding a protein in *E.coli* that is quite highly expressed, has affinity for the S-hexylglutathion resin, and is biotinylated is must be very low.

There are online databases for predictions of protein interactions. One such database is STRING that uses genomic context, high-throughput experiments, co-expression data, and previous knowledge to predict protein interactions.[110] The top results for human GSTA1 are other human GSTs and MAPEGS but also some Cytochrome P450 proteins. This is interesting since Cytochrome P450s are also detoxification enzymes. No Cytochrome P450 proteins have yet been identified in *E.coli* so the contaminating band must be another protein.[111] What E.coli does express in is an alpha class GST. If a search is done for *E.coli* GSTA one of the best hits is for Methionyl tRNA-synthetase, a 65kDa protein involved in protein biosynthesis. Why GST would interact with this protein or why this protein would have affinity towards the S-hexylglutathione resin is unclear. Since GSH contains glutamate Glutaminyl tRNA-synthetase would have been a more expected to co-purify with GST. The prediction of a protein of the right size does not mean this is the identity of the contaminating protein. Further characterization of the protein or mass spectrometry would have to be done to confirm this.

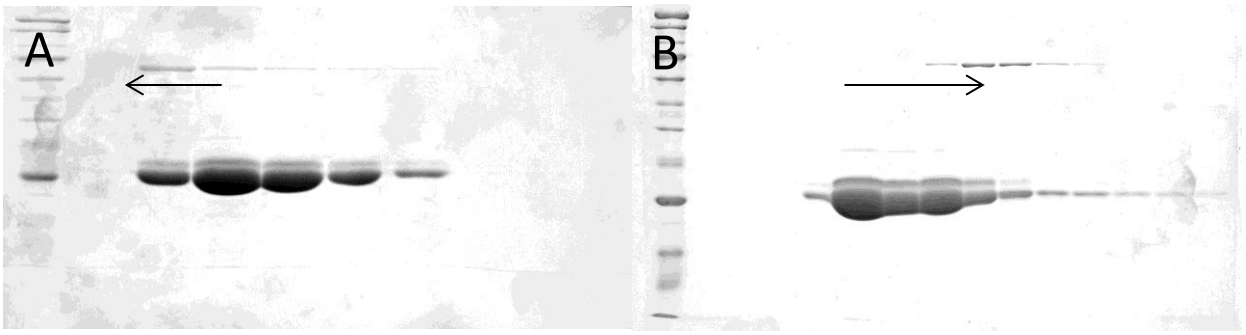

Figure 5.1: SDS-PAGE gel from Gel filtration of GSTA1-1 using Sephadex G-75 (**A**). The contaminating peak shifts to earlier elution, as expected for a larger protein, but cannot be separated from GSTA1-1. SDS-PAGE gel with fractions from anion exchange chromatography of GSTA1-1 using DEAE-Sephacel resin (**B**). The contaminating protein elutes after GSTA1-1, suggesting a more negatively charged protein, lower isoelectric point.

Appendix 1:

GST monomer reaction scheme - pseudo-equilibrium model of steady-state site occupancy

The enzyme-catalyzed reaction sequence for coupling of glutathione (A) to substrate (B) has two branches, one in which A binds first to the enzyme (E) followed by B, and the other in which B binds first to E followed by A:

(1) $A + E \leftrightarrow AE$ (2) $AE + B \leftrightarrow AEB$

(3) $E + B \leftrightarrow EB$ (4) $A + EB \leftrightarrow AEB$

The branches merge at the ternary complex AEB in which catalysis produces bound product C:

(5) $AEB \leftrightarrow EC$

Dissociation releases C and frees up the catalyst:

(6) $EC \leftrightarrow E + C$

Each of the six reactions has a forward (k_x) and reverse (k_x') rate constant:

(1) k_A, k_A' (2) k_{AB}, k_{AB}'

(3) k_B, k_B' (4) k_{BA}, k_{BA}'

(5) k_{cat}, k_{cat}'

(6) k_R, k_R'

In the equilibrium state for the overall reaction $A + B \leftrightarrow C$, the ratio of each pair of rate constants defines an equlibrium constant for the corresponding reaction:

$K_1 = k_A' / k_A = [A]_{eq} [E]_{eq} / [AE]_{eq}$ $K_2 = k_{AB}' / k_{AB} = [AE]_{eq} [B]_{eq} / [AEB]_{eq}$

$K_3 = k_B' / k_B = [B]_{eq} [E]_{eq} / [EB]_{eq}$ $K_4 = k_{BA}' / k_{BA} = [EB]_{eq} [A]_{eq} / [AEB]_{eq}$

$K_5 = k_{cat}' / k_{cat} = [AEB]_{eq} / [EC]_{eq}$

$K_6 = k_R' / k_R = [EC]_{eq} / ([E]_{eq} [C]_{eq})$

Since the free-energy change in reactions 1+2 must equal that in 3+4, it is a thermodynamic requirement that $K_1K_2 = K_3K_4$. This is also apparent algebraically, using the above expressions valid for dilute solutions.

Steady-state kinetics

The throughput of the enzyme is the rate of appearance of product, C. The simplest assay condition is [C] = 0, maintained by a flow cell supplying only reactants A and B, for example. However, experimentally, the simplest setup is a finite volume of solution, where [C] = 0 initially, but increases with time. These are equivalent, as long as $k_R'[E][C]$ is insignificant, and the reactants are not limiting. Define $\Phi_C = d[C]/dt$ as the product flux. Because the overall reaction is A + B $\rightarrow$ C, it always must hold in steady-state that d[C]/dt = – d[A]/dt = – d[B]/dt.

In this model "A" represents glutathione (GSH) and "B" represents the substrate chloro-dinitrobenzene (CDNB). The reaction produces the adduct "C", S-dinitrophenyl-glutathione.

Addition of an *inhibitor* ("I") to the above reaction scheme introduces another equilibrium expression:

$K_I = k_I' / k_I = [E]_{eq} [I]_{eq} / [EI]_{eq}$

Standard assay conditions - pseudo-equlibrium model

To model the standard inhibitor rate-suppression assay with CDNB as a colorimetric substrate, we reduce the system to steady-state in which the rate equation for each chemical component other than C is set equal to zero. The reaction scheme is further simplified by taking the initial condition [C] = 0 as fixed (no product inhibition). The reactants A and B are set at A_0 and B_0, respectively. In the **pseudo-equilibrium limit**, the substrate binding and dissociation reactions occur quickly relative to catalysis so that the equilibrium expressions for reactions (1)-(4) accurately relate the concentrations of intermediates. In this limit, the steady-state reaction rate is equal to the forward rate of reaction #5:

$d[C]/dt = \text{Reaction Rate} = R = k_R [EC] = k_{cat} [AEB]$

To obtain R in terms of $[A]=A_0$, $[B]=B_0$, and $[I]_{eq}$ (and dropping the 'eq' subscripts for convenience);

$$[AEB] = [EB] [A] / K_4$$

$$= ([B] [E] / K_3) [A] / K_4$$

$$= [A] [B] [E] / K_3K_4$$

[E] is found by summing all states of the enzyme to get the partition function:

$$E_0 = [E] + [AE] + [EB] + [AEB] + [EI]$$

$$= [E] + [A] [E] /K_1 + [B] [E] /K_3 + [A] [B] [E] /K_3K_4 + [I] [E] /K_I$$

$$= [E] (1 + [A]/K_1 + [B]/K_3 + [A][B]/K_3K_4 + [I]/K_I)$$

$$[E] = E_0 / (1 + [A]/K_1 + [B]/K_3 + [A][B]/K_3K_4 + [I]/K_I)$$

$$[AEB] = ([A]/K_4) ([B]/K_3) E_0 / (1 + [A]/K_1 + [B]/K_3 + [A][B]/K_3K_4 + [I]/K_I)$$

which is proportional to the rate:

$$R = k_{cat}[AEB]$$

$$= k_{cat}([A]/K_4)([B]/K_3)E_0 / (1 + [A]/K_1 + [B]/K_3 + [A][B]/K_3K_4 + [I]/K_I)$$

The **fractional rate** is R/R_0, where R_0 is the unsuppressed rate in the absence of inhibitor:

$$R/R_0 = (1 + [A]/K_1 + [B]/K_3 + [A][B]/K_3K_4) / (1 + [A]/K_1 + [B]/K_3 + [A][B]/K_3K_4 + [I]/K_I)$$

$$= 1 / \{ 1 + ([I]/K_I) / (1 + [A]/K_1 + [B]/K_3 + [A][B]/K_3K_4) \}$$

from which it can easily be seen that $[I]/K_I = (1 + [A]/K_1 + [B]/K_3 + [A][B]/K_3K_4)$ defines the IC50;

$$[I]_{50} = K_I (1 + [A]/K_1 + [B]/K_3 + [A][B]/K_3K_4)$$

which is also the apparent inhibitor equilibrium constant;

$$K_I^{eff} = K_I (1 + [A]/K_1 + [B]/K_3 + [A][B]/K_3K_4)$$

Since the assay is typically conducted with [GSH] and [CDNB] far above their binding constants K_1 and K_3, the effective inhibitory constant may be much higher than K_I.

Independent binding model

Thermodynamics requires that $K_1K_2 = K_3K_4$ so that the free energy of the ternary complex AEB is the same whether the first step is E + A or E + B. But, there is no further requirement on the numeric values of the four binding constants. If the simplifying assumption is made that ligands A and B bind to the enzyme independently (not affecting the structure of the enzyme in such a way that alters the binding of the other ligand), then $K_1=K_4$ and $K_2=K_3$, reducing the number of constants in the reaction scheme to k_{cat}, K_1, K_3, and K_I;

$$[E] = E_0 / (1 + [A]/K_1 + [B]/K_3 + [A][B]/K_1K_3 + [I]/K_I)$$

$$R = k_{cat}[AEB]$$

$$= k_{cat}([A]/K_1)([B]/K_3)E_0 / (1 + [A]/K_1 + [B]/K_3 + [A][B]/K_1K_3 + [I]/K_I)$$

$$R/R_0 = 1 / \{ 1 + ([I]/K_I) / (1 + [A]/K_1 + [B]/K_3 + [A][B]/K_1K_3) \}$$

and

$$K_I^{eff} = K_I (1 + [A]/K_1 + [B]/K_3 + [A][B]/K_1K_3)$$

The steady-state (pseudo-equilibrium) concentrations of all states of the enzyme can also be derived;

$$[E] = E_0 / (1 + [A]/K_1 + [B]/K_3 + [A][B]/K_1K_3 + [I]/K_I)$$

$$[EI] = ([I]/K_I)\, E_0 / (1 + [A]/K_1 + [B]/K_3 + [A][B]/K_1K_3 + [I]/K_I)$$

$$[AE] = ([A]/K_1)\, E_0 / (1 + [A]/K_1 + [B]/K_3 + [A][B]/K_1K_3 + [I]/K_I)$$

$$[EB] = ([B]/K_3)\, E_0 / (1 + [A]/K_1 + [B]/K_3 + [A][B]/K_1K_3 + [I]/K_I)$$

$$[AEB] = ([A]/K_1)\,([B]/K_3)\, E_0 / (1 + [A]/K_1 + [B]/K_3 + [A][B]/K_1K_3 + [I]/K_I)$$

References:

1. Grant, D. Detoxification pathways in the liver. *J. Inherit. Metab. Dis.* **14,** (1991).

2. Kim, S. K., Abdelmegeed, M. A. & Novak, R. F. Identification of the Insulin Signaling Cascade in the Regulation of Alpha-Class Glutathione S -Transferase Expression in Primary Cultured Rat Hepatocytes. *J. Pharmacol. Exp. Ther.* **316,** 1255–1261 (2006).

3. Eaton, D. L. & Bammler, T. K. Concise review of the glutathione S-transferases and their significance to toxicology. *Toxicol. Sci.* **49,** 156–164 (1999).

4. Blikstad, C., Shokeer, A., Kurtovic, S. & Mannervik, B. Emergence of a novel highly specific and catalytically efficient enzyme from a naturally promiscuous glutathione transferase. *Biochim. Biophys. Acta* **1780,** 1458–63 (2008).

5. Park, H., Koh, J., Ahn, S. & Kong, K. Functional studies of tyrosine 108 residue in the active site of human glutathione S-transferase P1-1. *Bull Korean Chem Soc* **26,** 24–27 (2005).

6. Laborde, E. Glutathione transferases as mediators of signaling pathways involved in cell proliferation and cell death. *Cell Death Differ.* **17,** 1373–1380 (2010).

7. Tew, K. D. *et al.* The role of glutathione S-transferase P in signaling pathways and S-glutathionylation in cancer. *Free Radic. Biol. Med.* **51,** 299–313 (2011).

8. Hayes, J. D., Flanagan, J. U. & Jowsey, I. R. Glutathione transferases. *Annu. Rev. Pharmacol. Toxicol.* **45,** 51–88 (2005).

9. Sheehan, D., Meade, G., Foley, V. M. & Dowd, C. A. Structure, function and evolution of glutathione transferases: implications for classification of non-mammalian members of an ancient enzyme superfamily. *Biochem. J.* **360,** 1–16 (2001).

10. Armstrong, R. N. Structure, catalytic mechanism, and evolution of the glutathione transferases. *Chem. Res. Toxicol.* **10,** 2–18 (1997).

11. Le Trong, I., Stenkamp, R. E., Ibarra, C., Atkins, W. M. & Adman, E. T. 1.3-A resolution structure of human glutathione S-transferase with S-hexyl glutathione bound reveals possible extended ligandin binding site. *Proteins* **48,** 618–27 (2002).

12. Grahn, E. *et al.* research papers New crystal structures of human glutathione transferase A1-1 shed light on glutathione binding and the conformation of the C-terminal helix research papers. 197–207 (2006).

13. Frova, C. Glutathione transferases in the genomics era: new insights and perspectives. *Biomol. Eng.* **23,** 149–69 (2006).

14. Ladner, J. E., Parsons, J. F., Rife, C. L., Gilliland, G. L. & Armstrong, R. N. Parallel evolutionary pathways for glutathione transferases: structure and mechanism of the mitochondrial class kappa enzyme rGSTK1-1. *Biochemistry* **43,** 352–61 (2004).

15. Jakobsson, P. J., Morgenstern, R., Mancini, J., Ford-Hutchinson, A. & Persson, B. Common structural features of MAPEG -- a widespread superfamily of membrane associated proteins with highly divergent functions in eicosanoid and glutathione metabolism. *Protein Sci.* **8,** 689–92 (1999).

16. Atkins, W. M., Wang, R. W., Bird, a W., Newton, D. J. & Lu, a Y. The catalytic mechanism of glutathione S-transferase (GST). Spectroscopic determination of the pKa of Tyr-9 in rat alpha 1-1 GST. *J. Biol. Chem.* **268,** 19188–91 (1993).

17. Sinning, I. *et al.* Structure determination and refinement of human alpha class glutathione transferase A1-1, and a comparison with the Mu and Pi class enzymes. *J. Mol. Biol.* **232,** 192–212 (1993).

18. Lyon, R. P. *et al.* Novel Class of Bivalent Glutathione S -Transferase Inhibitors †. 10418–10428 (2003).

19. Ricci, G. *et al.* 7-Nitro-2,1,3-benzoxadiazole derivatives, a new class of suicide inhibitors for glutathione S-transferases. Mechanism of action of potential anticancer drugs. *J. Biol. Chem.* **280,** 26397–405 (2005).

20. Mahajan, S. & Atkins, W. M. The chemistry and biology of inhibitors and pro-drugs targeted to glutathione S-transferases. *Cell. Mol. Life Sci.* **62,** 1221–33 (2005).

21. Fabrini, R. *et al.* The extended catalysis of glutathione transferase. *FEBS Lett.* **585,** 341–5 (2011).

22. Litwack, G., KETTERER, B. & ARIAS, I. M. Ligandin: a hepatic protein which binds steroids, bilirubin, carcinogens and a number of exogenous organic anions. *Group* (1971).

23. Gildenhuys, S. *et al.* Arginine 15 stabilizes an S(N)Ar reaction transition state and the binding of anionic ligands at the active site of human glutathione transferase A1-1. *Biophys. Chem.* **146,** 118–25 (2010).

24. Dourado, D. F. A. R., Fernandes, P. A. & Mannervik, B. Glutathione Transferase A1-1 : Catalytic Importance of Arginine 15. 1690–1697 (2010).

25. Kuhnert, D. C. *et al.* Tertiary interactions stabilise the C-terminal region of human glutathione transferase A1-1: a crystallographic and calorimetric study. *J. Mol. Biol.* **349,** 825–38 (2005).

26. Lien, S., Gustafsson, A., Andersson, A. & Mannervik, B. Human Glutathione Transferase A1-1 Demonstrates Both Half-of-the-sites and All-of-the-sites Reactivity *. **276,** 35599–35605 (2001).

27. Zhan, Y. & Rule, G. S. Glutathione induces helical formation in the carboxy terminus of human glutathione transferase A1-1. *Biochemistry* **43,** 7244–7254 (2004).

28. Nieslanik, B. S., Ibarra, C. & Atkins, W. M. The C-terminus of glutathione S-transferase A1-1 is required for entropically-driven ligand binding. *Biochemistry* **40,** 3536–43 (2001).

29. Misquitta, S. a & Colman, R. F. Communication between the two active sites of glutathione S-transferase A1-1, probed using wild-type-mutant heterodimers. *Biochemistry* **44,** 8608–8619 (2005).

30. Widersten, M., Björnestedt, R. & Mannervik, B. Involvement of the carboxyl groups of glutathione in the catalytic mechanism of human glutathione transferase A1-1. *Biochemistry* **35,** 7731–42 (1996).

31. Nilsson, L. O., Edalat, M., Pettersson, P. L. & Mannervik, B. Aromatic residues in the C-terminal region of glutathione transferase A1-1 influence rate-determining steps in the catalytic mechanism. *Biochim. Biophys. Acta* **1598,** 199–205 (2002).

32. Nieslanik, B. S., Dietze, E. C. & Matkins, W. The Locally Denatured State of Glutathione S-Transferase AI-I: Transition State Analysis of Ligand-dependent Formation of the C-Terminal Helix. *Symp. A Q. J. Mod. Foreign Lit.* **565,** 554–565 (1999).

33. Balchin, D. *et al.* Stability of the domain interface contributes towards the catalytic function at the H-site of class alpha glutathione transferase A1-1. *Biochim. Biophys. Acta* **1804,** 2228–33 (2010).

34. Lien, S., Gustafsson, a, Andersson, a K. & Mannervik, B. Human glutathione transferase A1-1 demonstrates both half-of-the-sites and all-of-the-sites reactivity. *J. Biol. Chem.* **276,** 35599–605 (2001).

35. Vargo, M. a & Colman, R. F. Heterodimers of wild-type and subunit interface mutant enzymes of glutathione S-transferase A1-1: interactive or independent active sites? *Protein Sci.* **13,** 1586–1593 (2004).

36. Fabrini, R. *et al.* Monomer-dimer equilibrium in glutathione transferases: a critical re-examination. *Biochemistry* **48,** 10473–82 (2009).

37. Dirr, H., Reinemer, P. & Huber, R. X-ray crystal structures of cytosolic glutathione S-transferases. Implications for protein architecture, substrate recognition and catalytic function. *Eur. J. Biochem.* **220,** 645–61 (1994).

38. Cornish-Bowden, A. Understanding allosteric and cooperative interactions in enzymes. *FEBS J.* **281,** 621–32 (2014).

39. Ricard, J. & Cornish-bowden, A. Co-operative and allosteric enzymes: 20 years on. *Eur. J. …* **272,** 255–272 (1987).

40. Pettersson, P. L. & Mannervik, B. The role of glutathione in the isomerization of delta 5-androstene-3,17-dione catalyzed by human glutathione transferase A1-1. *J. Biol. Chem.* **276,** 11698–704 (2001).

41. Fedulova, N. & Mannervik, B. Experimental conditions affecting functional comparison of highly active glutathione transferases. *Anal. Biochem.* **413,** 16–23 (2011).

42. Atkins, W. M. Biological messiness vs. biological genius: Mechanistic aspects and roles of protein promiscuity. *J. Steroid Biochem. Mol. Biol.* 1–9 (2014).

43. Holden, S. J. *et al.* Defining the limits of single-molecule FRET resolution in TIRF microscopy. *Biophys. J.* **99,** 3102–11 (2010).

44. Boehr, D. D. & Wright, P. E. Biochemistry. How do proteins interact? *Science* **320,** 1429–30 (2008).

45. Baumann, M. & Meri, S. Techniques for studying protein heterogeneity and post-translational modifications. *Expert Rev. Proteomics* **1,** 207–17 (2004).

46. Rowe, J. D., Nieves, E. & Listowsky, I. Subunit diversity and tissue distribution of human glutathione S-transferases: interpretations based on electrospray ionization-MS and peptide sequence-specific antisera. *Biochem. J.* **325,** 481–6 (1997).

47. Spange, S., Wagner, T., Heinzel, T. & Krämer, O. H. Acetylation of non-histone proteins modulates cellular signalling at multiple levels. *Int. J. Biochem. Cell Biol.* **41,** 185–98 (2009).

48. Xie, X. Enzymology and life at the single molecule level. *Single Mol. Spectrosc. Chem. Phys.* **i,** (2010).

49. Min, W., Xie, X. S. & Bagchi, B. Two-dimensional reaction free energy surfaces of catalytic reaction: effects of protein conformational dynamics on enzyme catalysis. *J. Phys. Chem. B* **112,** 454–66 (2008).

50. Daniel, R. M., Dunn, R. V, Finney, J. L. & Smith, J. C. The role of dynamics in enzyme activity. *Annu. Rev. Biophys. Biomol. Struct.* **32,** 69–92 (2003).

51. Nagel, Z. D. & Klinman, J. P. A 21st century revisionist's view at a turning point in enzymology. *Nat. Chem. Biol.* **5,** 543–550 (2009).

52. Eisenmesser, E. Z., Bosco, D. a, Akke, M. & Kern, D. Enzyme dynamics during catalysis. *Science* **295,** 1520–3 (2002).

53. Boehr, D. D., Dyson, H. J. & Wright, P. E. An NMR Perspective on Enzyme Dynamics. (2006).

54. English, B. P. *et al.* Ever-fluctuating single enzyme molecules: Michaelis-Menten equation revisited. *Nat. Chem. Biol.* **2,** 87–94 (2006).

55. Axelrod, D. Cell-substrate contacts illuminated by total internal reflection fluorescence. *J. Cell Biol.* (1981).

56. Thompson, N., McConnell, H. & Burhardt, T. Order in supported phospholipid monolayers detected by the dichroism of fluorescence excited with polarized evanescent illumination. *Biophys. J.* 739–747 (1984).

57. Thompson, N., Wang, X. & Navaratnarajah, P. Total internal reflection with fluorescence correlation spectroscopy: Applications to substrate-supported planar membranes. *J. Struct. Biol.* **168,** 95–106 (2009).

58. Lipman, E. A. Single-Molecule Measurement of. **1233,** 10–13 (2011).

59. Ha, T. Single-molecule fluorescence resonance energy transfer. *Methods* **25,** 78–86 (2001).

60. Roy, R., Hohng, S. & Ha, T. A practical guide to single-molecule FRET. *Nat. Methods* **5,** 507–16 (2008).

61. Hwang, H., Kim, H. & Myong, S. Protein induced fluorescence enhancement as a single molecule assay with short distance sensitivity. *Proc. Natl. Acad. Sci. U. S. A.* **108,** 7414–8 (2011).

62. Klehs, K. *et al.* Increasing the brightness of cyanine fluorophores for single-molecule and superresolution imaging. *Chemphyschem* **15,** 637–41 (2014).

63. Magde, D., Elson, E. & Webb, W. Thermodynamic fluctuations in a reacting system—measurement by fluorescence correlation spectroscopy. *Phys. Rev. Lett.* **29,** 705–708 (1972).

64. Widengren, J. & Schwille, P. Characterization of Photoinduced Isomerization and Back-Isomerization of the Cyanine Dye Cy5 by Fluorescence Correlation Spectroscopy. *J. Phys. Chem. A* **104,** 6416–6428 (2000).

65. Elson, E. L. Fluorescence correlation spectroscopy: past, present, future. *Biophys. J.* **101,** 2855–70 (2011).

66. Kogelnik, H. & Li, T. Laser beams and resonators. *Appl. Opt.* **54,** (1966).

67. Aitken, C. E., Marshall, R. A. & Puglisi, J. D. An oxygen scavenging system for improvement of dye stability in single-molecule fluorescence experiments. *Biophys. J.* **94,** 1826–35 (2008).

68. Cordes, T., Vogelsang, J. & Tinnefeld, P. On the mechanism of Trolox as antiblinking and antibleaching reagent. *J. Am. Chem. Soc.* **131,** 5018–5019 (2009).

69. Widengren, J. & Chmyrov, A. Strategies to improve photostabilities in ultrasensitive fluorescence spectroscopy. *J. Phys. Chem.* 429–440 (2007).

70. Ernst, L., Gupta, R., Mujumdar, R. & Waggoner, A. Cyanine dye labeling reagents for sulfhydryl groups. *Cytometry* **10,** 3–10 (1989).

71. Stone, K. M. *et al.* Electron Spin Resonance Shows Common Structural Features for Different Classes of Eco RI-DNA Complexes. *Angew. Chemie Int. Ed.* **47,** 10192–10194 (2008).

72. Yang, Z. *et al.* ESR spectroscopy identifies inhibitory Cu2+ sites in a DNA-modifying enzyme to reveal determinants of catalytic specificity. *Proc. Natl. Acad. Sci. U. S. A.* **109,** E993–1000 (2012).

73. Jeschke, G. DEER distance measurements on proteins. *Annu. Rev. Phys. Chem.* **63,** 419–46 (2012).

74. Merski, M., Fischer, M., Balius, T. E., Eidam, O. & Shoichet, B. K. Homologous ligands accommodated by discrete conformations of a buried cavity. *Proc. Natl. Acad. Sci. U. S. A.* **112,** 5039–5044 (2015).

75. Pearson, A., Mills, J., Song, Y. & Nasertorabi, F. Trapping a transition state in a computationally designed protein bottle. *Science (80-.).* (2015).

76. Ulusu, N. N. Evolution of Enzyme Kinetic Mechanisms. *J. Mol. Evol.* **80,** 251–257 (2015).

77. Chronopoulou, E. G. & Labrou, N. E. Glutathione transferases: emerging multidisciplinary tools in red and green biotechnology. *Recent Pat. Biotechnol.* **3,** 211–223 (2009).

78. Jochum, C. *et al.* Glutathione-S-transferase subtypes α and π as a tool to predict and monitor graft failure or regeneration in a pilot study of living donor liver transplantation. *Eur. J. Med. Res.* **16,** 34–40 (2011).

79. Zhang, J. *et al.* Synthesis and characterization of a series of highly fluorogenic substrates for glutathione transferases, a general strategy. *J. Am. Chem. Soc.* **133,** 14109–19 (2011).

80. Liu, Y., Hyde, A. S., Simpson, M. a & Barycki, J. J. *Emerging regulatory paradigms in glutathione metabolism. Adv. Cancer Res.* **122,** 69–101 (Elsevier Inc., 2014).

81. Koumaravelou, K. *et al.* Analysis of human glutathione S-transferase alpha 1 (hGSTA1) gene promoter polymorphism using denaturing high performance liquid chromatography (DHPLC). *Clin. Chim. Acta.* **412,** 1465–1468 (2011).

82. Modén, O. & Mannervik, B. *Glutathione transferases in the bioactivation of azathioprine. Adv. Cancer Res.* **122,** 199–244 (2014).

83. Hou, L. *et al.* Functional promiscuity correlates with conformational heterogeneity in A-class glutathione S-transferases. *J. Biol. Chem.* **282,** 23264–74 (2007).

84. Honaker, M. T., Acchione, M., Sumida, J. P. & Atkins, W. M. Ensemble perspective for catalytic promiscuity: calorimetric analysis of the active site conformational landscape of a detoxification enzyme. *J. Biol. Chem.* **286,** 42770–6 (2011).

85. Habig, W., Pabst, M. & Jakoby, W. Glutathione S-transferases the first enzymatic step in mercapturic acid formation. *J. Biol. Chem.* 7130–7140 (1974).

86. Kurtovic, S., Shokeer, A. & Mannervik, B. Diverging catalytic capacities and selectivity profiles with haloalkane substrates of chimeric alpha class glutathione transferases. *Protein Eng. Des. Sel.* **21,** 329–41 (2008).

87. Ploemen, J. Inhibition of rat and human glutathione S-transferase isoenzymes by ethacrynic acid and its glutathione conjugate. *Biochem. …* **40,** 1631–1635 (1990).

88. Hayeshi, R., Mutingwende, I., Mavengere, W., Masiyanise, V. & Mukanganyama, S. The inhibition of human glutathione S-transferases activity by plant polyphenolic compounds ellagic acid and curcumin. *Food Chem. Toxicol.* **45,** 286–95 (2007).

89. Chronopoulou, E. G., Papageorgiou, A. C., Markoglou, A. & Labrou, N. E. Inhibition of human glutathione transferases by pesticides: Development of a simple analytical assay for the quantification of pesticides in water. *J. Mol. Catal. B Enzym.* **81,** 43–51 (2012).

90. Fernández-Checa, J. & Kaplowitz, N. The use of monochlorobimane to determine hepatic GSH levels and synthesis. *Anal. Biochem.* **219,** 212–219 (1990).

91. Van Iersel, M. L., van Lipzig, M. M., Rietjens, I. M., Vervoort, J. & van Bladeren, P. J. GSTP1-1 stereospecifically catalyzes glutathione conjugation of ethacrynic acid. *FEBS Lett.* **441,** 153–157 (1998).

92. Howard, P. K., Shaw, J. & Otsuka, A. J. Nucleotide sequence of the birA gene encoding the biotin operon repressor and biotin holoenzyme synthetase functions of Escherichia coli. **35,** 321–331 (1985).

93. Cull, M. G. & Schatz, P. J. Biotinylation of proteins in vivo and in vitro using small peptide tags. *Methods Enzymol.* **326,** 430–40 (2000).

94. GREEN, N. M. A SPECTROPHOTOMETRIC ASSAY FOR AVIDIN AND BIOTIN BASED ON BINDING OF DYES BY AVIDIN. *Biochem. J.* **94,** 23C–24C (1965).

95. Humbert, N., Zocchi, A. & Ward, T. Electrophoretic behavior of streptavidin complexed to a biotinylated probe: A functional screening assay for biotin-binding proteins. *Electrophoresis* 47–52 (2005).

96. Cheng, Y. & Prusoff, W. H. Relationship between the inhibition constant (K1) and the concentration of inhibitor which causes 50 per cent inhibition (I50) of an enzymatic reaction. *Biochem. Pharmacol.* **22,** 3099–108 (1973).

97. Lamichhane, R., Solem, A., Black, W. & Rueda, D. Single-molecule FRET of protein-nucleic acid and protein-protein complexes: surface passivation and immobilization. *Methods* **52,** 192–200 (2010).

98. Cordes, T., Vogelsang, J. & Tinnefeld, P. On the mechanism of Trolox as antiblinking and antibleaching reagent. *J. Am. Chem. Soc.* **131,** 5018–5019 (2009).

99. Mehlert, A. & Diplock, A. T. The glutathione S-transferases in selenium and vitamin E deficiency. **227,** 823–831 (1985).

100. Ibarra, C. A., Chowdhury, P., Petrich, J. W. & Atkins, W. M. The anomalous pKa of Tyr-9 in glutathione S-transferase A1-1 catalyzes product release. *J. Biol. Chem.* **278,** 19257–65 (2003).

101. Parsons, J. F., Xiao, G., Gilliland, G. L. & Armstrong, R. N. Enzymes harboring unnatural amino acids: mechanistic and structural analysis of the enhanced catalytic activity of a glutathione transferase containing 5-fluorotryptophan. *Biochemistry* **37,** 6286–94 (1998).

102. Mosebi, S., Sayed, Y., Burke, J. & Dirr, H. Residue 219 impacts on the dynamics of the C-terminal region in glutathione transferase A1-1: implications for stability and catalytic and ligandin functions. *Biochemistry* 15326–15332 (2003).

103. Malitson, I. Interspecimen comparison of the refractive index of fused silica. *JOSA* **55,** (1965).

104. Kedenburg, S. & Vieweg, M. Linear refractive index and absorption measurements of nonlinear optical liquids in the visible and near-infrared spectral region. *Opt. Mater. Express* **2,** 8148–8154 (2012).

105. Cole, J. Horita, D. R. Stable isotope partitioning in aqueous and hydrothermal systems to elevated temperatures, in Aqueous systems at elevated temperatures and pressures. *Phys. Chem. water, steam hydrothermal Solut.* 277–319 (2004).

106. Glycerine Producers' Association. Physical Properties of Glycerine and Its Solutions. (1963).

107. Matko, J., Ohki, K. & Edidin, M. Luminescence quenching by nitroxide spin labels in aqueous solution: studies on the mechanism of quenching. *Biochemistry* (1992).

108. Zhu, P., Clamme, J.-P. & Deniz, A. a. Fluorescence quenching by TEMPO: a sub-30 A single-molecule ruler. *Biophys. J.* **89,** L37–9 (2005).

109. Cameron, A. D. *et al.* Structural analysis of human alpha-class glutathione transferase A1-1 in the apo-form and in complexes with ethacrynic acid and its glutathione conjugate. *Structure* **3,** 717–27 (1995).

110. Szklarczyk, D. *et al.* STRING v10: protein-protein interaction networks, integrated over the tree of life. *Nucleic Acids Res.* **43,** D447–52 (2015).

111. Lamb, D. C. *et al.* The First Virally Encoded Cytochrome P450. *J. Virol.* **83,** 8266–8269 (2009).